Investigations on the mechanism of Host-Induced Gene Silencing of the fungal *CYP51* genes in the *Fusarium – Arabidopsis* pathosystem

Dissertation zur Erlangung des Doktorgrades (Dr. rer. nat.) der Naturwissenschaftlichen Fachbereiche der Justus-Liebig-Universität Gießen

durchgeführt am Institut für Phytopathologie

vorgelegt von

M. Sc. Lisa Höfle

Gießen, 2018

Dekan: Prof. Dr. Volker Wissemann

1. Gutachter: Prof. Dr. Karl-Heinz Kogel

2. Gutachterin: Prof. Dr. Annette Becker

Selbstständigkeitserklärung

„Ich erkläre: Ich habe die vorgelegte Dissertation selbstständig und ohne unerlaubte fremde Hilfe und nur mit den Hilfen angefertigt, die ich in der Dissertation angegeben habe. Alle Textstellen, die wörtlich oder sinngemäß aus veröffentlichten Schriften entnommen sind, und alle Angaben, die auf mündlichen Auskünften beruhen, sind als solche kenntlich gemacht. Ich stimme einer evtl. Überprüfung meiner Dissertation durch eine Antiplagiat-Software zu. Bei den von mir durchgeführten und in der Dissertation erwähnten Untersuchungen habe ich die Grundsätze guter wissenschaftlicher Praxis, wie sie in der „Satzung der Justus-Liebig-Universität Gießen zur Sicherung guter wissenschaftlicher Praxis" niedergelegt sind, eingehalten."

Datum	Unterschrift

Parts of this work are already or will be published.

Talk: "Functional characterization of essential fungal CYP51 ergosterol biosynthesis genes using Host-Induced Gene Silencing (HIGS) as well as Spray-Induced Gene Silencing (SIGS) approaches."
Tagung der Deutschen Phytomedizinischen Gesellschaft, 16.-17. März 2017, Universität Rostock

Table of contents

Abbreviations

APS	ammonium persulfate
At	*Arabidopsis thaliana*
cDNA	complementary DNA
Cm	*Cucurbita maxima*
Col-0	*At* wild-type Col-0 Köln
ddH$_2$O	double-distilled water
dpi	days past infection
dsRNA	double-stranded RNA
E. coli	*Escherichia coli*
EVs	extracellular vesicles
Fg	*Fusarium graminearum*
FHB	Fusarium head blight
h	hours
HEPES	N-2-hydroxyethylpiperazine-N-2-ethanesulfonic acid
HIGS	Host-Induced Gene Silencing
LB	lysogeny broth
miRNA	microRNA
mRNA	messenger RNA
MS	Murashige & Skoog Medium
Nb	*Nicotiana benthamiana*
PBS	phosphate buffered saline
PTGS	post-transcriptional gene silencing
qRT-PCR	quantitative real-time PCR
RBP	RNA-binding protein
RNAi	RNA interference
RT	room temperature
SAM	shoot apical meristem
SDS	sodium dodecyl sulfate
SDS-PAGE	SDS polyacrylamide gel electrophoresis
SIGS	Spray-Induced Gene Silencing
siRNA	small interfering RNA
SNA-agar	synthetic nutrient-poor agar

TBS	Tris buffered saline
TE	Tris-EDTA
TEM	transmission electron microscopy
Temed	Tetramethylethylendiamin
TGS	transcriptional gene silencing
Tris	Tris(hydroxymethyl)-aminomethan
VIB	vesicle isolation buffer
wk	week
wt	wild-type
YEB	yeast extract broth

1. Introduction

1.1 *Fusarium graminearum*

Fusarium graminearum (*Fg*) is a species of the large genus *Fusarium* in the division of Ascomycota. Some Fusarium species are harmless and live as saprophytes in the soil. Others like *Fg* are plant pathogenic and have major economic impacts on the agriculture industry (Doll and Danicke, 2011). The genome of *Fg* is completely sequenced and the fungus can be cultivated easily under lab conditions. This together with his high economical relevance make *Fg* to one of the best studied fungal pathogens. Biological research focuses mainly on the study of the infection process and the life cycle in order to identify weak points for the generation of resistant plants (Ding et al., 2017; Lu and Edwards, 2017; Machado et al., 2017).

1.1.1 *Fg* life cycle and mycotoxins

Fg can reproduce asexually via macroconidia and sexually via ascospores (Stack, 1989). Under the microscope macroconidia of *Fg* can be observed as sickle-shaped structures that contain multiple septa. At the beginning of the life cycle the fungus produces macroconidia that overwinter in the soil or on plant residues. The next step is the development of fruiting bodies. These so-called perithecia release ascospores that can infect cereal heads during flowering. High humidity further promotes the germination of the fungus. The infection causes Fusarium head blight (FHB) and manifests as premature bleaching of cereal heads and results as further consequences in the reduction of grain yield and quality. Grain quality is particularly affected by the production of mycotoxins such as zearalenone (ZEA) and deoxynivalenol (DON) in the grain what makes it useless for human consumption (Fig. 1; Trail, 2009). Several studies show that trichothecene mycotoxins like DON represent a severe threat for human and animal health. Among others they can cause cell death, have immunological effects and are suspected to cause cancer (Arunachalam and Doohan, 2013; Rocha et al., 2005). Whereas *Fg* was classified as necrotrophic fungus, some studies support the idea that *Fg* exhibits a biotrophic lifestyle during the early stages of infection (Brown et al., 2010; Kazan et al., 2012). Microscopic analysis of wheat heads revealed that fungal hyphae remain intercellular at the infection front. Necrosis and cell death started later after fungal hyphae colonized the intracellular space (Brown et al., 2010). Others argue that the lack of intracellular growth do not conform with the traditional definition of biotrophy (Kazan et al., 2012; Trail, 2009).
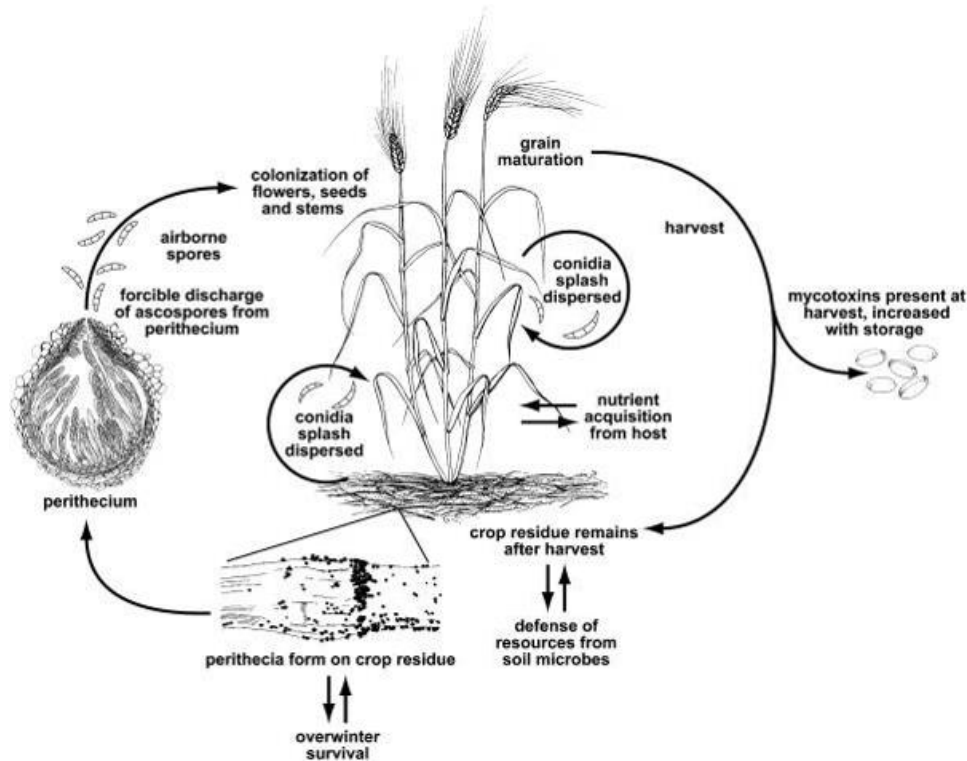
Fig. 1 Life cycle of *Fusarium graminearum* on wheat. (Trail, 2009)

1.1.2 *Fg* in crop production

Crop plants are challenged by a multitude of different pathogens, insects, animals and weeds that cause many different plant diseases and constitute a constant threat to food supply. It is estimated that they are responsible for yield losses up to 40% of the global agricultural production what constitutes extremely high costs for our growing world population (Alexander et al., 2017; Oerke and Dehne, 2004). Mycotoxin producing fungi like *Fusarium* have a huge impact on food and feed supply as mycotoxin contamination of grains has become one of the biggest challenges for plant pathologists in these days. FHB is caused by many fungi of the genus *Fusarium* and affects several of the most important crop plants like wheat, barley, maize and oats (Brown et al., 2017; Osborne and Stein, 2007). Each year the fungus causes billions of dollars in economic losses worldwide (Doll and Danicke, 2011; Savary et al., 2012). Current plant protection strategies against *Fusarium* are crop rotation, breeding for resistance (Mesterházy et al., 2012), tillage practices (Lori et al., 2009) and the chemical treatment with fungicides. Though the latter strategies can contribute to FHB resistance, the application of fungicides is essential for consistent disease control and limitation of mycotoxin contamination. Thereby the most common chemicals are azole fungicides that were extensively used since their development in the 1970s against several plant pathogenic fungi. They are targeting the sterol 14α-demethylase encoded by the *CYP51* gene, an enzyme which is important for the ergosterol biosynthesis of the fungi. By binding to CYP51, the enzyme is inactivated leading to the

accumulation of ergosterol intermediates and as consequence the inhibition of ergosterol synthesis. Ergosterol is essential for the fungi to maintain membrane fluidity and stability (Yoshida, 1988). Seeing the intensive exposure to azole fungicides it is not surprising that increasing rates of insensibilities could be observed in several plant pathogenic fungi including *Fg* (Becher et al., 2010). Possible mechanisms for resistance development are point mutations in the *CYP51* gene, *CYP51* overexpression or the overexpression of efflux transporters (Price et al., 2015). These transporters, naturally exporting toxins and fungicides out of the cell, reduce the intracellular concentration of fungicides (Price et al., 2015; Stefanato et al., 2009). Additionally, it could be shown that ascomycetes like *Fusarium* possess multiple paralogous *CYP51* genes. This could cause an enhanced resistance against azole fungicides by maintaining the enzyme activity due to multiple gene copies (Fan et al., 2013). *Fg* for example has three *CYP51* genes, *FgCYP51A*, *FgCYP51B* and *FgCYP51C* (Becher et al., 2011). Knowledge on specific gene functions of individual *FgCYP51* genes is based on few studies showing partly opposing results. Fan et al. 2013 showed by *CYP51* gene deletion that *FgCYP51B* encodes the major demethylase, whereas *FgCYP51A* encodes an additional enzyme that can be upregulated under CYP51B deficiency. In the same study *FgCYP51C,* which is found exclusively in *Fusarium* species (Fernández-Ortuño et al., 2010), is described as genus specific virulence factor that is not involved in ergosterol synthesis (Fan et al., 2013). Indeed, an earlier study showed that deletion of *CYP51A* or *CYP51B* can partly reduce conidiation but had no influence on ergosterol content, virulence as well as growth of the fungus (Liu et al., 2011). In support to this finding, (Fan et al., 2013) showed that only double deletion mutants restrict fungal growth. The loss of effective treatment against *Fusarium* diseases would have a large impact on agricultural production and global food security so there is a need for alternatives. Genetic engineering of plants expressing antifungal genes such as chitinases (Shin et al., 2008) and plant defensins (Li et al., 2011) or mycotoxin reducing enzymes like glycosyltransferases are recent research examples (Karlovsky, 2011). However, the applicability of these approaches under field conditions is not proven (Kazan et al., 2012). Current examples of alternative plant protection measures against *Fusarium* are based on RNA interference (RNAi) like Host-Induced Gene Silencing (HIGS) (Machado et al., 2017; Majumdar et al., 2017).

1.2   RNA interference (RNAi)

RNAi is a conserved biological process where double stranded RNA (dsRNA) leads to a gene specific inhibition of gene expression or translation. Beside the role in regulation of gene expression, RNAi constitutes an important part of the immune response to viruses and foreign nucleic acids and can be found in nearly all eukaryotes including animals (Cerutti and Casas-

Mollano, 2006). Since the discovery in 1998 in the model nematode *C. elegans* that injection of dsRNA caused effective and specific gene silencing, the high potential of RNAi in suppression of requested genes has become evident and revolutionized experimental biology (Fire et al., 1998). In eukaryotes RNAi is initiated by DICER, an RNAse III enzyme, that cleaves the dsRNA precursor into small (double-stranded) interfering RNAs (siRNAs) of 20-25 nt in length (Borges and Martienssen, 2015; Papp, 2003). These siRNAs are each composed of an antisense strand, which is complementary to the target mRNA, and a sense strand. The sense strand, which is identical to the target mRNA, has no function and is degraded in the next steps, while the antisense strand is loaded onto ARGONAUTE (AGO) proteins to form together with other proteins an active RNA-induced silencing complex (RISC). The antisense strand can then bind to the target mRNA by sequence complementarity, which leads in case of perfect sequence identity to target degradation by the action of activated AGO proteins (Pratt and MacRae, 2009). In case of only partial homology of siRNA and target mRNA the target is not degraded. Gene silencing is here the result of translational inhibition (Fig. 2; Borges and Martienssen, 2015; Majumdar et al., 2017; Pratt and MacRae, 2009).

RNAi can be triggered endogenously by foreign DNA or viral dsRNA, aberrant transcripts from repetitive sequences like transposons as well as pre-microRNA (Nosaka et al., 2012; Plasterk, 2002). The possibility of triggering RNAi by introduction of foreign dsRNA together with the high specificity make RNAi a precious tool for experimental biology. Amongst others, RNAi was used in functional genomics for the establishment of loss-of-function phenotypes in a variety of organisms including plants (Hamakawa and Hirotsu, 2017; Lu, 2003; Nybakken et al., 2005).
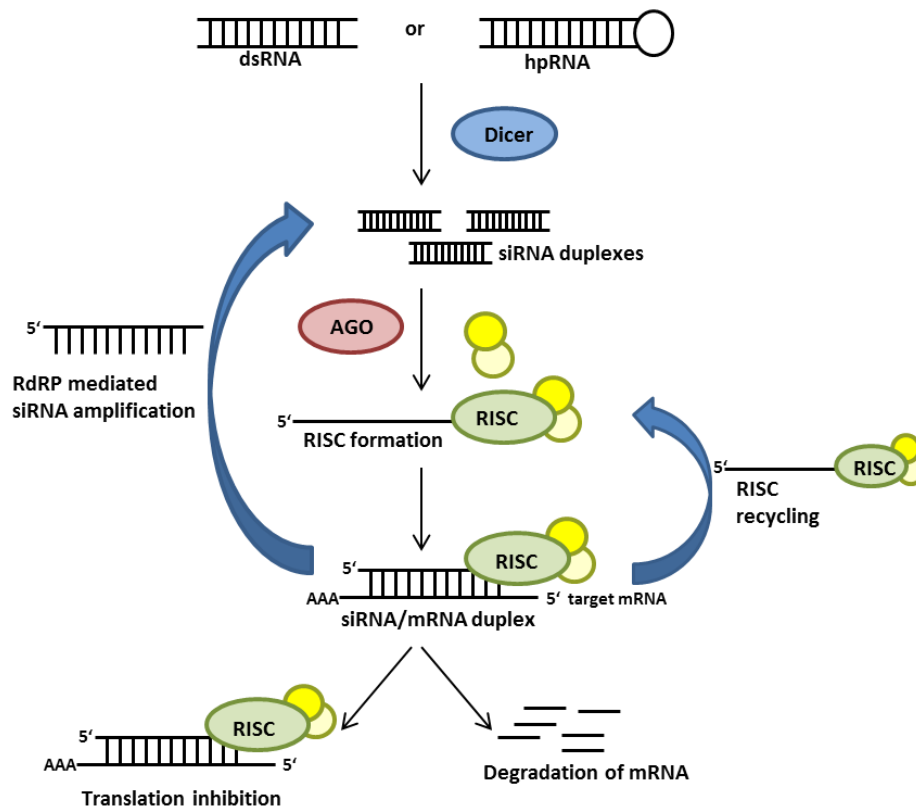
Fig. 2 Mechanisms of RNAi-mediated gene silencing in eukaryotes. Double-stranded RNA (dsRNA), hairpin RNA (hpRNA), ARGONAUTE (AGO), RNA-induced silencing complex (RISC), RNA-dependent RNA polymerase (RdRP) (modified after Majumdar et al., 2017).

1.2.1 RNAi-based plant protection

Modern plant protection in conventional agriculture relies on effective chemical pathogen and pest control. Especially in the case of mycotoxin producing fungi like *Fusarium* spec. chemical fungicides are indispensable to limit mycotoxin contamination of grains. However, recently an increasing number of resistances and decreased sensibility of pathogens against the available chemicals have been observed (Becher et al., 2010), indicating the need for alternative control strategies. RNAi-mediated plant protection strategies like Host-Induced Gene Silencing (HIGS), Virus-Induced Gene Silencing (VIGS) as well as Spray-Induced Gene Silencing (SIGS) demonstrated a great potential for modern crop protection (Koch et al., 2016; Koch and Kogel, 2014; Majumdar et al., 2017; Zhang et al., 2017). The mechanism of HIGS relies on the integration of an inverted repeat transgene in the plant genome. The expression of the transgene triggers RNAi by production of dsRNA and subsequently procession by the plants RNAi machinery and finally gene silencing of target genes in the pathogen. Several HIGS vectors are available that drive the production of dsRNA through inverted promotor sequences or by expression of inverted repeat transgenes. Both, long dsRNA as well as hairpin constructs have been shown to function in HIGS (Ghag et al., 2014; Koch et al., 2013; Koch and Kogel, 2014).

In contrast, VIGS is based on the natural RNAi-mediated defence mechanism against viruses. By exchanging the viral genes, the production of dsRNA targeting the gene of interest can be triggered in the plant (Unver and Budak, 2009). HIGS has been shown to protect several different plants species against infection by nematodes (Shivakumara et al., 2017), insects (Bhatia et al., 2012), bacteria (Walawage et al., 2013) and fungi (Koch et al., 2013) as well as invasion by parasitic plants (Alakonya et al., 2012). RNAi based plant protection has a great potential in controlling *Fusarium* diseases and could provide an alternative for the resistance compromised fungicides. The expression of a 791 nt dsRNA construct *in planta* targeting the three *CYP51* genes of *Fg* could confer resistance to *Arabidopsis* and barley. All three genes were silenced via HIGS, which has been proven by quantitative real-time PCR (qRT-PCR). This leaded to an extremely strong resistance phenotype in detached leave assays (Koch et al., 2013). In further studies, it could be proven that the same dsRNA, when externally applied on leaves, could protect barley plants in a similar way than shown before with transgenic plants. This, so-called Spray-Induced Gene Silencing (SIGS), represents a really new and innovative plant protection strategy against pathogenic fungi like *Fg* (Koch et al., 2016). During SIGS, the host plant is treated externally with dsRNA that is transported via still unknown mechanisms into the plant as well as the pathogen where it leads to silencing of the targeted genes. SIGS is really innovative and shown by only few studies against the two necrotrophic fungi *Fg* as well as *Botrytis cinerea* so far (Koch et al., 2016; Mitter et al., 2017; Wang et al., 2016). Recently, Mitter et al. showed that dsRNA spraying works efficiently against two different plant viruses when combined with clay nanosheets (Mitter et al., 2017). One of the latest publications indicates that this silencing approach also functions against insects. After external application of dsRNA on tomato leaves, the dsRNA could be detected in insects after feeding on the plant (Gogoi et al., 2017). In contrast to HIGS, SIGS does not require a transformation event what makes it really attractive as plant transformation is often time consuming and also not available for some important crop plants. Especially in Europe it could constitute an alternative to HIGS as transgenic plants are here not under consideration.

1.2.2 Function of small RNAs (sRNA) in plants

In plants, several classes of endogenous small RNAs can be differentiated including microRNAs (miRNAs), hairpin derived siRNAs (hp-siRNAs), natural antisense siRNAs (natsiRNAs), secondary siRNAs (secsiRNAs) and heterochromic siRNAs (hetsiRNAs) (Borges and Martienssen, 2015). There exist three main biogenesis pathways that cover for the majority of plant small RNAs. One for the biogenesis of 20-22 nt miRNAs, one for the biogenesis of 21-22 nt secondary siRNAs and the last for the biogenesis of 24 nt hetsiRNAs. All of them are

modified at the 3'-end by 2'O-methylation which is necessary for small RNA stability and protection from degradation (Borges and Martienssen, 2015). The biogenesis of small RNAs requires the activity of Dicer-like proteins (DCL) which are RNAse III enzymes composed of multiple domains responsible for dsRNA binding and cleavage. In *A. thaliana*, there exist four genes encoding DICER proteins DCL1, DCL2, DCL3 and DCL4 that are responsible for the processing of different classes of small RNAs (Mukherjee et al., 2013).

Plant miRNAs are mainly involved in post-transcriptional gene silencing (PTGS) by transcript cleavage or translational repression. In contrast to animals, where miRNAs bind through imperfect homology mostly to the 3'-UTR of mRNAs and lead to translational repression, most plant miRNAs mediate cleavage of target mRNAs via perfect sequence complementarity (Saumet and Lecellier, 2006). In the first biogenesis step long, primary miRNAs are transcribed by RNA polymerase II from endogenous genes. The single stranded precursor folds into hairpin-like structures and is then cleaved by DCL1 into smaller stem loop structures, which are processed again by DCL1 into mature miRNA duplexes (Baulcombe, 2004; Borges and Martienssen, 2015).

Most endogenous plant siRNAs are needed for RNA-directed DNA methylation (RdDM) or transcriptional gene silencing (TGS) and their procession requires DCL2, DCL3 and DCL4 (Borges and Martienssen, 2015). RdDM is an epigenetic pathway essential for the silencing of transposable elements and a subset of genes via TGS. It is established and maintained by the 24 nt hetsiRNAs, which represent beside secondary siRNAs, the most abundant class of siRNAs in plants (Law and Jacobsen, 2010). Their biogenesis is initiated by the transcription of long RNA precursors at target sites through RNA polymerase IV. Precursor RNA is used as a template for RNA-dependent RNA polymerase 2 (RDR2) to produce dsRNA which is finally processed by DCL3 into 24 nt hetsiRNAs (Kuo et al., 2017; Matzke and Mosher, 2014).

The ability to amplify RNA silencing by the production of secsiRNAs is an important feature of plant RNAi. Thereby RNAs that are targeted and cleaved through the action sRNAs become targets for RNA-dependent RNA polymerase 6 (RDR6) what leads subsequently to their conversion into dsRNA and procession by DCL2 and DCL4 to 21-22 nt siRNAs (Borges and Martienssen, 2015; Felippes et al., 2017). The miRNA-mediated cleavage of a target mRNA can trigger the production of secsiRNAs which can in turn silence other genes. This allows the silencing of genes that are sequence-related to the original target and in this way the control of large gene families by single miRNAs (Manavella et al., 2012). Most secsiRNAs are involved in PTGS and are subdivided again in different classes including the highly conserved trans-acting siRNAs (tasiRNAs) (Borges and Martienssen, 2015; Felippes et al., 2017). Additionally,

secsiRNAs play important roles for the local as well as systemic spreading of RNA silencing. In both cases the transported silencing signals include siRNAs. However, whether the movement requires single- and/or double-stranded siRNAs and also whether they are bound to RNA-binding proteins is unclear (Vazquez and Hohn, 2013). The generation of secsiRNAs can also be induced artificially by inverted repeat transgenes as well as by Virus-Induced Gene Silencing (VIGS) vectors. Especially in the case of transgenes the spreading of RNA silencing is dependent on RDR6-mediated amplification (Vazquez and Hohn, 2013).

1.2.3 The double-stranded RNA-binding proteins of *Arabidopsis*

In *Arabidopsis*, the five dsRNA-binding proteins named DRB1-5 are promoting cofactors of the four DCLs to ensure efficient and precise production of sRNA. DRBs are characterized by two conserved dsRNA-binding motifs (dsRBM) that are located at the N-terminus (Curtin et al., 2008). It was believed that each DCL must interact with one DRB for the production of sRNAs and that similar to the four DCL they would act redundantly (Hiraguri et al., 2005). Recent studies showed that this is not the case. DRB1 seems to interact exclusively with DCL1 to produce miRNAs, whereas DRB4 interacts with DCL4 to promote the production of 21 nt siRNAs from viral or hairpin-RNA (Curtin et al., 2008). DRB4 is additionally involved in defence against pathogens (Zhu et al., 2013). Both are localized in the nucleus, in contrast to DRB2, which seems to locate in the cytoplasm (Curtin et al., 2008). By the generation of a triple mutant it was shown that DRB2, DRB3 and DRB5 are not involved in the general production of sRNAs and that none of them interact with DCL2 or DCL3. The high sequence similarity and their overlapping localization to the shoot apical meristem (SAM) region suggest a functional redundancy, possibly in an unknown developmental pathway (Curtin et al., 2008). Although their exact function remain to be elucidated, there are hints that DRB2, DRB3 and DRB5 could be involved in a non-canonical miRNA pathway and that they might play important roles under stress conditions (Eamens et al., 2012b; Sawano et al., 2017).

1.3 RNA trafficking during RNAi-based plant protection

The efficient gene silencing in the pathogen via HIGS relies on the production and transport of enough siRNAs between the two organisms. Accordingly, it was originally speculated that HIGS cannot function against necrotrophic fungi as their lifestyle includes the immediate destruction of the host tissue what could negatively impact the plants ability to provide sufficient amounts of siRNAs. Nevertheless, several studies have shown that HIGS can protect host plants from infection by necrotrophic fungi such as *Fg*, *Sclerotinia*, *Botrytis* and others (Andrade et al., 2016; Koch et al., 2013; Wang et al., 2016; Zhou et al., 2016). In contrast to

insects (Zhang et al., 2017), nematodes (Lilley et al., 2012) as well as parasitic plants (Alakonya et al., 2012), it is virtually unresolved how RNAs cross the plant fungal interface. Several studies have shown that siRNAs as well as dsRNA can be taken up efficiently by fungi (Jöchl et al., 2009; Khatri and Rajam, 2007; Koch et al., 2016; Majumdar et al., 2017; Wang et al., 2016). In *Aspergillus*, significant uptake of siRNAs was proven by *in vitro* incubation with siRNAs what resulted in specific gene silencing (Jöchl et al., 2009; Khatri and Rajam, 2007). External application of siRNAs and dsRNAs protected plants from infection by *Botrytis cinerea* also suggesting an efficient RNA uptake (Wang et al., 2016). However, until now it is unclear whether only siRNAs and/or dsRNAs are transported and consequently whether intact RNAi machineries of both organisms are required. In the SIGS process applied to control *Fg* the long CYP3RNA precursor was transported into the fungus and an intact fungal RNAi machinery, in this case DCL1, is required for effective gene silencing and disease control (Koch et al., 2016). There exist different theories how RNAs could be transported from plant into fungal cells including the transfer via plant extracellular vesicles or via specific transporters (Koch and Kogel, 2014; Majumdar et al., 2017). During HIGS against insects, the plant originating dsRNA is imported into insect cells through feeding on the plant (Zhang et al., 2017). It is likely that this process is enabled by homologs of the dsRNA transport protein Systemic RNA interference deficient (SID), that has been originally identified in *Caenorhabditis elegans* and recently described to selectively bind long dsRNA (Li et al., 2015). Expression of SID-1 in *Drosophila* S2 cells enables passive uptake of dsRNA from the culture medium (Shih and Hunter, 2011). Homologs of SID or similar RNA transporters have not been discovered in fungi until now.

The second hypothesis is the incorporation and transfer of siRNAs via plant extracellular vesicles, in mammalian cells known as exosomes. Several studies provide evidence that vesicle-mediated transfer of sRNAs takes place in fungi and that these vesicles can be taken up by host cells (Peres da Silva et al., 2015). In great support to this finding, Weiberg et al. identified small RNAs from the necrotrophic fungus *Botrytis cinerea* that silence genes in host plants (Weiberg et al., 2013) and that could be possibly transported via vesicles. Recently, it was shown that plant pathogenic bacteria as well as nematodes release vesicles that modulate plant immunity (Katsir and Bahar, 2017; Quintana et al., 2017). A lot of information is available on vesicle-mediated RNA communication between animals and different pathogens (Buck et al., 2014; Zhu et al., 2016). There exist studies showing that plant-derived miRNAs are transferred to animals, viruses as well as mammals and that they are able to regulate expression of target genes (Han and Luan, 2015; Zhang et al., 2012). It was often postulated but until now there is

lacking evidence that plant-derived vesicles transmit RNAs to pathogenic fungi (Koch and Kogel, 2014; Majumdar et al., 2017).

1.3.1 Exosomes and plant extracellular vesicles

The study of extracellular vesicles (EVs) has largely focused on mammalian systems and only few studies describe exosome biogenesis in typical model organisms like *Caenorhabditis elegans* (Liegeois et al., 2006) and *Drosophila* (Gross et al., 2012). First declined as waste delivery system, extracellular vesicles have emerged as key players in intercellular communication by shuttling various biological signals including sRNAs between cells and as diagnostic biomarkers for diverse diseases (Skog et al., 2014). Exosomes are defined as endosome originating vesicles of 40-150 nm in diameter (Kalluri, 2016). They are released as consequence of fusion of multivesicular bodies (MVBs) with the plasma membrane (Colombo et al., 2014; Crescitelli et al., 2013; Johnstone et al., 1987). Though the nomenclature of extracellular vesicles is still under consideration, it can be distinguished beside exosomes between apoptotic bodies with diameters of 800-5000 nm that are released by apoptotic cells and microvesicles within a size range of 150-1000 nm that are shed from the plasma membrane (Gould and Raposo, 2013). Exosomes have been routinely isolated from the cell culture supernatant of different mammalian cell lines as well as from various body fluids like blood (Caby et al., 2005), breast milk (Admyre et al., 2007), urine (Pisitkun et al., 2004) and saliva (Kim et al., 2017). Despite the fact that already 50 years ago it was proposed for higher plants that the fusion of MVBs with the plasma membrane (PM) results in the release of small vesicles into the extracellular space, the research on plant extracellular vesicles is an emerging field (Halperin and Jensen, 1967). Studies using transmission electron microscopy (TEM) showed that MVBs proliferate in barley next to papillae during pathogen attack. These MVBs would be able to release their vesicles into the paramural space what led to the speculation that exosomes exist in plants (An et al., 2006b). Plant exosomes are speculated to function in the transport of defence compounds into the extracellular space, supported by the observation that both, hydrogen peroxide and callose could be identified inside MVBs next to the PM (An et al., 2006b; Xu and Mendgen, 1994). Moreover, vesicles were identified by TEM in the extrahaustorial matrix of powdery mildew, favouring the idea of an exosome-mediated secretion pathway of fungal effectors. Due to the fact that they failed to identify whether these vesicles are of fungal or plant origin, also the reciprocal transport would be conceivable (Micali et al., 2011). Ultrastructural analysis of the plant – powdery mildew interface shows vesicles not only in the extrahaustorial matrix but also in the paramural space as well as inside papillae of attacked host cells. Altogether these facts strengthen the hypothesis that vesicle secretion

from both organism takes place at the plant – fungus interface (An et al., 2006a; Hückelhoven and Panstruga, 2011). Attempts to isolate plant exosomes were performed on fruits and vegetables as well as from the apoplast of sunflower seeds. In all cases exosome-like particles containing protein and RNA cargo could be identified (Mu et al., 2014; Regente et al., 2009). Recently, Rutter and Innes isolated, for the first time, extracellular vesicles (EVs) of endosomal origin from the apoplast of intact *Arabidopsis* leaves, indicating the existence of exosomes in plants. The EV proteome was enriched for proteins involved in abiotic and biotic stress responses as well as defence-related proteins. This leads together with the observation that vesicle proliferation is enhanced during pathogen attack to the suggestion that EVs play important roles during plant immune responses and contribute to intercellular communication like in animals (Rutter and Innes, 2017).

1.3.2 RNA long-distance trafficking in plants

One key feature of plant RNAi is that RNA silencing is mobile. The silencing signal can travel over long distances and trigger silencing in distant plant tissues (Melnyk et al., 2011). It has been shown by grafting experiments that siRNAs are detectable in tissues of DICER mutants that are defective for siRNA biogenesis (Molnar et al., 2010). This led to the speculation that siRNAs and not their precursors are the mobile silencing signals (Dunoyer et al., 2013). Whereas cell-to-cell movement occurs through plasmodesmata, the systemic movement of a silencing signal involves the vascular system comprising phloem and xylem (Brosnan and Voinnet, 2011; Lough and Lucas, 2006). It is likely that the phloem rather than the xylem is involved as there exist studies suggesting that xylem sap is free of RNA (Buhtz et al., 2008). The direct sampling of phloem sap from several plant species revealed a population of sRNAs further supporting the idea that sRNAs contribute to long distance signaling (Yoo et al., 2004). However, until now the molecular forms of mobile RNAs are not resolved (Parent et al., 2012). In general, long distance transport of RNAs through the phloem appears to be mediated by RNA-binding proteins (RBPs). The first phloem RPB, PHLOEM PROTEIN16 (PP16), was characterized in pumpkin as homologue of viral movement proteins (Xoconostle-Cázares et al., 1999). Later, another 50 kDa pumpkin phloem RNA-binding protein (RBP50) was identified that interacts with PP16 and other proteins in ribonucleoprotein complexes. The protein translocated from source to sink and possess a specificity for transcripts containing polypyrimidine tract binding motifs (Ham et al., 2009).

Besides being a question of basic research, the elucidation of RNA long-distance trafficking will also have a practical application in crop protection. RNAi-based plant protection strategies like HIGS and SIGS arise questions about amplification and transport of the silencing signal in

the plant. Local spraying of barley leaves with a dsRNA targeting the *CYP51* genes of *Fg* protected distant leave parts from infection, suggesting a systemic transport of either the precursor or siRNAs. Microscopic analysis with labeled RNA revealed that the long precursor is transported into the fungus, supporting the idea of dsRNA as mobile silencing signals (Koch et al., 2016). The same is true for HIGS against insects where dsRNA is taken up upon feeding on the plant (Abdellatef et al., 2015). In contrast, whether dsRNA also contributes to gene silencing during HIGS against fungi or whether only siRNAs are transported into fungal cells where they provoke silencing is unresolved. Accordingly also the nature of mobile silencing signals in the plant itself is unresolved (Koch and Kogel, 2014; Majumdar et al., 2017).

1.4   Aim of the study

Recently, it was shown that CYP3RNA targeting the three *CYP51* genes of the necrotrophic fungus *Fg*, limits fungal growth on leaves in HIGS as well as SIGS approaches (Koch et al., 2013; Koch et al., 2016). Whether targeting all *FgCYP51* genes at once is necessary to control fungal infection was unclear and is explained by the fact that *FgCYP51* gene functions are only partly resolved. This study aims to answer this question by the creation of different CYP3RNA-based dsRNA constructs targeting a single or two *FgCYP51* genes. The analysis of these constructs with different dsRNA delivery strategies (HIGS, SIGS) in different plant species (*Arabidopsis*, barley) could further elucidate possible mechanistic differences between these approaches. Furthermore, it was assessed whether gene silencing efficiency of individual *FgCYP51* genes is influenced by the length of the dsRNA precursor by creating constructs from 400 bp to over 1000 bp. Due to unpublished sequencing data gained from CYP3RNA expressing plants, it was known that most siRNAs originated from the *FgCYP51A* fragment of the precursor (Fig. 3), clarifying that further research is needed concerning the design of HIGS respectively SIGS constructs. To assess whether this was caused by positional and/or sequence based effects, different CYP3RNA based constructs were created. Different approaches included, changing positions of the individual target sequences of *FgCYP51A*, *FgCYP51B* and *FgCYP51C*, cloning of the peak hot-spot of *FgCYP51A*, changing positions of the dsRNA in the original target mRNA (5' vs. 3') as well multiplication of single constructs containing three times the same target sequence. All approaches aim to characterize whether gene silencing effectivity is influenced by the design of the dsRNA, what is until now virtually unresolved for RNAi-based plant protection approaches. All constructs were assessed by transgenic expression of dsRNAs in *Arabidopsis thaliana* (*At*) as well as partly in barley *Hordeum vulgare* (*Hv*).

It is clear that efficiency of gene silencing depends on the number of functional siRNAs in the fungus. How and which silencing signals, so whether siRNAs and/or dsRNA precursors, are

transferred from plant into fungal cells is unclear. Hypothesis include amongst others a vesicle based transport mechanism of siRNAs. To prove this, a method for the isolation of exosome-like nanoparticles was established for *Arabidopsis* as well as barley and combined with RNA sequencing.

Another open question is how transgenically expressed dsRNAs and/or siRNAs are transported in the plant itself. Long distance transport is probably mediated through the phloem and assisted by RNA-binding proteins. Due to missing knowledge about phloem RBPs from *Arabidopsis*, RBPs from other species were assessed in this study. Best studied phloem RNA binding proteins are PP16 and RBP50 from *Cucurbita maxima*. These proteins were cloned and together with CYP3RNA expressed in *Arabidopsis*. By co-RNA-Immunoprecipitation and RNA sequencing, it should be assessed whether these two proteins bind CYP3RNA-originating siRNAs, which would suggest a phloem based siRNA transport. Additionally, the five DRBs from *Arabidopsis* were cloned and assessed similarly. DRB-bound siRNAs could give further inside into the procession mechanism of transgenic dsRNA and involvement of different RNA binding proteins. The functions of the five *At*DRBs are only partly resolved. Involvement of them in RNAi-based plant protection could clarify new DRB functions and help to understand procession mechanisms of transgenically expressed dsRNA.
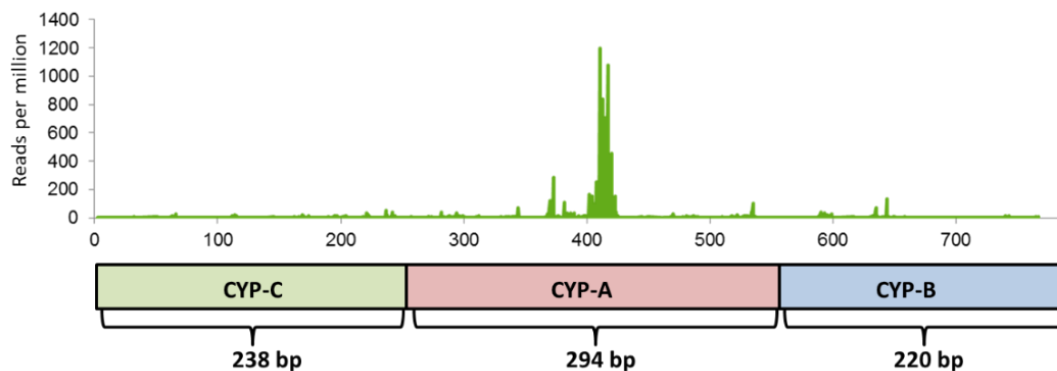
Fig. 3 RNA sequencing of CYP3RNA-expressing *Arabidopsis thaliana* plants. CYP3RNA originating antisense siRNA hits are shown as reads per million. Below CYP3RNA precursor and lengths of the individual target sequences of *FgCYP51A*, *FgCYP51B* and *FgCYP51C* are shown (unpublished data).

2.   Material and Methods

2.1   Material

2.1.1   Plant material and growth conditions

All transformations of *Arabidopsis* were done in the Col-0 Köln background. Seeds from *Arabidopsis* CYP3RNA plants were obtained from previous studies (Koch et al., 2013) and used in T3 generation. Transformations of barley (*Hordeum vulgare*) were done in the Golden Promise background. Other mutant lines from *Arabidopsis* that were used in this study are listed below (Tab. 1).

Tab. 1 Plant material and mutants that were used in this study.

Mutant	Mutant allele	Stock number	Disposition
DRB1	drb1	Salk_064863, N859864	DRB immunoprecipitation (IP)
DRB2	drb2	N433321 GK-348A09	DRB IP
DRB3	drb3	Salk_003331, N503331	DRB IP
DRB4	drb4	Salk_000736, N9970	DRB IP
DRB5	drb5	Salk_031307C, N656337	DRB IP
#41	CYP3RNA	L19 P1 T3	(Koch et al., 2013)

Arabidopsis Col-0 wt and transgenic *Arabidopsis* plants were grown in a climate chamber with 8 h photoperiod at 22°C with 60% relative humidity. For floral dip transformation of *Arabidopsis,* flowering was induced by switching to 16 h photoperiod at 22°C with 60% relative humidity.

Barley cv. Golden Promise and transgenic barley plants were grown in a climate chamber with a 16 h photoperiod at 22°C with 60% relative humidity.

Nicotiana benthamiana (*Nb*) was grown at 24°C with 16 h photoperiod and 70% relative humidity.

2.1.2   Fungi and bacteria material

Fungal and bacterial strains used in this study are listed below (Tab. 2). *Escherichia coli* (*E. coli*) was grown at 37°C on lysogeny broth (LB) agar plates or as LB liquid culture. *Agrobacterium tumefaciens* was grown at 28°C on yeast extract broth (YEB) agar plates or as liquid culture.

Fusarium graminearum (*Fg*) was grown on synthetic nutrient-poor (SNA) agar plates at 25°C with 12 h photoperiod in an incubator (BINDER, Germany).

Tab. 2 Bacterial strains that were used in this study.

Organism	Strain	Disposition
Escherichia coli	DH5α	cloning
Escherichia coli	Xl1 blue	cloning
Agrobacterium tumefaciens	AGL1	Transformation of *Arabidopsis* and *Hv*
Agrobacterium tumefaciens	GV3101	Protein expression in *Nb*
Fusarium graminearum (Fg)	IFA65	Plant infection assays

2.1.3 Plasmids

Tab. 3 List of plasmids used in this study.

Plasmid	Company/Reference	Disposition
pGEM-T	Promega	stacking of CYP51 constructs
p7U10 RNAi	DNA cloning service	*Arabidopsis* transformation for HIGS
p7i-Ubi-RNAi2	DNA cloning service	*Hv* transformation for HIGS
p6i	DNA cloning service	*Hv* transformation for HIGS
pAUL17	(Lyska et al., 2013)	expression of RBPs in *Arabidopsis* and *Nb*
pAUL1	(Lyska et al., 2013)	expression of RBPs in *Arabidopsis* and *Nb*
pAUL19	(Lyska et al., 2013)	expression of RBPs in *Arabidopsis* and *Nb*
pDONR™/Zeo	ThermoScientific	Gateway cloning

2.1.4 Primers

All Primers were purchased from Eurofins Scientific.

Tab. 4 List of primers used in this study

No.	Primer name	Primer sequence	Application
1	Cyp51A(HindIII)_fw	ATTTAAAGCTTCGGTCCATTGACAATCCCCGT	Cloning CYP-A
2	Cyp51A(XmaI)_rev	ATTTACCCGGGGCAGCAAACTCGGCAGTGAG	Cloning CYP-A
3	Cyp51B(HindII)_fw	ATTTAAAGCTTCAGCAAGTTTGACGAGTC	Cloning CYP-B
4	Cyp51B(XmaI)_rev	ATTTACCCGGGAGAGTTCATAAGGTGCTTCA	Cloning CYP-B
5	Cyp51C(HindIII)_fw	ATTTAAAGCTTATTGGAAGCACCGTACAAT	Cloning CYP-C
6	Cyp51C(XmaI)_rev	ATTTACCCGGGCATTGGAGCAGTCATAAACAA	Cloning CYP-C
7	CYP51A4_F	CCTTTGGTGCCGGTAGACAT	qRT-PCR *FgCYP51A*
8	CYP51A4_R	CCCATCGAATAAACGCAG GC	qRT-PCR *FgCYP51A*
9	CYP51B_F	TCTACACCGTTCTCACTACTCC	qRT-PCR *FgCYP51B*
10	CYP51B_R	GCTTCTCTTGAAGTAATCGC	qRT-PCR *FgCYP51B*
11	CYP51C2_F	CGAGTCCCTGGCACTGAATG	qRT-PCR *FgCYP51C*
12	CYP51C2_R	GCTCATCACCCCAAAACCGT	qRT-PCR *FgCYP51C*
13	EF1a_F	CAAGGCCGTCGAGAAGTCCAC	qRT-PCR *Fg*
14	EF1a_R	TGCCAACATGATCATTTCGTCGTA	qRT-PCR *Fg*

No.	Primer name	Primer sequence	Application
15	Cyp51A(T7)_fw	TAATACGACTCACTATAGGGCGGTCCATTGACAATCCCCG	dsRNA synthesis
16	Cyp51A(T7)_rev	AATACGACTCACTATAGGGCATTGGAGCAGTCATAAACAA	dsRNA synthesis
17	Cyp51B(T7)_fw	TAATACGACTCACTATAGGGCAGCAAGTTTGACGAGTC	dsRNA synthesis
18	Cyp51B(T7)_rev	TAATACGACTCACTATAGGGAGAGTTCATAAGGTGCTTCA	dsRNA synthesis
19	Cyp51C(T7)_fw	TAATACGACTCACTATAGGGATTGGAAGCACCGTACAAT	dsRNA synthesis
20	Cyp51C(T7)_rev	TAATACGACTCACTATAGGGCATTGGAGCAGTCATAAACA	dsRNA synthesis
21	Ubideg60_fw	ACCCTCGCCGACTACAACAT	qRT-PCR barley
22	Ubideg60_fw	CAGTAGTGGCGGTCGAAGTG	qRT-PCR barley
23	Ubi4_F	GCTTGGAGTCCTGCTTGGACG	qRT-PCR *Arabidopsis*
24	Ubi4_R	CGCAGTTAAGAGGACTGTCCGGC	qRT-PCR *Arabidopsis*
25	qCYPA_trans_F1	TGGCCTTACGCAAAAAGCAC	expression CYP-A
26	qCYPA_trans_R1	CGATGGTGCTAGTTCTGCCA	expression CYP-A
27	qCYPB_trans_F1	CCTCGATATGGGCTTCACCC	expression CYP-B
28	qCYPB_trans_R1	CGGATTCGTTGTTGCCCTTG	expression CYP-B
29	qCYPC_trans_F1	ACGGCGACTGCTTTACCTTT	expression CYP-C
30	qCYPC_trans_R1	TTCCCATAAACGTCCTCGGC	expression CYP-C
31	CYPA_F_full	ATAAT AAGCTT TTCCATCTACTCATCTATCCCTTATG	Cloning CYP-A_f
33	CYPA_R_full	ATAAT CCCGGG TATCTTCTTCCTACGCTCCCATC	Cloning CYP-A_f
34	CYPA_F_500bp	ATAAT AAGCTT GGATGCCAATGCAGAAGAAGTTTAC	Cloning CYP-A_500
35	CYPA_R_500bp	ATAAT CCCGGG TGGCTATCATATCAGTACCATCTTC	Cloning CYP-A_500
36	CYPA_R_800bp	ATAAT CCCGGG GCAGGATTGAGTGGATGGAAGAG	Cloning CYP-A_800
37	CYPB_F_full	ATAAT AAGCTT GGTCTCCTTCAAGAACTGGCGGG	Cloning CYP-B_f
38	CYPB_R_full	ATAAT CCCGGG CTGGCGTCGCTCCCAGTGAATG	Cloning CYP-B_f
39	CYPB_F_400bp:	ATAAT AAGCTT GCATTGCCGATATCCCCAAGAAG	Cloning CYP-B_400
40	CYPB_R_400bp:	ATAAT CCCGGG CATGAGCTGGTGGAAGAAGAAGAG	Cloning CYP-B_400
41	CYPB_F_800bp:	ATAAT AAGCTT GAGATCTACACCGTTCTCACTACTC	Cloning CYP-B_800
42	CYPB_R_800bp:	ATAAT CCCGGG ACGGGCATGGGAGACTTGACG	Cloning CYP-B_800
43	CYPC_F_full	ATAAT AAGCTT GAATCGCTCTACGAGACTCTGC	Cloning CYP-C_f
44	CYPC_R_full	ATAAT CCCGGG TTCTACTGTCTCGCGTCGACGC	Cloning CYP-C_f
45	CYPC_F_400bp:	ATAAT AAGCTT CGTTGTATTCCATATCTTCCCCTTC	Cloning CYP-C_400
46	CYPC_R_400bp:	ATAAT CCCGGG GATTCCTGTGTCACCCTTGAAG	Cloning CYP-C_400
47	CYPC_R_800bp	ATAAT CCCGGG GAAGCCAAGCACCACTAACAGC	Cloning CYP-C_800
48	CYPB_fw	CAGCAAGTTTGACGAGTC	Cloning CYP-ABC
49	CYPB_rev	AGAGTTCATAAGGTGCTTCA	Cloning CYP-ABC
50	CYPA_fw(AatII)	ATTTAGACGTCCGGTCCATTGACAATCCCCGT	Cloning CYP-ABC
51	CYPA_rev(NcoI)	ATTTACCATGGGCAGCAAACTCGGCAGTGAG	Cloning CYP-ABC
52	CYPC_fw((BcuI/SpeI)	ATTTAACTAGTATTGGAAGCACCGTACAAT	Cloning CYP-ABC
53	CYPC_rev(SacI)	ATTTAGAGCTCCATTGGAGCAGTCATAAACAA	Cloning CYP-ABC
54	CYPA_fw(SacI)	ATTTAGAGCTCCGGTCCATTGACAATCCCCGT	Cloning CYP-BCA
55	CYPA_rev(NsiI)	ATTTAATGCATGCAGCAAACTCGGCAGTGAG	Cloning CYP-BCA
56	HS_F_CYPA(HindIII)	ATTTAAAGCTTCGCAAAAAGCACTCGAGTC	Cloning CYP-HSA

No.	Primer name	Primer sequence	Application
57	HS_R_CYPA(XmaI)	ATTTACCCGGGTCGATGGTGCTAGTTCTGC	Cloning CYP-HSA
58	5prime_F_CYPA:	ATTTAAAGCTTTTCCATCTACTCATCTATCCCTTATG	Cloning CYP-A5'
59	5prime_R_CYPA:	ATTTACCCGGGATTGGCATCCTGGAGGCGAC	Cloning CYP-A5'
60	5prime_F_CYPB:	ATTTAAAGCTTGGTCTCCTTCAAGAACTGGCGGG	Cloning CYP-B5'
61	5prime_R_CYPB:	ATTTACCCGGGTGGGGGGGTCCATTCCGTATG	Cloning CYP-B5'
62	middle_F_CYPC:	ATTTAAAGCTTGATGATGGCTTCCAACCCATTA	Cloning CYP-Cmiddle'
63	middle_R_CYPC:	ATTTACCCGGG GGATAGCAATCAACATACGCG	Cloning CYP-Cmiddle'
64	CYPA_F(AatII+HindIII)	ATTTAGACGTCAAGCTTCGGTCCATTGACAATCCCCGT	Cloning CYP-AAA
65	CYPA_R(NcoI)	ATTTACCATGGGCAGCAAACTCGGCAGTGAG	Cloning CYP-AAA
66	CYPA_F_SpeI:	ATTTAACTAGTCGGTCCATTGACAATCCCCGT	Cloning CYP-AAA
67	CYPA_R_SacI+XmaI:	ATTTAGAGCTC CCCGGG GCAGCAAACTCGGCAGTGAG	Cloning CYP-AAA
68	CYPB_F_AatII+HindIII:	ATTTAGACGTCAAGCTTCAGCAAGTTTGACGAGTC	Cloning CYP-BBB
69	CYPB_R_NcoI:	ATTTACCATGGAGAGTTCATAAGGTGCTTCA	Cloning CYP-BBB
70	CYPB_F_SpeI:	ATTTAACTAGTCAGCAAGTTTGACGAGTC	Cloning CYP-BBB
71	CYPB_R_SacI+XmaI:	ATTTAGAGCTCCCCGGGAGAGTTCATAAGGTGCTTCA	Cloning CYP-BBB
72	CYPC_fw:	ATTGGAAGCACCGTACAAT	Cloning CYP-CCC
73	CYPC_rev:	CATTGGAGCAGTCATAAACAA	Cloning CYP-CCC
74	CYPC_F_AatII+HindIII:	ATTTAGACGTCAAGCTTATTGGAAGCACCGTACAAT	Cloning CYP-CCC
75	CYPC_R_NcoI:	ATTTACCATGGCATTGGAGCAGTCATAAACAA	Cloning CYP-CCC
76	CYPC_F_SpeI:	ATTTAACTAGTATTGGAAGCACCGTACAAT	Cloning CYP-CCC
77	CYPC_R_SacI+XmaI:	ATTTAGAGCTCCCCGGGCATTGGAGCAGTCATAAACAA	Cloning CYP-CCC
78	AttB1_PP16_1	AAAAAGCAGGCTCCGGGATGGGAATGATGGAGGTCC	Cloning PP16 in pAUL17
79	AttB2_PP16_1	AGAAAGCTGGGTTTAGTTTTCCCATGGGTAACATCC	Cloning PP16 in pAUL17
80	AttB1_RBP50_1	AAAAAGCAGGCTCCACTGAACCCTCAAAGGTTATTC	Cloning PP16 in pAUL17
81	AttB2_RBP50_1	AGAAAGCTGGGTTCATATACTCTGCAGCTGGGAAAAC	Cloning PP16 in pAUL17
82	AttB1_RBP50_2	AAAAAGCAGGCTCCACCATGACTGAACCCTCAAAGGTTATTC	Cloning PP16 in pAUL1
83	AttB2_RBP50_2	AGAAAGCTGGGTCTATACTCTGCAGCTGGGAAAAC	Cloning PP16 in pAUL1
84	DRB1_AttB1	AA AAAGCAGGCTCCACCTCCACTGATGTTTCCTCTG	Cloning DRB1 in pAUL17
85	DRB1_AttB2	A GAAAGCTGGGTTTATGCGTGGCTTGCTTCTGT	Cloning DRB1 in pAUL17
86	DRB2_AttB1	AAAAAGCAGGCTCCTATAAGAACCAGCTACAAGAGTTG	Cloning DRB2 in pAUL17
87	DRB2_AttB2	AGAAAGCTGG GTTCAGATCTTTAGGTTCTCCAG	Cloning DRB2 in pAUL17
88	DRB3_AttB1	AA AAAGCAGGCTCCTATAAGAATCAGTTGCAAGAGC	Cloning DRB3 in pAUL17
89	DRB3_AttB2	A GAAAGCTGGGTCTAATTTGGTAATGACTTCTTCTC	Cloning DRB3 in pAUL17
90	DRB4_AttB1	AAAAAGCAGGCTCCGATCATGTATACAAAGGTCAACTG	Cloning DRB4 in pAUL17
91	DRB4_AttB2	AGAAAGCTGGGTTTATGGCTTCACAAGACGATA	Cloning DRB4 in pAUL17
92	DRB5_AttB1	AAAAAGCAGGCTCCTATAAGAATCAGCTTCAAGAGC	Cloning DRB5 in pAUL17
93	DRB5_AttB2	A GAAAGCTGG GTCTAACTATCATGGGTTTGATCC	Cloning DRB5 in pAUL17
94	attB1_fw	GGGG ACAAGTTTGTACA	fusion of attB1 sites
95	attB2_rev	GGGGACCACTTTGTACA	fusion of attB2 sites
96	M13_fw	GTTTTCCCAGTCACGAC	sequencing/colony PCR
97	M13_rev	AACAGCTATGACCATG	sequencing/colony PCR

No.	Primer name	Primer sequence	Application
98	qCYPA-500/800_f	TTGGAAACGCAGTCGCTTAC	qRT-PCR *FgCYP51A*
99	qCYPA-500/800_r	AAGCGACGATTTTTCGACCG	qRT-PCR *FgCYP51A*
100	qCYPB-500/800_f	GGCCAGCAAGTTGGAATTGG	qRT-PCR *FgCYP51B*
101	qCYPB-500/800_r	CAATGCGGCTGTATCGAACG	qRT-PCR *FgCYP51B*
102	qCYPC-500/800_f	ATCCCACACACTGCTTTCGT	qRT-PCR *FgCYP51C*
103	qCYPC-500/800_r	TCCAGCTCCAAAGGGCAAAT	qRT-PCR *FgCYP51C*
104	qCYP-A5'_f	GCCTCACAACCGAAAACGAG	qRT-PCR *FgCYP51A*
105	qCYP-A5'_r	GGAACAGGCTGTCCGTTCTT	qRT-PCR *FgCYP51A*
106	qCYP-Cmid_f	TCAACGCCGAGGACGTTTAT	qRT-PCR *FgCYP51C*
107	qCYP-Cmid_r	CTGCACACAAGGAGGGGTTA	qRT-PCR *FgCYP51C*
108	oligo(dT)Primer	TTTTTTTTTTTTTTTTTTT	cDNA synthesis
109	random Hexamer	$d(n)_6$	cDNA synthesis

2.2   Methods

2.2.1   Polymerase chain reaction (PCR)

PCR for genotyping of transgenic *Arabidopsis* and *Hv* plants or colony PCR for selection of bacterial transformants were performed using DCS-Taq DNA Polymerase (DNA cloning service). Standard 20 µl PCR approach and temperature protocol are shown below (Tab. 5). Annealing temperature and elongation time were adjusted according to primer melting temperature and length of template respectively.

Tab. 5 Standard 20 µl PCR approach and temperature protocol for DNA amplifications with the DCS-Taq DNA Polymerase.

component	amount [µl]	temperature [°C]	time	
10x BD buffer	2	94	5 min	
dNTPs (2 mM)	2.5	94	30 sec	
MgCl$_2$	1.5	50-60	30 sec	x 30
Primer forward	10 pmol	72	1 min/kb	
Primer reverse	10 pmol	72	5 min	
DCS Taq	0.5	4	∞	
template	x µl			
ddH2O	ad 20 µl			

For vector cloning, PCR was performed with the Phusion High-Fidelity DNA polymerase (Thermo Scientific). Standard 25 µl PCR approach and temperature protocol are shown below (Tab. 6). Optional 1 µl DMSO was added to the PCR reaction. Annealing temperature and elongation time were adjusted according to primer melting temperature and length of template respectively.

Tab. 6 Standard 25 µl PCR approach and temperature protocol for DNA amplifications with the Phusion High-Fidelity DNA Polymerase.

component	amount [µl]	temperature [°C]	time	
5x HF/GC buffer	5	98	30 sec	
dNTPs (10 mM)	2	98	10 sec	
Primer forward	10 pmol	50-60	30 sec	x 35
Primer reverse	10 pmol	72	30 sec/kb	
Phusion	0.3	72	5 min	
template	x µl	4	∞	
DMSO	1 µl (optional)			
ddH$_2$O	ad 25 µl			

Before the ligation of blunt-end Phusion Polymerase amplified DNA fragments with pGEM-T (Promega), A-tailing reaction was performed with the DCS-Taq Polymerase in a standard 20 µl PCR approach (Tab. 7). A-tailing reaction was used directly for ligation.

Tab. 7 A-tailing reaction for ligation of DNA fragments with pGEMT-T.

component	amount [µl]	temperature [°C]	time
10 x BD buffer	2	72	30 min
dATPs (2 mM)	3	4	∞
MgCl$_2$	1.5		
DCS Taq	1		
Insert	ad 20 µl		

2.2.2 Vector cloning by ligation

Before ligation of CYP51 constructs with p7U10-RNAi for *Arabidopsis* transformation or p7i-Ubi-RNAi2 for *Hv* transformation, inserts were stacked into pGEM-T vector (Promega). Therefore, single dATP overhangs were generated by the DCS-Taq Polymerase (2.2.1). For restriction enzyme cloning, insert and vector were digested in a 20 µl reaction using the supplied buffers and according to the manufacturer's instructions. Restriction enzymes were obtained from New England BioLab (NEB) or Thermo Scientific. After digestion, DNA fragments were either purified or used directly for ligation.

Equimolar ratios for vector and insert were calculated with the following formula. For ligation ratios of 3:1 or 5:1 of insert to vector were used.

$$\frac{ng\ vector\ x\ size\ of\ insert\ (bp)}{size\ of\ vector\ (bp)} = ng\ insert$$

Ligation was performed for 1 h at room temperature (RT) or overnight at 4°C in a 20 µl reaction using the T4 DNA ligase from Thermo Scientifc (Tab. 8).

Tab. 8 Reaction approach for sticky-end ligation.

component	amount [µl]
10 x T4 ligase buffer	2
vector	100 ng
insert	3:1 to 5:1 ratio over vector
T4 ligase	1
ddH$_2$O	add 20 µl

2.2.3   Gateway vector cloning of RBP containing pAUL vectors

The pAUL vectors for transient expression of RBPs in *Nicotiana benthamiana* (*Nb*) or transformation of *Arabidopsis* were obtained by Gateway cloning. *Cm*RBP50, *Cm*PP16 and sequences of *At*DRB1-5 were first amplified from the respective cDNA using specific primers (Tab. 4) and inserted into pGEM-T. Afterwards attB1 and attB2 recombination sites were added using Phusion DNA Polymerase (Thermo Scientific) and specific primers (Tab. 4) by a two-step PCR protocol (2.2.1) to avoid usage of extremely long oligonucleotides. In the first step attB1/2 mini sites containing only half of the attB sites were fused in a short five cycle PCR using gene specific primers (Tab. 4). In the second PCR, these fragments were further amplified after purification by the Wizard PCR purification kit (Promega) using primer pair 94/95 (Tab. 4), that contains the 5' end of attB sites. Entry clones were obtained after BP reaction of attB site containing DNA fragments and pDONR^{TM}/Zeo (Thermo Scientific). BP reaction was performed in a 10 µl reaction overnight at RT using the supplied buffers (Tab. 9). After the reaction, BP clonase was denatured by adding 1 µl Proteinase K (Thermo Scientific) and incubation for 10 min at 37°C.

Tab. 9 BP reaction for the generation of entry clones

component	amount [µl]
5x BP clonase reaction buffer (Invitrogen^{TM})	1
attB-PCR product	150-300 ng
pDONR^{TM}/Zeo	300 ng
TE buffer	ad 10 µl

For selection of positive plasmids, 5-10 µl of BP reaction were transformed into chemically competent *E. coli* DH5α cells by heat-shock transformation (2.2.5) and plated on selective agar plates. Grown colonies were analysed by colony PCR (2.2.1) using the M13 primer pair. After re-isolation, positive plasmids were verified by enzymatic digest and sequencing (2.2.4). Afterwards LR reaction was performed in a 16 µl reaction overnight at RT (Tab. 10). Before transformation of 5-10 µl of the reaction into competent *E. coli* DH5α cells, LR clonase was denatured by adding 1 µl proteinase K (Thermo Scientific) and incubation for 10 min at 37°C.

Transformants were selected as described above and all plasmids were verified by restriction digest as well as sequencing (2.2.4) of the final destination vector.

Tab. 10 LR reaction between entry clone and destination vector.

component	amount [µl]
5x LR clonase reaction buffer (Invitrogen^{TM})	4
Entry clone	150-300 ng
Destination vector	300 ng
TE buffer	ad 16 µl

2.2.4 DNA sequencing

For sequencing, plasmid DNA was sent to LGC Genomics according to the manufacturer's instructions. DNA sequencing results were analyzed using the ApE – A plasmid Editor software.

2.2.5 Heat-shock transformation of chemically competent *Escherichia coli* cells

For the transformation of chemically competent *E. coli* DH5α or Xl1blue cells with plasmids, 100 µl cells were thawed on ice for 30 min. In the case of previously ligated plasmids or plasmids generated by Gateway cloning, 5-10 µl of the ligation respectively Gateway reaction were used. For retransformation of plasmids 50 ng DNA was used. The DNA and the cells were mixed carefully and incubated on ice for 20 min. Heat-shock was performed in a 42°C tempered water bath for 90 sec. After that, the cells were cooled on ice for 2 min and mixed with 500 µl sterile LB media. Before plating on LB-agar plates containing the appropriate antibiotics, cells were regenerated for 60 min at 37°C with agitation. The plates were incubated overnight at 37°C and growing colonies were analyzed by colony PCR (2.2.1).

2.2.6 Electroporation of *Agrobacterium tumefaciens*

For the transformation of *A. tumefaciens* AGL1 or GV3101 with plasmids, 40 µl competent cells were thawed on ice and mixed with 100 ng plasmid DNA. After that the cells were transferred to precooled cuvettes for electroporation (Bio-Rad) and pulsed twice in the Gene Pulser Xcell™ Electroporation Systems (Bio-Rad). They were cooled on ice for 5 min and resuspended in 1 ml YEB media. The cell suspension was transferred to a 1.5 ml reaction tube and incubated at 28°C for 2 h without agitation. For the selection of successfully transformed bacteria, 50-100 µl of the cell suspension were plated on YEB agar plates containing the appropriate antibiotics. Plates were incubated at 28°C for 2 days and growing colonies were analyzed by colony PCR (2.2.1)

2.2.7   Isolation of genomic DNA from plant leaves

For genotyping of transgenic *Arabidopsis* or *Hv* plants, genomic DNA was extracted with the Quick & Dirty method. Therefore, single leaves of potential transgenic plants were harvested in 2.0 ml reaction tubes, frozen in liquid nitrogen and crushed to a fine powder using tissue lyzer II (Qiagen). Then 500 µl DNA extraction buffer (200 mM Tris-HCl pH 7.5, 250 mM NaCl, 25 mM EDTA, 0.5%SDS) was added to the frozen powder, mixed vigorously and incubated for 10 min at RT. After addition of 500 µl chloroform, samples were mixed for 20 sec and centrifuged for 10 min at 13,000 xg. The upper phase was transferred to a new 1.5 ml reaction tube and DNA was precipitated by adding 500 µl isopropanol, incubation for 10 min at RT and centrifugation for 10 min at 13,000 xg. The pellet was washed with 70% EtOH and dried completely before resuspension in 30-100 µl ddH$_2$O depending on leave size.

2.2.8   RNA extraction from plant leaves

RNA extraction was performed using TRIzol (Thermo Scientific) or GENEzol (Geneaid) reagent according to the manufacturer's instructions. Leaves were grind to a fine power in liquid nitrogen with pestle and mortar or in the case of single leaves by using tissue lyzer II (Qiagen). All centrifugation steps were performed in an Eppendorf 5417R centrifuge at 4°C. For RNA extraction 1 ml TRIzol respectively GENEzol reagent was added to the frozen plant powder, resuspended by vortexing and incubated for 5 min at RT. Phase separation was performed for 20 min at 13,000 rpm. The upper phase (~ 500 µl) was transferred to a new 1.5 ml reaction tube, mixed with 500 µl isopropanol and incubated for 15 min at RT. RNA was precipitated by centrifugation at 13,000 rpm for 30 min, supernatant was removed carefully, and the pellet was washed with 1 ml ice-cold 70% EtOH. After a final centrifugation at 13,000 rpm for 5 min and removal of the supernatant, pellet was dried completely at RT. For resuspension 50 µl DEPC-ddH$_2$O was added to the pellet and incubated for 10 min at 70°C. RNA concentration was determined by using NanoDrop Spektralphotometer (Peqlab) and RNA was stored at -80°C.

2.2.9   RNA extraction for RNA sequencing

Before isolation of RNA from plant EVs, RNAse digest was performed using 0.4 ng µl^{-1} RNAse A (Thermo Scientific). Samples were incubated for 10 min at 37°C and kept on ice until proceeding with RNA extraction. RNA from plant exosome-like nanoparticles, EVs or after immunoprecipitation of RBPs was isolated using the Single Cell RNA Purification Kit (Norgen Biotek) according to the manufacturer's instructions described for cells growing in suspension. RNA concentrations were determined using the NanoDrop Spektralphotometer (Peqlab) and RNA was stored at -80°C.

2.2.10 DNAse I digest and cDNA synthesis

Before cDNA synthesis, remaining DNA was digested by DNAse I (Thermo Scientific) using RiboLock RNAse Inhibitor (Thermo Scientific) for 30 min at 37°C (Tab. 11).

Tab. 11 Reaction mixture for DNAse I digest

component	amount [µl]
10x DNAse I buffer	1 µl
RNA	1-2 µg
DNAse I	1 µl
RiboLock (40 U/µl)	0.5 µl
DEPC-ddH$_2$O	ad 10 µl

For cDNA synthesis 1 µg digested RNA was used. For pathogen assays cDNA synthesis was performed using qScript^{TM} cDNA synthesis kit (Quanta). Standard reaction approach of 20 µl is shown below (Tab. 12).

Tab. 12 Reaction assembly for cDNA synthesis using qScript^{TM} cDNA synthesis kit

component	amount [µl]	temperature [°C]	time
5x qScript reaction mix	4	22	5 min
qScript RT	1	42	40 min
RNA (DNAse digested)	1 µg (5-10 µl)	85	5 min
nuclease-free water	5-10		

cDNA synthesis for expression studies of dsRNA expressing *Arabidopsis* or barley was performed with RevertAid first strand cDNA synthesis kit (Thermo Scientifc) using OligodT and Random Hexamer Primer (Tab. 4). Standard 20 µl reaction approach is shown below (Tab. 13).

Tab. 13 Reaction assembly for cDNA synthesis using RevertAid first strand cDNA synthesis kit

component	amount [µl]	temperature [°C]	time
5x qScript reaction mix	4	22	5 min
qScript RT	1	42	60 min
RNA (DNAse digested)	1 µg (5-10 µl)	85	5 min
nuclease-free water	5-10		

Before using the cDNA for qRT-PCR, reaction was filled up to 100 µl with ddH$_2$0 and analyzed by PCR using the respective reference primer (Tab. 4).

2.2.11 Quantitative Real-Time PCR (qRT-PCR)

Quantitative Real-Time PCR (qRT-PCR) was performed with freshly synthetized cDNA (2.2.10) in the QuantStudio 5 Real-Time PCR system (Applied Biosystems) in 384-well plates using SYBR$^{®}$ green JumpStart Taq ReadyMix (Sigma-Aldrich). For each sample three replicates were performed and target transcript levels were determined via the $2^{-\Delta\Delta Ct}$ method (Livak and Schmittgen, 2001) by normalizing the amount of target transcript to the amount of reference transcript. Primers used for qRT-PCR are shown in Tab. 4.

Tab. 14 Reaction assembly and temperature protocol for qRT-PCR in 384-well plates.

component	amount [µl]	temperature [°C]	time	
SYBR$^{®}$ Mix	5	95	5 min	
Primer forward	0.25	95	30 sec	
Primer reverse	0.25	60	30 sec	x 40
cDNA	1.5 (10 ng)	72	30 sec	
ddH2O	3	4	∞	

2.2.12 *Agrobacterium tumefaciens* mediated transformation of *Arabidopsis thaliana*

Plasmids for transformation of *Arabidopsis* were introduced into the *A. tumefaciens* strain AGL1 by electroporation (2.2.6). Transformation of *Arabidopsis* was performed with the floral dip method as described (Bechtold and Pelletier, 1998) and transgenic plants were selected on ½ MS agar plates containing BASTA (7 µg/ml) or Hygromycin B (Invitrogen 50 µg/ml) depending on the vector.

2.2.13 *Agrobacterium tumefaciens* mediated transformation of barley

Plasmids for transformation of barley were introduced into the *A. tumefaciens* strain AGL1 by electroporation (2.2.6). The transformation of immature barley embryos was performed as described (Imani et al., 2011).

2.2.14 Plant infection assays and spray application of dsRNA

Fg IFA65 was grown on SNA agar plates at 22°C in an incubator (BINDER). For all leaf inoculation assays, *Fg*-IFA65 conidia concentration was adjusted to 5×10^4 macroconidia ml^{-1} in ddH$_2$0 containing 0.002% Tween-20. After inoculation, plates were stored at RT and infection symptoms were assessed at 5 dpi. To evaluate infection severity, fungal growth was determined by measuring the size of chlorotic and necrotic lesions using the ImageJ software (https://imagej.nih.gov/ij/index.html).

For the *Arabidopsis* – *Fg* infection 15 rosette leaves of ten different 5-wk-old plants of each transgenic line and control plants [Col-0 wild-type (wt)] were detached and transferred in

square petri dishes containing 1% agar. Inoculation of *Arabidopsis* was done by wound inoculation of detached leaves with 5 µl *Fg* conidia suspension on each leaf side. Wounding was performed by scratching of the leave surface with a pipette tip. At 5 dpi leaves were frozen in liquid nitrogen and subjected to RNA extraction.

For the barley – *Fg* infection ten second leaves of ten different 3-wk-old plants of each transgenic line (T1) as well as control plants (empty vector (ev)) were detached and transferred in square petri dishes containing 1% agar. Inoculation was performed by drop inoculation of 3x 20 µl *Fg* conidia suspension per leaf. The leaf surface was scraped with the pipette tip before placement of the droplet to the leaf. At 5 dpi leaves were frozen in liquid nitrogen and subjected to RNA extraction.

For spray application, dsRNA was generated using MEGAscript RNAi Kit (Invitrogen) following the manufacturer's instructions. The stacked pGEM-T clones or p7U10 plasmids containing single and double CYP51 constructs (2.2.2) or the CYP3RNA (Koch et al., 2013) were used as template. Primer pairs with T7 promoter sequences at the 5`end of both forward and reverse primers were designed for amplification of dsRNA (Tab. 4). The dsRNA, eluted in TE-Buffer (10 mM Tris-HCl pH 8.0, 1 mM EDTA), was diluted in 500 µl water to a final concentration of 20 ng µl^{-1}. For the TE-control, TE-buffer was diluted in 500 µl water corresponding to the amount that has been used for dilution of the dsRNA. Typical RNA concentration after elution was 500 ng µl^{-1}, representing a buffer concentration of 400 µM Tris-HCL and 40 µM EDTA in the final dilution. Detached barley leaves were covered before spraying with a plastic tray leaving only the upper part (approximately 1 cm) uncovered. After spraying, dishes were kept open until the surface of each leaf was dried. After 48 h, leaves were drop-inoculated as described above.

2.2.15 Isolation of exosome-like nanoparticles from *Arabidopsis thaliana*

Rosette leaves of 4-5-wk old *Arabidopsis* plants were harvested. To get the cell extract, leaves were grind with pestle and a mortar in a small amount of PBS buffer. The cell lysate was collected and stored on ice. To separate the larger particles, the cell extract was sequentially centrifuged at 1000 xg for 10 min (Eppendorf Centrifuge 5810R), 3000 xg for 20 min and 10,000 xg for 40 min at 4°C (Beckmann J2-21M/E). After the last centrifugation step the supernatant was centrifuged at 160,000 xg for 90 min in an ultracentrifuge (SW 41 Ti, Beckmann Coulter), the exosome containing pellet was resuspended in 1 ml PBS and loaded on top of a sucrose gradient (8%-/15%-/30%-/45%-/60% sucrose in 20 mM HEPES, pH 7.3). The gradient was centrifuged at 160,000 xg for 2 h and the bands between the 30%/45% and the 45%/60% layer were harvested separately. To concentrate and wash the exosome-like

nanoparticles the respective fraction was filled up to 10 ml with PBS and centrifuged again for 90 min at 160,000 xg. The pelletized vesicles were resuspended in a small amount of PBS and analyzed by transmission electron microscopy (TEM; 2.2.17) or subjected to RNA extraction (2.2.9) and RNA sequencing (2.2.18).

2.2.16 Isolation of extracellular vesicles from apoplastic washes of *Arabidopsis thaliana* and barley

For the isolation of EVs from apoplastic washes of *Arabidopsis,* a previously published protocol has been adjusted (Rutter and Innes, 2017). 5-wk-old *Arabidopsis* Col-0 wt and CYP3RNA plants (Koch et al., 2013) were harvested at the rosette and the leaves were vacuum infiltrated with vesicle isolation buffer (VIB: 20 mM MES, 2 mM CaCl$_2$ and 0.1 M NaCl, pH 6) until infiltration sites were visible as dark green spots. The infiltrated plants were drained carefully on filter paper and centrifuged in 30 ml syringes placed in 50 ml Falcons for 20 min at 700 xg and 4°C (Eppendorf Centrifuge 5810R). The resulting apoplastic fluid was filtered through 45 µm sterile filters and larger particles were separated by centrifugation at 10,000 xg for 30 min at 4°C (Eppendorf Centrifuge 5417R). The supernatant was then filled up to 10 ml with VIB and centrifuged for 1 h at 48,000 xg and 4°C (Beckmann J2-21M/E). The resulting pellet containing EVs was washed with 10 ml PBS before resuspension of the vesicles in a small amount of PBS and analysis by TEM or proceeding with RNA extraction (2.2.9) and RNA sequencing (2.2.18).

For the isolation of EVs from apoplastic washes of barley, leaves were pretreated with CYP3RNA as described (Koch et al., 2016). Ten detached second leaves of 3-wk-old plants were transferred in square Petri dishes containing 1% agar. Upper leave parts were sprayed with 500 µl CYP3RNA (20 ng µl^{-1}) or TE-buffer in H$_2$O and incubated for two days at RT. Only unsprayed leave parts were harvested, washed in H$_2$O and vacuum infiltrated with VIB until infiltration sites were visible as dark green spots. The infiltrated leaves were drained carefully on filter paper and centrifuged in 30 ml syringes placed in 50 ml falcons for 30 min at 1000 xg and 4°C (Eppendorf Centrifuge 5810R). The next steps were done as described above.

2.2.17 Negative staining and transmission electron microscopy (TEM)

For TEM, formvar and carbon coated 300-mesh electron microscopy grids were glow discharged prior to sample application for 40 s. Afterwards 5 µl of plant vesicles resuspended in PBS were applied to the grids for 5 minutes. Then the fluid was drawn off using filter paper (whatman no. 4) and grids were washed three times (1 min. each) in 50 µl of 2% uranyl acetate. Finally, the solution was wicked away and the grids were air dried. Preparations were inspected

in the TEM (EM912a/b - ZEISS) at 120 kV under zero-loss conditions and images were recorded at slight underfocus using a cooled 2k x 2k slow-scan ccd camera (SharpEye / TRS) and the iTEM software package (Olympus-SIS).

2.2.18 Small RNA sequencing and bioinformatic analysis

Indexed sRNA libraries were constructed from vesicle isolated RNA (2.2.9) with the TruSeq® Small RNA Library Prep Kit for Illumina according to the manufacturer's instructions. Indexed sRNA libraries were pooled and sequenced on the Illumina HiSeq and NextSeq 500 platforms and the sequences sorted into individual datasets based on the unique indices of each sRNA library. The quality of the datasets was examined with fastqc before and after trimming. The adapters were trimmed using cutadapt (Martin, 2011) version 1.14 (Tab. 15). The trimmed reads were mapped to the CYP3RNA sequence using bowtie2 (Langmead and Salzberg, 2012) version 2.3.2. to identify siRNAs derived from the precursor sequence. The mappings were first converted into bedgraph using bedtools (Quinlan and Hall, 2010) version 2.26.0 and then to bigwig using bedGraphToBigWig (Kent et al., 2010). These files were used for visualization with IGV (Thorvaldsdóttir et al., 2013). Read coverage is defined as the number of reads that batch at a certain position of the sequence.

Tab. 15 Number of reads in datasets from small RNA sequencing of vesicle contained RNAs. Read number in million is shown before and after adapter trimming.

Dataset	No. of reads in million	No. of reads after trimming
vesicles-whole leaves (CYP)	2.3	2.2
vesicles-whole leaves (control)	5.7	5.3
vesicles apoplast (CYP)	5.4	2.4
vesicles apoplast (control)	2.9	0.8
vesicles barley (CYP)	2.8	2.6
vesicles barley (TE)	2.8	2.6

2.2.19 "Quick & Dirty" protein extraction from plant leaves

"Quick & Dirty" protein extraction was done with 4x Laemlli buffer (125 mM Tris-HCl pH 6.8, 4% SDS, 50% glycerol, 0.02% bromophenol blue). Before usage, 1 ml Laemlli buffer was heated at 95°C and mixed with 30 mg freshly weighed DTT. Approximately 50-100 mg frozen plant material were filled in a 1.5 ml reaction tube, mixed with 50-100 µl 4x Laemlli buffer and heated for 5 min at 95°C. Insoluble particles were separated at 14,000 rpm for 5 min (Eppendorf centrifuge 5417R) and the supernatant was transferred to a new 1.5 ml reaction tube. The samples were used directly for SDS-PAGE (2.2.20).

2.2.20 Sodium dodecyl sulfate polyacrylamide gel electrophoresis (SDS-PAGE)

For the separation of proteins, discontinuous polyacrylamide gels were used containing a 12% resolving gel and a 3% stacking gel. The protocol for two gels is shown below (Tab. 16). Protein extracts were mixed with 4x SDS-buffer (1M Tris pH 6.8, 80% Glycerol, 4% SDS, 0.05% bromophenol blue) and denatured in a 95°C heating block for 5 min before loading into the pockets of the SDS gel. After "Quick & Dirty" protein extraction, protein extracts were used directly. After immunoprecipitation, proteins were released by incubation in SDS-buffer at 95°C for 5 min. Separation of proteins was done at 100 V for 2 h or until the blue color of the buffer came out depending on the size of the proteins.

Tab. 16 Protocol for two 12% SDS-gels for the 1 mm BioRad Mini-Protean gel system

component	Resolving gel	Stacking gel
30% acrylamide mix	4 ml	1 ml
1.5 M Tris-HCl pH 8.8	2.5 ml	-
1 M Tris-HCl pH 6.8	-	600 µ
H_2O	3.4 ml	3.6 ml
10% SDS	100 µl	100 µl
TEMED	10 µl	10 µl
10% APS	100 µl	50 µl

2.2.21 Western Blot

For the immunodetection after separation by SDS-PAGE, proteins were transferred from the SDS gel to a PVDF membrane (Roth) by application of an electric tension. The blot was built from bottom to top by 6x whatman paper (GE Healthcare), PVDF membrane, SDS-gel, 6x whatman paper. Before, whatman paper was soaked in towbin buffer (25 mM Tris, 192 mM glycin, 20% methanol) and the PVDF membrane in methanol additionally. Electric tension of 25 V and 1.0 ampere was applied for 30 min (BioRad TransBlot Turbo) and the membrane was washed in distilled water before proceeding with the immunodetection. Optional, the membrane was stained with the ponceau reagent (1% ponceau in 5% (v/v) acetic acid) to verify successful transfer of the proteins. For immunoprecipitation experiments ponceau stained rubisco complex was used as a loading control for input samples.

2.2.22 Immunodetection

After western blot the PVDF membrane was washed 2 x with TBS-T buffer (100 mM Tris-HCl pH 7.5, 150 mM NaCl, 0.1% tween-20) and then incubated with 20 ml 5% milk powder in TBS-T for 1 h at RT or overnight at 4°C. After two additional washing steps in TBS-T, the membrane was incubated with 10 ml of a 1:8000 dilution of anti-HA high affinity 3F10 (Roche) in 1%

milk powder in TBS-T for 3 h at RT. The membrane was washed 5 x with TBS-T for 5 min before detection of bound antibodies with the Amersham ECL™ Prime western blotting detection reagent. The developing chemiluminescence was detected with the ChemiDoc XRS+ system from BioRad using the ImageLab Software.

2.2.23 Immunoprecipitation

All centrifugation steps were performed at 4°C in the Eppendorf 5417R centrifuge. For the immunoprecipitation of HA-tagged RBPs, the leaves of RBP expressing *Arabidopsis* plants (T1) were ground to a fine powder with liquid nitrogen. The proteins of 100-500 mg plant powder were extracted with 1 ml IP lysis buffer (Tab. 17) containing 40 U/ml RNAseOUT (Invitrogen), 0.5 mM PMSF and complete proteinase inhibitor cocktail (Roche). IP lysis buffer was adopted with slight changes from (Carbonell et al., 2012). Insoluble particles were separated by centrifugation at 12,000 xg for 5 min and 20 µl of the supernatant were kept as input sample. The rest was mixed with 1-2 µg anti-HA 12CA5 antibody (Roche). After 1 h incubation at 4°C on a tube rotator, 50-100 µl protein-A agarose (Roche) was added and incubated for another hour at 4°C. Agarose-antibody-protein complexes were sedimented at 12,000 xg for 1 min and washed 6x for 10 min at 4°C with 1 ml IP lysis buffer (Tab. 17). For analysis of RBP bound RNA, beads were divided after the last washing step into protein and RNA fraction. In most cases 20% of the beads were used for protein and 80% for the RNA fraction. Immunoprecipitated proteins were released by incubation with SDS buffer and heating at 95°C for 5 min, beads were separated by centrifugation and the supernatant was loaded in the pockets of a 12% SDS gels (see 2.2.20). Bound RNA was released by incubation of the beads in 0,5 volume proteinase K buffer (Tab. 17) for 15 min at 65°C. Agarose was separated by centrifugation and RNA was purified with the Single Cell RNA purification kit (Norgen Biotek).

Tab. 17 Buffers used for immunoprecipitation of RBPs

IP lysis buffer	Proteinase K buffer
50 mM Tris-HCl pH 7.4	100 mM Tris-HCl pH 7.4
100 mM KCl	10 mM EDTA
2.5 mM $MgCl_2$	300 mM NaCl
0.1% Nonidet-P40	2% SDS
	1 mg/ml Proteinase K

2.2.24 Transient expression of RBPs in *Nicotiana benthamiana*

*Cm*PP16, *Cm*RBP50 and *Arabidopsis* DRB containing pAUL17 plasmids were introduced into the *A. tumefaciens* strain GV3101 by electroporation (2.2.6). Bacterial precultures were

incubated overnight at 28°C in 5 ml YEB media containing the appropriate antibiotics (25 µg/ml Rifampicin, 25 µg/ml Gentamycin, 50 µg/ml Kanamycin). On the next day 50 ml fresh YEB media containing 200 µM acetosyringone as well as antibiotics were inoculated with the preculture and bacteria were incubated for another night at 28°C. Bacterial cells were harvested by centrifugation and washed with MES buffer (10 mM MES pH 5.7, 10 mM $MgCl_2$) before dilution of the bacteria to an OD_{600} of 0.5-1.0 in MES buffer containing 200 µM acetosyringone. The cultures were incubated for 3-4 h at RT in the dark. Protein expression in *Nb* was induced by infiltration of bacterial cultures into the leaves of 4-5-wk-old plants. Leave samples were taken 24 h and 48 h post-infiltration, frozen in liquid nitrogen and stored at -80°C. Before immunodetection of the proteins, leaves were ground to a fine powder in liquid nitrogen and proteins were extracted by the "Quick & Dirty" method (2.2.19).

2.2.25 Off-target prediction

The precursor sequences of CYP51-dsRNAs were split into k-mers of 18 bases. These sequences were mapped to the coding sequences (CDS) of *Fg* strain PH-1 (GCA_000240135.3) with Segemehl (Hoffmann et al., 2009) using the following settings: accuracy of 60, report all targets, max seed distance of 4, max e-value of 20. The hits were filtered for an edit distance of 0, 1, 2 and 3. For each sequence the mapping depth per position and edit distance was plotted with Matplotlib (Hunter, 2007; Michael DroettboomNIH et al., 2017). Furthermore, every matched CDS was annotated with PFAM domains (Eddy, 2011; Finn et al., 2016) (e-value cut-off: 10e-5) in order to enrich the annotation with further data. The results were reported as plots and a respective table containing the matching intervals and the annotation. The analysis is implemented as an internal pipeline using Nextflow (Di Tommaso et al., 2017).

2.2.26 Statistical analysis

For statistical analysis, two-tailed students t-test was performed with data gained in plant infection assays and qRT-PCR.

3. Results

3.1 Host-Induced Gene Silencing of single and double *FgCYP51* genes

3.1.1 Silencing of single and double *FgCYP51* genes in *Arabidopsis thaliana*

Previous work has shown that HIGS of all three *FgCYP51* genes by the CYP3RNA construct can reduce growth of *Fg in planta* (Koch et al., 2013). However, functions of individual *FgCYP51* genes are only partly known from studies using *Fg* deletion mutants and remain to be elucidated (Fan et al., 2013; Liu et al., 2011). In order to assess whether single and double silencing of *FgCYP51* genes can influence fungal growth in a similar way, the respective sequences of *FgCYP51A*, *FgCYP51B* and *FgCYP51C* were amplified from the CYP3RNA construct and cloned into p7U10-RNAi to obtain CYP-A, CYP-B, CYP-C, CYP-AC, CYP-BC and CYP-AB (Fig. 4). The vector contains two inverted 35S promotors that drive the constitutive expression of dsRNA.
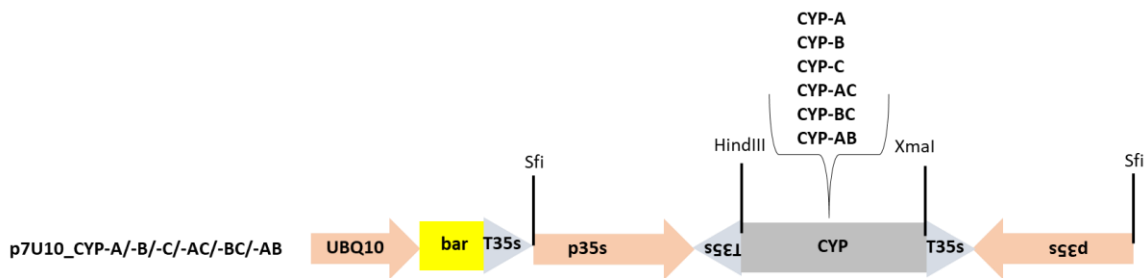

Fig. 4 Schematic representation of single and double *FgCYP51* dsRNA constructs in p7U10-RNAi. The respective target sequences of *FgCYP51A*, *FgCYP51B* and *FgCYP51C* were first arranged in the pGEM-T cloning vector and then inserted between the HindIII and XmaI restriction sites of p7U10-RNAi. UBQ10 = *Arabidopsis* ubiquitin-10 promoter, bar = bialaphos resistance, T35S = 35S terminator, p35s = 35S promotor. (Höfle et al., 2018 in revision)

To assess antifungal potential of CYP3RNA derived dsRNAs in planta, all six constructs were transformed into *Arabidopsis* Col-0 wt by the floral dip method (Bechtold and Pelletier, 1998). After ripening of the seeds, transgenic plants were selected by glufosinat resistance (BASTA) and insertion of the transgene was verified by PCR using gene specific primers. Positive plants were propagated until T2 generation and used in pathogen assays with *Fg*. For the infection assays, rosette leaves of 5-wk-old plants were wound-inoculated with a conidia suspension of *Fg* IFA65 and incubated for five days at RT. As controls Col-0 wt and CYP3RNA expressing plants were assessed. After five days typical symptoms of *Fg* infection like chlorotic and necrotic lesions were visible on wt plants. In contrast CYP3RNA plants were nearly completely resistant against *Fg* infection as seen before (Koch et al., 2013). Moreover, leaves of plants

expressing single and double CYP constructs showed only minor infection symptoms at the inoculation sites in comparison to the wt. The only exception was CYP-C where chlorotic lesions were bigger than seen for the other constructs (Fig. 5A). Analysing the size of chlorotic and necrotic lesions by ImageJ further supports a significant reduction of the infection area that was measured for all constructs except CYP-C. Infection areas were reduced from 35% for the wt to 15% for CYP-A, 12% for CYP-B, 24% for CYP-C, 13% for CYP-AC, 17% for CYP-BC, 14% for CYP-AB and 15% for CYP3RNA (Fig. 5B).

In order to prove that resistance against *Fg* was caused by downregulation of *FgCYP51* gene expression, qRT-PCRs were performed. For all constructs, expression of target genes was reduced in comparison to wt plants. Target genes of single constructs CYP-A, CYP-B and CYP-C were reduced by about 85%, 50% and 75% respectively (Fig. 5C). CYP-AC was the most efficient construct in terms of target gene silencing by reducing the expression of both target genes by at least 95%. Generally, except CYP-C, there was no clear difference in resistance enhancement as well as gene silencing efficiency between single and double constructs. Surprisingly, for all single and double constructs expression of non-target genes was reduced in a similar level explaining why all plants showed enhanced resistance against *Fg* that was comparable to the CYP3RNA plants. In contrast to the phenotype, also CYP-C caused downregulation of both non-target genes by 60% (Fig. 5). In general, the resistance enhancement of single and double CYP construct expressing plants was provoked by co-silencing of non-target *FgCYP51* genes. This further masked the influence of the individual genes on fungal growth as well as pathogenicity leaving the above asked question about *FgCYP51* gene function unresolved.
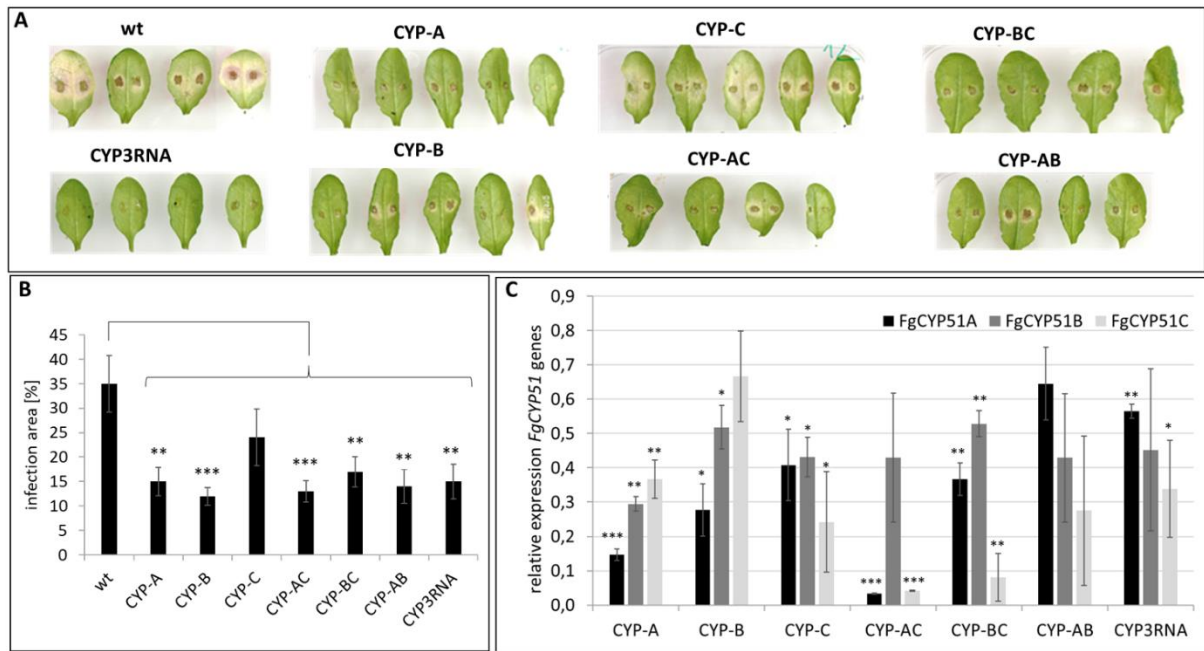
Fig. 5 Host-Induced Gene Silencing in *Fg* on leaves of transgenic *Arabidopsis* expressing single and double CYP51-dsRNA. A, fifteen detached rosette leaves of CYP51-dsRNA-expressing *Arabidopsis* plants (T2 generation) were drop-inoculated with 5 x 10⁴ conidia ml⁻¹. Infection symptoms were evaluated at 5 dpi. **B**, quantification of the visibly infected area at 5 dpi shown as percent of the total leaf area. Error bars represent SE of two independent experiments each using 15 leaves of ten different plants for each transgenic line. **C**, gene-specific expression of *FgCYP51A, FgCYP51B* and *FgCYP51C* was measured by qRT-PCR and normalized to fungal *EF1-α* (FGSG_08811) as reference gene. cDNA was generated after total RNA extraction from infected leaves at 5 dpi. The reduction in *CYP51* gene expression in the *Fg*-inoculated dsRNA-expressing leaves compared to the wt control was statistically significant. Error bars represent SD of two independent experiments each using 15 leaves of ten different plants for each transgenic line. Asterisks indicate statistical significance (*p<0.05; **p<0.01; ***p < 0.001; students t-test). (Höfle et al., 2018 in revision)

3.1.2 Bioinformatics prediction of off-targets in the *FgCYP51* genes caused by single constructs CYP-A, CYP-B and CYP-C

To further analyse and confirm off-target effects detected by qRT-PCR a bioinformatics analysis using the Segemehl software has been performed. Sequences of single constructs CYP-A, CYP-B and CYP-C were split into k-mers of 18 bp and mapped to the coding sequences of *FgCYP51A, FgCYP51B* and *FgCYP51C*. Off-targets for each single construct were predicted for siRNAs with one to maximal three mismatches. As expected each construct has a long perfect match on the corresponding CDS. Besides that, potential off-target regions with non-perfect matches could be observed (Fig. 6). CYP-A showed off-targets in *FgCYP51B* and *FgCYP51C* what correlates with the downregulation of all three genes as detected by qRT-PCR. For CYP-B off-targets were predicted only in *FgCYP51A* and for CYP-C only in *FgCYP51B* what contravenes the results of the qRT-PCR where downregulation of both non-target genes could be observed (compare Fig. 5C). One could argue that downregulation of *FgCYP51C* by

CYP-B was only minor and not significant congruent with the bioinformatics prediction (Fig. 5).
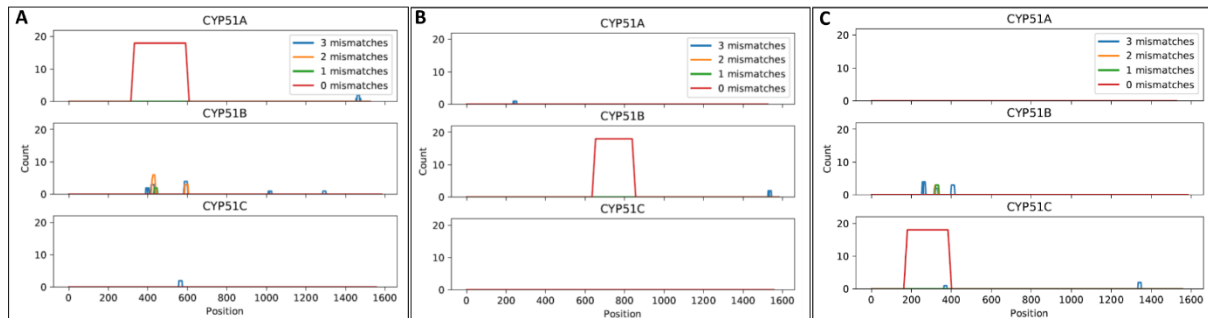
Fig. 6 Off-target prediction for single CYP51-dsRNA constructs. Sequences of CYP-A (**A**), CYP-B (**B**) and CYP-C (**C**) were split into k-mers of 18 bases. These were mapped against the corresponding coding sequences (CDS) of *FgCYP51A*, *FgCYP51B* and *FgCYP51C*. For each position within the CDS the number of k-mers (count) that match with a specified number of mismatches is plotted. (Höfle et al., 2018 in revision)

### 3.1.3 Silencing of single and double *FgCYP51* genes in barley

To assess the antifungal potential of single and double CYP constructs for plant protection, we transgenically expressed the same dsRNAs in the agronomical relevant plant *Hordeum vulgare* (*Hv*). Therefore, single and double CYP sequences were transferred to the vector p7i-Ubi-RNAi2 which contains two inverted Ubiquitin promotors. In favour of the hygromycin resistance gene, the whole cassette containing promotor as well as CYP sequences was transferred to the p6i-Ubi-RNAi2 vector using Sfi restriction sites (Fig. 7). As control, the GUS insert from p7i-Ubi-RNAi2 was transferred to p6i-Ubi-RNAi2, too. For transformation of barley embryos, the constructs were transformed in the *A. tumefaciens* strain AGL1 and confirmed by colony-PCR.
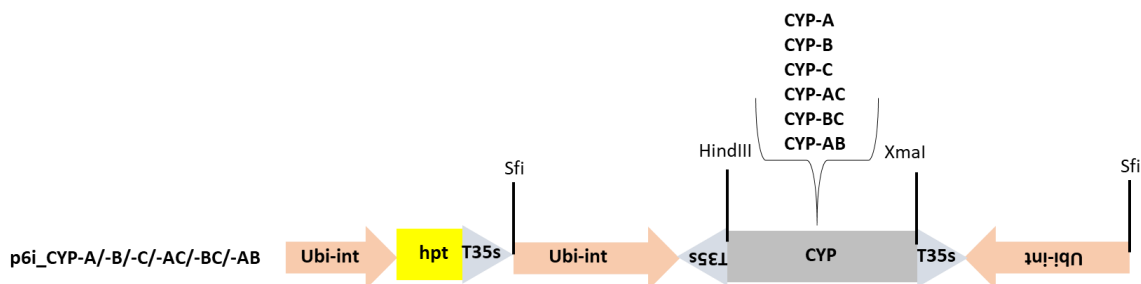
Fig. 7 Schematic representation of single and double *FgCYP51* dsRNA constructs in p6i vector. The respective target sequences of *FgCYP51A*, *FgCYP51B* and *FgCYP51C* were first inserted between HindIII and XmaI restriction sites of p7i-Ubi-RNAi2 and then transferred by Sfi restriction to p6i-Ubi-RNAi2. Ubi-int = plant ubiquitin promotor, hpt = hygromycin resistance, T35S = 35S terminator. (Höfle et al., 2018 in revision)

The transformation of barley (*Hv*) was performed as described in Imani et al., 2011. After regeneration of PCR positive plants, that integrated the transgene in their genome, expression

of the transgene was further analysed by qRT-PCR. Using construct specific primers (Tab. 4), the expression of dsRNA was determined, and best expressing plants were subjected to propagation. Seeds received from the T0 generation were then used for infection assays with *Fg*. Thereby lines were chosen based on expression analysis of the T0 generation. Again, the generated plants (T1) were tested by PCR and transgene expression was verified by qRT-PCR. Infection assays were performed on detached leaves of 3-wk-old plants that were inoculated with a conidia suspension of *Fg*. After five days necrotic lesions were visible at the inoculation sites of all leaves (Fig. 8A). Comparable to *Arabidopsis*, leaves expressing CYP-B, CYP-AC, CYP-BC and CYP-AB showed significantly reduced infection areas in comparison to the GUS-dsRNA expressing control. Infection areas were reduced from 54% for the GUS control to 33% for CYP-B and CYP-AC and to 21% and 26% for CYP-BC and CYP-AB respectively (Fig. 8B). However, and in contrast to *Arabidopsis,* leaves expressing CYP-A and CYP-C dsRNAs showed no difference in infection severity in comparison to the control. Phenotypes could be confirmed by expression analysis of the *FgCYP51* genes. CYP-A and CYP-C reduced the expression of the target genes by about 60% and 45% respectively, whereas silencing of non-target genes was in a range of 30% and lower. In contrast, CYP-B reduced the target gene expression by 40% and simultaneously expression of non-target genes was reduced by about 60% explaining why CYP-B showed a higher resistance in comparison to the other single constructs. In general infection severity seems to be reflected by the expression of *FgCYP51B* as CYP-A and CYP-C showed a higher expression as all other constructs (Fig. 8C).
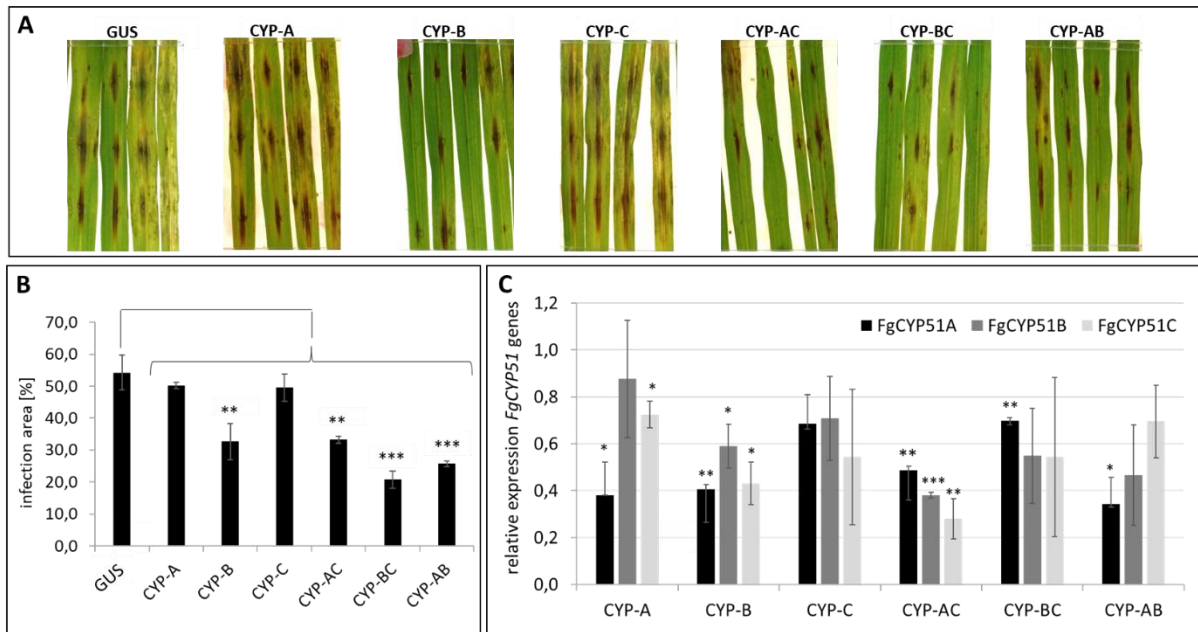
Fig. 8 *Fg* infections and Host-Induced Gene Silencing on leaves of transgenic barley lines expressing CYP51-dsRNAs. **A**, detached second leaves of 3-wk-old barley plants expressing CYP51-dsRNAs and dsRNA derived from the GUS gene sequence (GUS) were inoculated with 5×10^4 macroconidia ml^{-1}. Infection symptoms were assessed at 5 dpi. **B**, quantification of the infection area shown as percent of the total leaf area. Error bars represent SE of two independent experiments, each using ten leaves of ten different plants for each transgenic line. **C**, cDNA was generated at 5 dpi after total RNA extraction from infected leaves. Gene-specific expression of *FgCYP51A, FgCYP51B* and *FgCYP51C* was measured by qRT-PCR and normalized to fungal *EF1-α* as reference gene. Error bars represent SD of two independent experiments, each using ten leaves of ten different plants for each transgenic line. Asterisks indicate statistical significance (*p<0.05; **p<0.01; ***p < 0.001; students t-test). (Höfle et al., 2018 in revision)

3.1.4 Spray-Induced Gene Silencing of *FgCYP51* genes using single and double CYP constructs

Encouraged by the activity of single and double CYP constructs in HIGS approaches, the potential of these constructs in Spray-Induced Gene Silencing (SIGS) approaches was assessed. Earlier studies have proven that spraying of the CYP3RNA previous to *Fg* infection can confer resistance on detached barley leaves (Koch et al., 2016). To analyse whether this also holds true for single and double constructs, previously used plasmids (Fig. 4) were used for the generation of dsRNA. dsRNAs at a concentration of 20 ng µl^{-1} were sprayed on detached second leaves of 3-wk-old barley plants and after two days drop inoculated with *Fg*. As controls CYP3RNA and TE-buffer were sprayed, too. In comparison to the TE control, CYP3RNA-treated leaves showed significantly smaller lesion sizes that were reduced by over 90%. As already seen in the *Arabidopsis* HIGS approach but in clear contrast to barley HIGS plants, all single and double constructs reduced the infection area significantly by at least 80% (Fig. 9A, B). In general, resistance enhancement was more prominent than in the HIGS approaches.
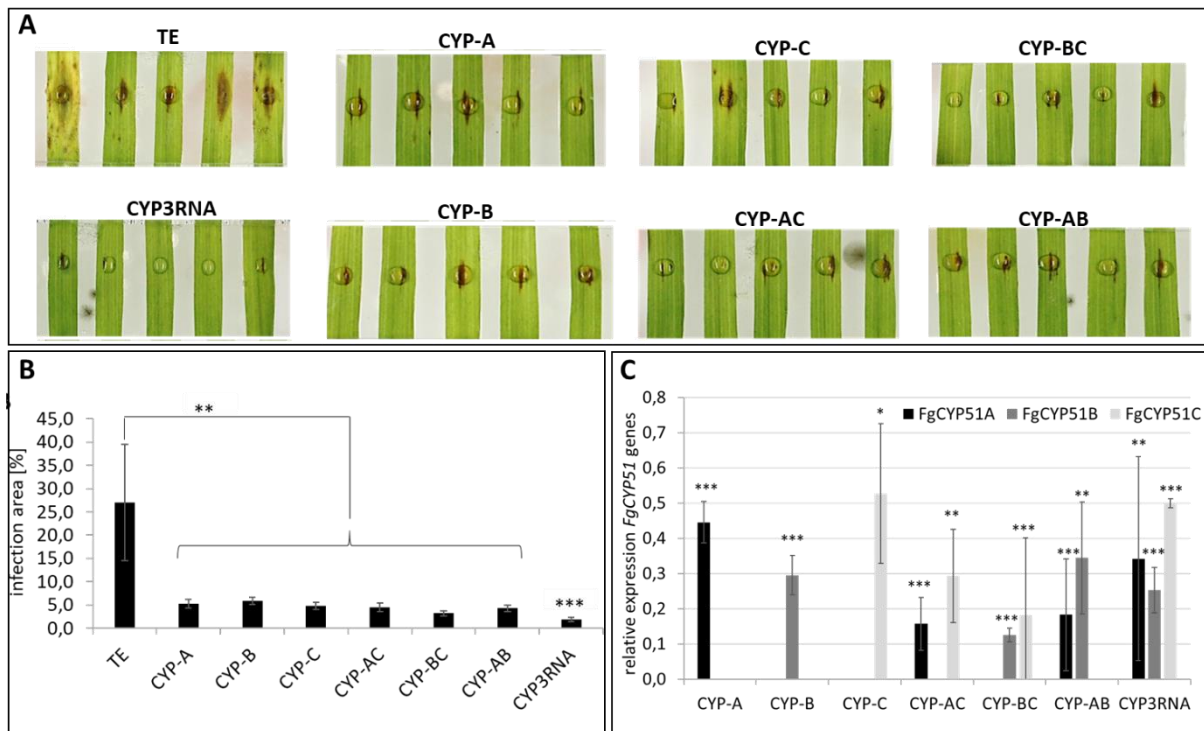
Fig. 9 Infection symptoms of *Fg* on barley leaves sprayed with CYP51-dsRNAs. A, detached leaves of 3-wk-old barley plants were sprayed with CYP51-dsRNAs or TE buffer. After 48 h, leaves were drop-inoculated with 5×10^4 conidia ml^{-1} and evaluated for infection symptoms at 5dpi. **B**, infection area, shown as percent of the total leaf area for ten leaves for each dsRNA and the TE control. Error bars indicate SE of two independent experiments. Asterisks indicate statistical significance (**p<0.01; ***p< 0.001; students t-test). **C**, gene-specific expression of *FgCYP51A, FgCYP51B* and *FgCYP51C* was measured by qRT-PCR and normalized to fungal *EF1-α* as reference gene. Detached leaves of 3-wk-old barley plants were sprayed with CYP51-dsRNA or TE buffer. After 48 h leaves were drop inoculated with 5×10^4 macroconidia ml^{-1}. cDNA was generated at 5 dpi after total RNA extraction from infected leaves. Error bars represent SD of two independent experiments. Asterisks indicate statistical significance (*p< 0.05; **p<0.01; ***p< 0.001; students t-test). (Höfle et al., 2018 in revision)

Higher resistance was caused for all construct by target gene silencing by at least 50% (Fig. 9C) as well as strong co-silencing in the range of 40% or more (Fig. 10). The only exception was CYP-AB where a high upregulation of *FgCYP51C* by over 400% occurred, which could not be explained by the observed phenotypes.
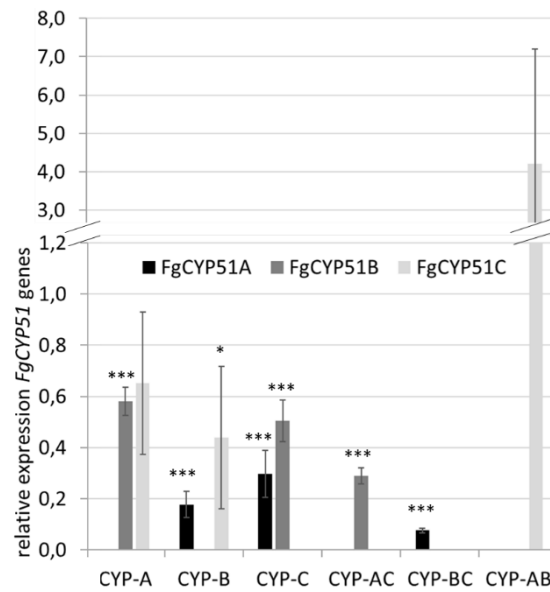
Fig. 10 Expression of non-target *FgCYP51* genes in barley leaves after spray treatment of single and double CYP dsRNAs. Gene-specific expression of *FgCYP51A, FgCYP51B* and *FgCYP51C* was measured by qRT-PCR and normalized to fungal *EF1-α* as reference gene. Detached leaves of 3-wk-old barley plants were sprayed with CYP51-dsRNA or TE buffer. After 48 h leaves were drop inoculated with 5 x 10^4 macroconidia ml^{-1}. cDNA was generated at 5 dpi after total RNA extraction from infected leaves. Error bars represent SD of two independent experiments. Asterisks indicate statistical significance (*p< 0.05; **p<0.01; ***p< 0.001; students t-test). (Höfle et al., 2018 in revision)

3.2   Efficiency analysis of dsRNAs with different lengths targeting the *FgCYP51* genes via HIGS

The above shown results prove that silencing of single *FgCYP51* genes via HIGS is possible with dsRNA constructs of about 200 bp to 300 bp in lengths. Besides, multiple off-target effects were provoked by these constructs leading to downregulation of all three *FgCYP51* genes and subsequent resistance against *Fg*. In theory, one could expect that longer precursor molecules could also be processed into a higher number of matching siRNAs resulting in stronger silencing of target genes. Additionally, and based on the results with single and double constructs, one could expect that also off-target effects are more likely with longer precursor molecules. In general, it is unknown how the length of the precursor dsRNA influences procession efficiency of siRNAs as well as amplification of the silencing signal in plants. To assess this question, dsRNA constructs of 400 bp to 500 bp and 800 bp were generated targeting single *FgCYP51* genes (CYPA-500/800, CYPB-400/800, CYPC-400/800). Additionally, the full-length cDNA of each *FgCYP51* gene (CYPA-full, CYPB-full, CYPC-full) was cloned without the start and the stop codon to avoid protein expression. The constructs were inserted into the vector p7U10-RNAi as described above (Fig. 4) and transgenic *Arabidopsis* plants were generated by the floral dip method (Bechtold and Pelletier, 1998). Cloning and plant

transformation were performed with help of Abhishek Shrestha in the context of his master thesis (Abhishek Shrestha, 2016).

After selection of transgenic plants by PCR and verification of successful transgene expression by qRT-PCR, positive lines were propagated into T2 generation. Afterwards, all constructs were tested in infection assays with *Fg*. Infection symptoms on wt leaves were visible after five days as chlorotic and necrotic lesions. Moreover, CYP51-dsRNA expressing plants showed typical symptoms of *Fg* infection at the inoculation sites (Fig. 11A). Similar to above tested single and double constructs, they were restricted to the inoculation sites and significantly smaller in comparison to wt leaves (Fig. 11B). There were no clear phenotypic differences between 400 bp and 800 bp or full-length constructs and the reduction of the infection area was for nearly all constructs in a similar extent of about 50% to 60% in comparison to the control. The only exceptions were CYPB-800 that showed a higher resistance and reduced infection area by 77% whereas CYPA-800 showed the lowest resistance by reducing infection areas by only 34%. In general resistance enhancement conferred by longer dsRNA constructs was comparable to single and double constructs that have been assessed before (compare Fig. 5 and Fig. 11). As expected resistance phenotypes were caused by target as well as non-target gene silencing of the *FgCYP51* genes (Fig. 11C). By comparing the 800 bp dsRNAs with the shorter 400 bp dsRNAs, the longer precursors showed a higher gene silencing efficiency and reduced the expression of all *FgCYP51* genes by 80% or more. For full-length constructs, only non-target gene expression could be determined because no gene specific primers, that would not also bind in the original construct sequence, were available for qRT-PCR. Silencing efficiency of non-target genes was high and over 60% in most cases. Generally, the overall gene silencing efficiency was higher than with single and double constructs that were about 200-300 bp in length (compare Fig. 5 and Fig. 11).
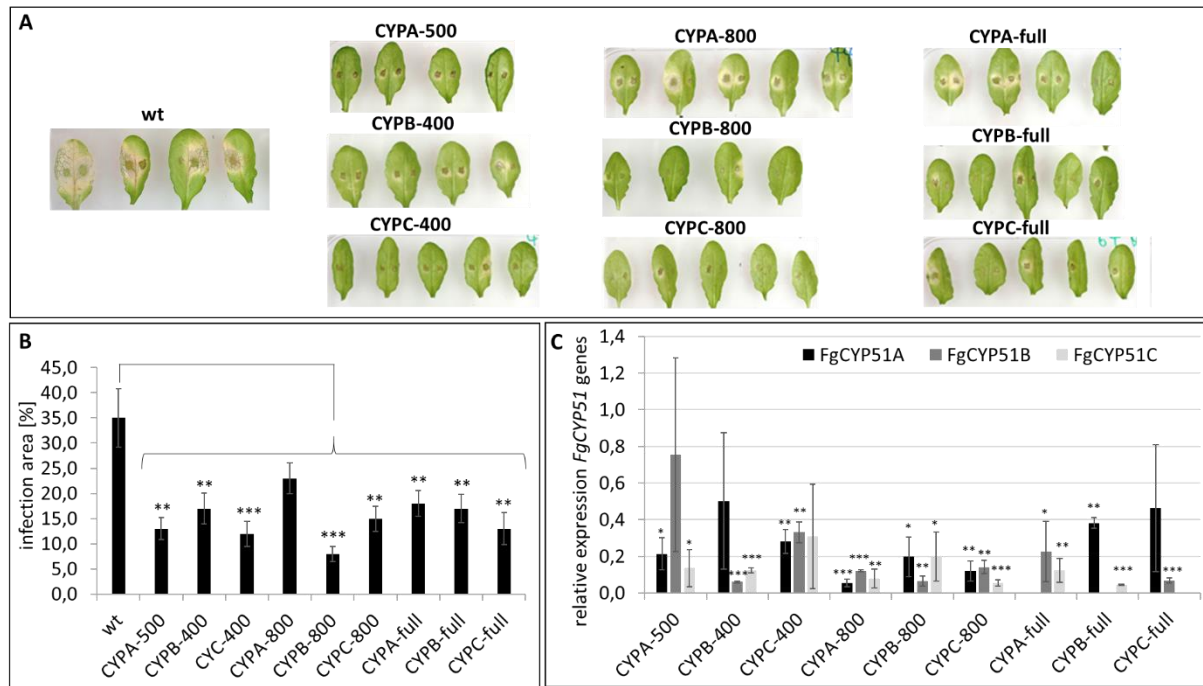
Fig. 11 Host-Induced Gene Silencing in *Fg* on leaves of transgenic *Arabidopsis* expressing CYP51-dsRNAs of different lengths. A, 15 detached rosette leaves of CYP51-dsRNA-expressing *Arabidopsis* plants (T2 generation) were drop-inoculated with 5 x 10^4 conidia ml^{-1}. Infection symptoms were evaluated at 5 dpi. **B**, quantification of the visibly infected area at 5 dpi shown as percent of the total leaf area. Error bars represent SE of two independent experiments each using 15 leaves of ten different plants for each transgenic line. **C**, gene-specific expression of *FgCYP51A, FgCYP51B* and *FgCYP51C* was measured by qRT-PCR and normalized to fungal *EF1-α* (FGSG_08811) as reference gene. cDNA was generated after total RNA extraction from infected leaves at 5 dpi. The reduction in *CYP51* gene expression in the *Fg*-inoculated dsRNA-expressing leaves compared to the wt control was statistically significant. Error bars represent SD of two independent experiments each using 15 leaves of ten different plants for each transgenic line. Asterisks indicate statistical significance (*p<0.05; **p<0.01; ***p < 0.001; students t-test).

Additionally, the results indicate that also co-silencing effects are more prominent with longer precursor molecules. This could be further proven after bioinformatics off-target prediction by applying the same parameters as shown above for single constructs CYP-A, CYP-B and CYP-C. A range of potential off-targets were identified for all constructs in the respective non-target *FgCYP51* genes (Fig. 12). In contrast to shorter single constructs (compare Fig. 6) all dsRNAs had potential off-target hits in both respective non-target *FgCYP51* genes confirming the results from qRT-PCR, showing that all dsRNAs decreased the expressing of both non-target genes, although this was not significant in some cases (Fig. 11C). Thereby the number of off-targets per construct increased with the length of the precursor RNA showing a maximum in the full-length constructs, as expected (Fig. 12). This was regardless of whether *FgCYP51A*, *FgCYP51B* or *FgCYP51C* was the actual target. Generally, *FgCYP51C*-derived constructs seem to have fewer off-targets in respective non-target genes than *FgCYP51A-* and *FgCYP51B*-derived constructs, although this was not reflected by qRT-PCR results (Fig. 11C).
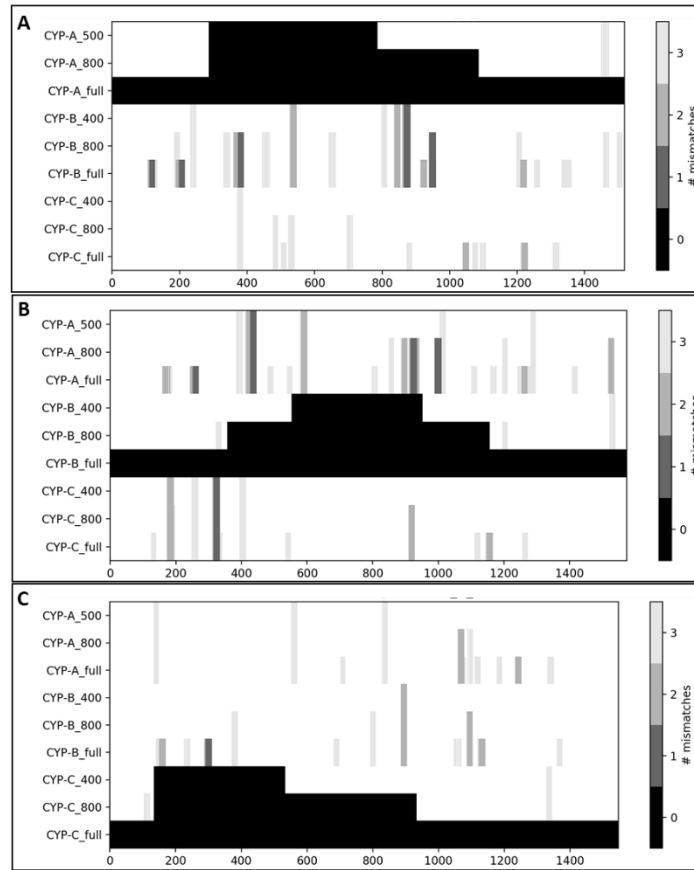
Fig. 12 Off-target prediction for single CYP-dsRNA constructs with different length. Sequences of CYP51-dsRNAs (y-axis) were split into k-mers of 18 bp. These were mapped against the corresponding coding sequences (CDS) of *FgCYP51A* (**A**), *FgCYP51B* (**B**) and *FgCYP51C* (**C**). For each position within the CDS (x-axis) the k-mers that match with a specified number of mismatches is plotted.

3.3 Influence of different dsRNA designs on the silencing efficiency of *FgCYP51* genes via HIGS

Based on unpublished RNA sequencing results of CYP3RNA-expressing *Arabidopsis,* it was known that most siRNAs originated from the *FgCYP51A* fragment in the precursor (Fig. 3). To resolve whether this is caused by the sequence of the CYP-A fragment itself and/or its position in the centre of the precursor RNA, several constructs targeting one or more *FgCYP51* genes were generated. The different designs included changing positions of the individual fragments in the CYP3RNA (CYP-ABC, CYP-BCA; Fig. 13A) and cloning of the CYP-A hot-spot (CYP-HSA; Fig. 13B). Another question concerning the dsRNA design was, if multiplication of the single constructs would cause a better gene silencing efficiency because of multiplication effects (CYP-AAA, CYP-BBB, CYP-CCC; Fig. 13C) and if the position (5' or 3' mRNA region) of the precursor RNA in the respective *FgCYP51* gene would make a difference on gene silencing efficiency (CYP-A5', CYP-B5', CYP-Cmiddle; Fig. 13D). RNAi vector generation

as well as plant transformation were done as described for other constructs and were performed by Maximilian Metze during his master thesis (Maximilian Metze, 2016).
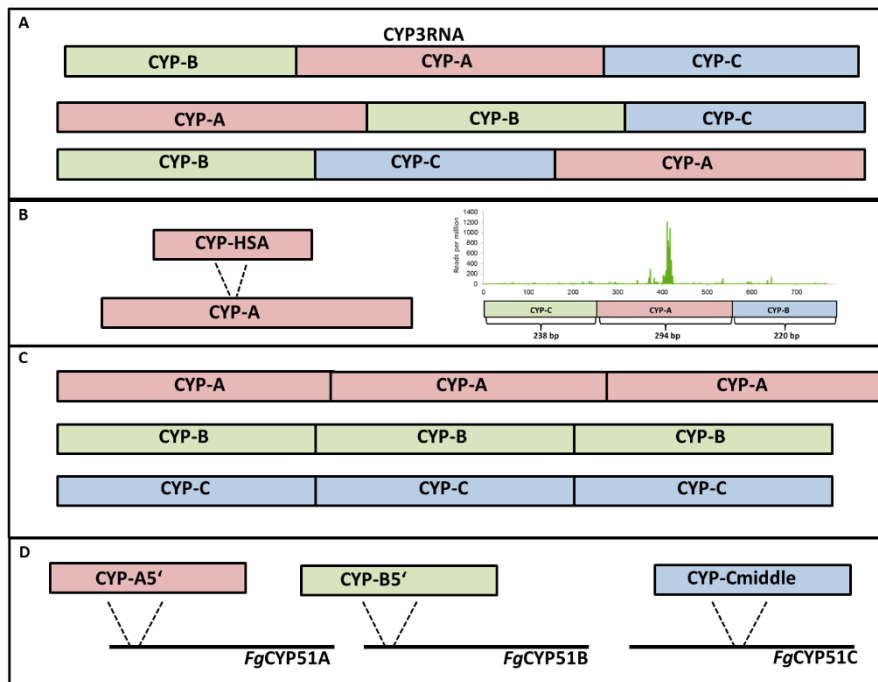
Fig. 13 Schematic representation of different dsRNA designs targeting *FgCYP51* genes. Designs were based on CYP3RNA precursor sequence and included changing positions of CYP51 fragments (**A**), the peak hot-spot in the CYP-A fragment (**B**), multiplication of individual CYP fragments (**C**) and changing positions of the precursor sequence in the corresponding *FgCYP51* gene (**D**).

After selection of positive transgenic lines by PCR and verification of successful transgene expression by qRT-PCR, phenotypes were assessed in infection assays with *Fg*. In contrast to above tested constructs, obvious phenotypic differences could be observed (Fig. 14A). Plants expressing CYP-ABC, CYP-Cmiddle and CYP-CCC showed similar lesion sizes than wt plants reflected also by the infection area. CYP-A5' showed slightly reduced infection symptoms but this reduction was not significant after determination of the infection area, whereas CYP-AAA and CYP-BBB significantly reduced infection areas by about 70% and CYP-HSA even by 80%. CYP-BCA and CYP-B5' caused reduction of the infection area of about 50% and 30% respectively (Fig. 14B). By comparison of the phenotypes with the gene expression analysis by qRT-PCR, some inconsistencies were found (Fig. 14C). Contrasting the phenotypes, all *FgCYP51* genes were downregulated in plants expressing CYP-ABC and CYP-Cmiddle, whereby CYP-Cmiddle showed the highest silencing of target as well as non-target expression among all constructs. Expression of target gene *FgCYP51C* was reduced by over 90%. For CYP-CCC on the other hand, upregulation of all *FgCYP51* genes could be detected explaining why plants were highly infected. Furthermore, the phenotypes of highly resistant plants CYP-

HSA, CYP-AAA and CYP-BBB were reflected by *FgCYP51* gene silencing. CYP-HSA reduced the expression of all *FgCYP51* genes by about 60% or more. In CYP-AAA- and CYP-BBB-expressing leaves, only *FgCYP51A* and *FgCYP51B* were downregulated by about 50% or more whereas *FgCYP51C* was upregulated. Triple construct CYP-BCA did only reduce the expression of two target genes and *FgCYP51B* expression was similar to wt plants. CYP-A5' and CYP-B5'reduced the expression of *FgCYP51A* and *FgCYP51C*, whereas *FgCYP51B* was slightly upregulated. Consequently, expression of CYP-B5' did not cause target gene silencing but only reduction of non-target genes. Generally, it was difficult to analyse the influence of the dsRNA design on *FgCY51* gene silencing efficiency because of off-target silencing as well as inconsistencies between phenotypes and gene expression analysis. Probably these experiments should be repeated with T2 generation plants as used before. This could also help to reduce high standard errors that were partly observed in qRT-PCR analysis.
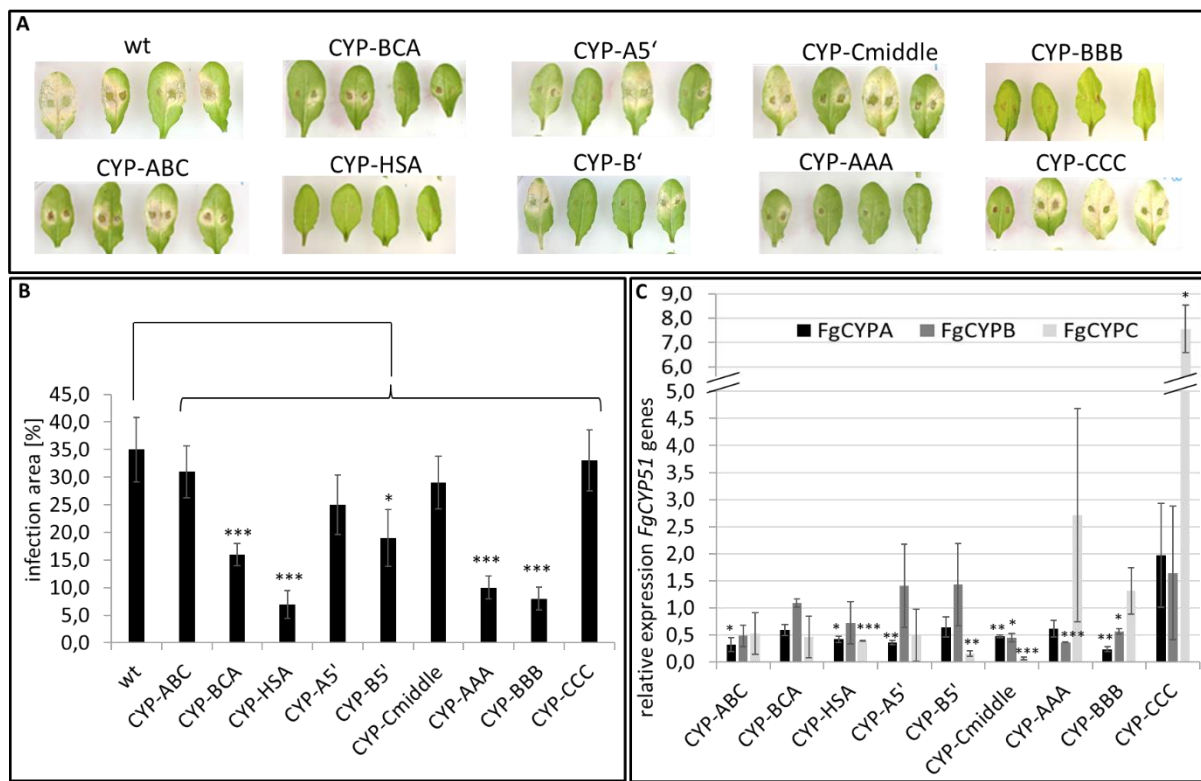

Fig. 14 Influence of dsRNA design on HIGS of *FgCYP51* genes. A, fifteen detached rosette leaves of CYP51-dsRNA-expressing *Arabidopsis* plants (T1 generation) were drop-inoculated with 5×10^4 conidia ml^{-1}. Infection symptoms were evaluated at 5 dpi. **B**, quantification of the visibly infected area at 5 dpi shown as percent of the total leaf area. Error bars represent SE of two independent experiments each using 15 leaves of ten different plants for each transgenic line. **C**, gene-specific expression of *FgCYP51A, FgCYP51B* and *FgCYP51C* was measured by qRT-PCR and normalized to fungal *EF1-α* (FGSG_08811) as reference gene. cDNA was generated after total RNA extraction from infected leaves at 5 dpi. The reduction in *CYP51* gene expression in the *Fg*-inoculated dsRNA-expressing leaves compared to the wt control was statistically significant. Error bars represent SD of two independent experiments each using 15 leaves of ten different plants for each transgenic line. Asterisks indicate statistical significance ($*p<0.05$; $**p<0.01$; $***p < 0.001$; students t-test).

3.4 Vesicle mediated transport of siRNAs during RNAi-based plant protection

### 3.4.1 Vesicle isolation from whole leaves of CYP3RNA expressing *Arabidopsis*

Many studies show that plant-derived siRNAs silence target genes in fungi (Chen et al., 2016; Cheng et al., 2015; Koch et al., 2013; Nowara et al., 2010). However, how these siRNAs cross the plant-fungal interface is literally unresolved. One possibility would be intracellular incorporation into plant vesicles that subsequently could be taken up by the fungus during the infection process. Previous attempts on the isolation of plant vesicles were performed with fruits and vegetables. Here a protocol successfully used for the isolation of exosome-like nanoparticles from grapes, grapefruit, ginger and carrots was established for *Arabidopsis* (Mu et al., 2014).

For vesicle isolation, plants expressing CYP3RNA were used (Koch et al., 2013). As control Col-0 wt plants were assessed. In the first step and to get a sufficient amount of starting material, whole leaves of *Arabidopsis* plants were crushed by pestle and mortar. The obtained cell lysate was sequentially centrifuged to separate larger particles (1000 xg for 10 min, 3000 xg for 20 min and 10,000 xg for 40 min at 4°C) and the remaining supernatant was subjected to ultracentrifugation (160,000 xg for 90 min at 4°C). The resulting pellet containing exosome-like nanoparticles was resuspended in PBS buffer and for further purification loaded on top of a sucrose gradient (8%/15%/30%/45%/60%). The gradient was centrifuged for 2 h at 160,000 xg. After the last centrifugation step, two distinct greenish bands were visible between the 60% and 45% and the 45% and 30% sucrose layer (Fig. 15). Both fractions of about 1 ml were harvested separately and filled up to 10 ml with PBS buffer. This was done as another washing step of the vesicles and dilution of the remaining sucrose as well as for concentration of the vesicles by another centrifugation step at 160,000 xg. The resulting pellets were finally resuspended in a small amount of PBS buffer and analyzed by negative staining and transmission electron microscopy (TEM). Microscopy revealed in the upper fraction numerous vesicle-like structures that were in a size range of about 50 nm to 200 nm. Most of them were cup-shaped and surrounded by a layer reminiscent of a membrane (Fig. 15).
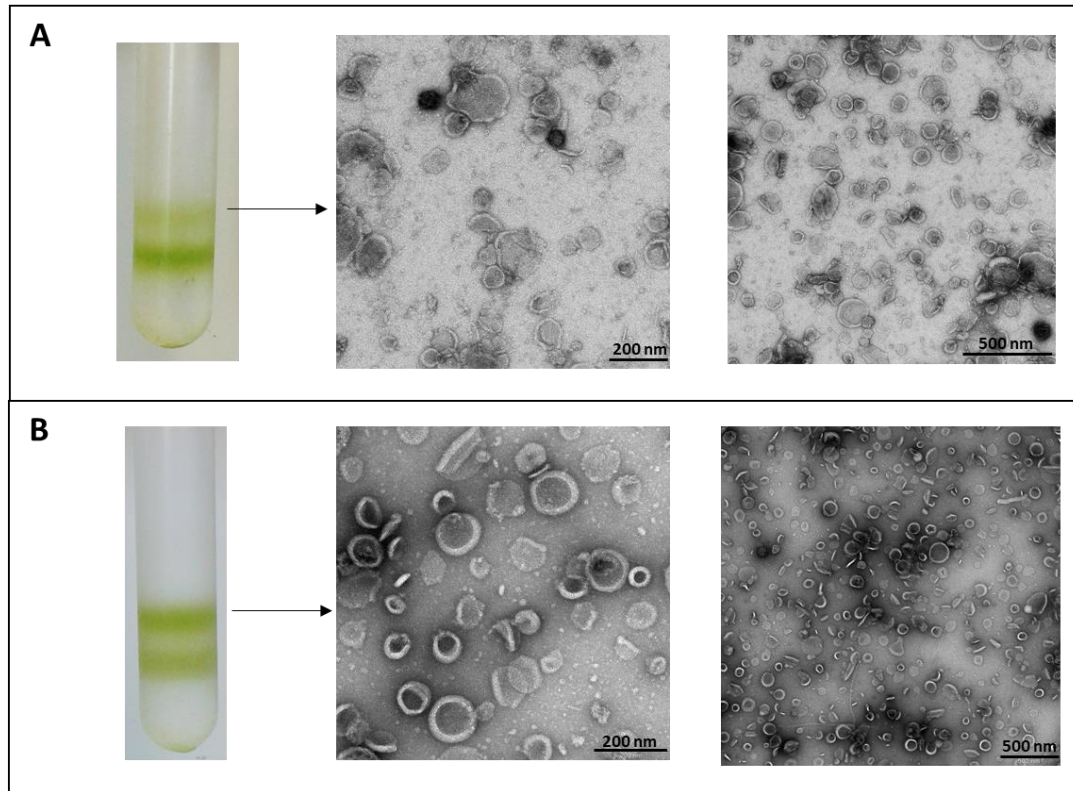
Fig. 15 Isolation of exosome-like nanoparticles from CYP3RNA-expressing (A) and wt (B) *Arabidopsis* leaves. Shown are plant vesicles that float in a sucrose gradient after ultracentrifugation as well as negative staining and transmission electron microscopy of the upper fractions with scales of 200 nm and 500 nm.

In contrast to this only few and also smaller particles could be observed in the lower fraction. Most of them seemed not to be surrounded by a membrane (Fig. 16A). The fraction between the two visible bands was mainly free of vesicle-like structures, suggesting that vesicles were concentrated in the visible bands (Fig. 16B). We continued only with the vesicles from the upper fraction as they were in the expected size range and analysed their average size using ImageJ. Analysis of the vesicle diameter revealed an average diameter of about 95 nm for vesicles isolated from wt and 105 nm for vesicles from CYP3RNA (Tab. 19). This fits with the size definition of exosomes having diameters of 30 nm to maximal 150 nm (Colombo et al., 2014).
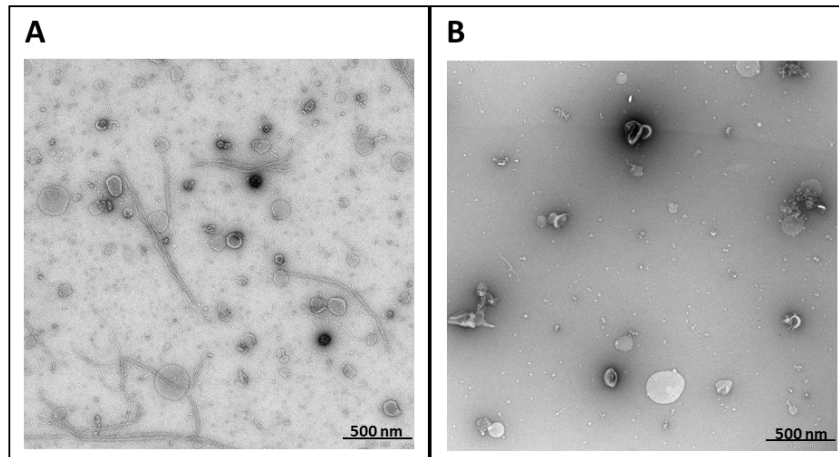
Fig. 16 Transmission electron microscopy of fractions harvested during vesicle isolation from *Arabidopsis* leaves. Shown are the lower fraction (**A**) and the fraction between the visible bands (**B**) (see also Fig. 15) in the sucrose gradient with a scale of 500 nm.

After proving that the used method is suitable to isolate exosome-like nanoparticles from *Arabidopsis* and that these vesicles can be purified by floating in a sucrose gradient, we wanted to know whether these vesicles contain CYP3RNA derived siRNAs. Therefore, vesicles from the upper fraction were washed, pelleted by ultracentrifugation and subjected to RNA extraction. As only few amounts of RNA were expected, RNA extraction was performed with the single Cell RNA Purification kit from Norgen Biotek. The RNA was analysed by small RNA sequencing and reads were mapped to the CYP3RNA precursor sequence what revealed a range of siRNAs originating from CYP3RNA (Fig. 17). Thereby more siRNA species mapped to the *FgCYP51A* fragment of the precursor than to *FgCYP51B* and *FgCYP51C* fragments. In contrast, no siRNAs isolated from wt samples mapped to the CYP3RNA. The results suggest that the isolated vesicles contain siRNAs originating from the transgenic CYP3RNA and probably also other RNA cargo.
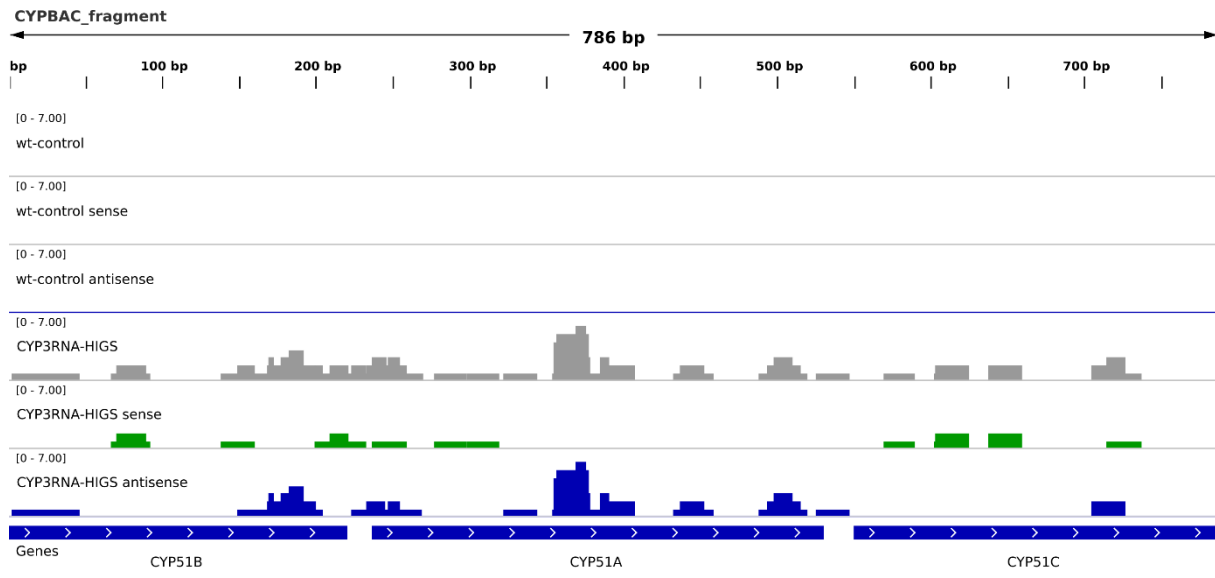
Fig. 17 Profiling of CYP3RNA-derived siRNAs in exosome-like nanoparticles from *Arabidopsis* leaves. Exosome-like nanoparticles were isolated from whole leaves and purified by sucrose-gradient centrifugation. Total RNAs were isolated from vesicles from the upper fraction of the gradient. sRNA reads of max. 25 nt from CYP3RNA-expressing (CYP3RNA-HIGS) and wt (wt-control) plants are mapped to the sequence of CYP3RNA. Read coverage varied from 0-7 as indicated. Sequencing data are gained from two separate vesicle isolations (gradients) of CYP3RNA and wt plants that were pooled and subjected to RNA extraction.

3.4.2 Vesicle isolation from apoplastic washing fluid of CYP3RNA-expressing *Arabidopsis*

Recently Rutter and Innes (2017) succeeded in isolating extracellular vesicles (EVs) from *Arabidopsis* and proved that they were of endosomal origin suggesting that exosomes exist in plants. The above described vesicles were isolated from whole plant leaves, so whether they derive from extracellular origin is questionable. To prove this, we applied the same method as in the mentioned paper for the isolation of EVs from CYP3RNA (Koch et al., 2013) and wt *Arabidopsis* plants. To ensure an extracellular origin, vesicles were exclusively isolated from the apoplastic fluid of *Arabidopsis* leaves. Apoplastic fluid was collected by vacuum infiltration of vesicle isolation buffer (see 2.2.16) and subsequent low speed centrifugation of infiltrated plants. Infiltration was done until infiltration sites were visible as dark green areas using a maximum of 30 sec for one infiltration cycle to minimize damaging of the cells and cell walls. The collected apoplastic fluid was filtered and sequentially centrifuged to separate larger particles. Two different centrifugation speeds were used in order to isolate different classes of vesicles. Vesicles were first pelleted by centrifugation at 40,000 xg (F40) before the resulting supernatant was subjected to another centrifugation step at 100,000 xg (F100). Both pellets were washed with PBS and analysed by negative staining and TEM. The F40 fraction revealed

multiple vesicular structures from approximately 50 nm to 300 nm in diameter (Fig. 18A). Analysis of the vesicle diameter using ImageJ revealed average diameters of 141 nm and 119 nm for CYP3RNA and wt plants, respectively (Tab. 19). This is in line with the observation of Rutter and Innes (2017) because most abundant particles in their F40 fraction had around 150 nm in diameter as detected by light-scattering. Thereby one has to consider that light-scattering measurement of the whole isolation approach is probably more exact than measurement of individual vesicle diameters by ImageJ. In contrast, the F100 fraction contained no vesicles, but mostly a high amount of small circular structures with diameters under 30 nm (Fig. 18B). Already Rutter and Innes determined that 40,000 xg is sufficient for the isolation of vesicle-like structures from apoplastic fluid (Rutter and Innes, 2017).
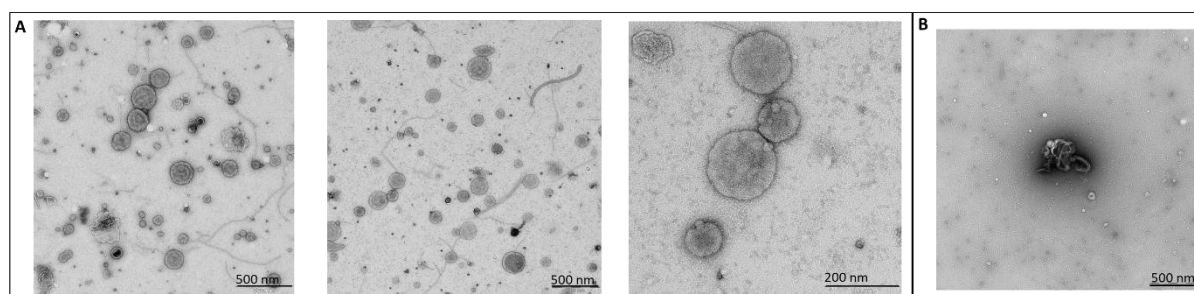
Fig. 18 Isolation of vesicle-like structures from the apoplastic fluid of *Arabidopsis* leaves. Shown are negative staining and TEM of pellets after centrifugation at 40,000 xg (F40, A) and 100,000 xg (F100, B). Pictures are shown exemplary for CYP3RNA expressing and wt plants and experiments were performed multiple times with similar results.

As described above, RNA isolated from vesicles contained in the F40 fraction were subjected to RNA sequencing. Before RNA extraction, vesicles were treated with RNAse A, what further proves that the isolated RNA was protected in the lumen of the vesicles. Mapping of RNA sequencing reads to the CYP3RNA precursor revealed CYP3RNA originating siRNAs as seen before. Again, siRNA species originating from the *FgCYP51A* fragment were more numerous than those from *FgCYP51B* and *FgCYP51C* fragments (Fig. 19).
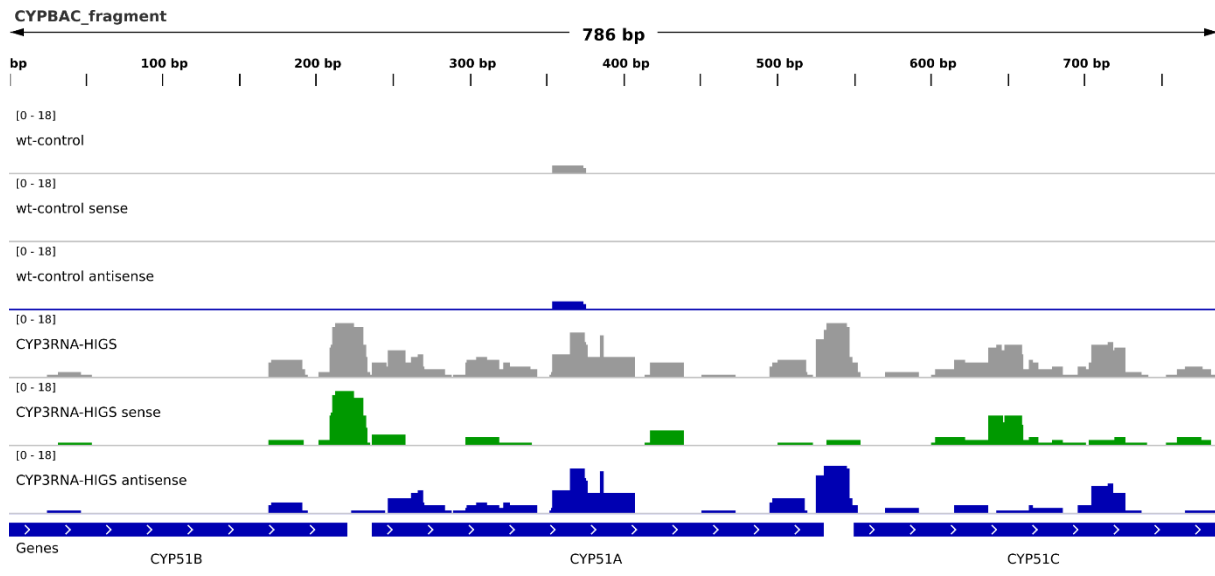
Fig. 19 Profiling of CYP3RNA derived siRNAs in extracellular vesicles from the apoplast of *Arabidopsis* leaves. Vesicles were isolated by apoplastic washes of *Arabidopsis* leaves and subjected to RNAse A treatment. Total RNA extraction was performed from purified vesicles and analysed by RNA sequencing. sRNA reads of max. 25 nt from CYP3RNA-expressing (CYP3RNA-HIGS) and wt (wt-control) plants are mapped to the sequence of the CYP3RNA. Read coverage varied from 0-18 as indicated. Sequencing data are gained from vesicle isolation from the apoplastic fluid of ten different CYP3RNA-expressing or wt plants.

3.4.3 Vesicle isolation from apoplastic washing fluid of barley leaves after spray treatment with CYP3RNA

The above shown results suggest that extracellular vesicles (EVs) play an important role for the transport of siRNAs during HIGS approaches against fungi. Whether vesicle transport plays a similar role during SIGS applications was unclear. To clarify this, the method for the isolation of EVs from *Arabidopsis* was adjusted for barley leaves. Detached leaves were pre-treated with CYP3RNA as described earlier (Koch et al., 2016). Only the upper leaf part was sprayed. After incubation of the sprayed leaves for 2 days, the unsprayed leaf parts were harvested. Two days were chosen based on infection assays where *Fg* inoculation was done 48 h after spraying of CYP3RNA (Koch et al., 2016). Before performing the apoplastic washes, the leaf segments were washed in distilled water to further minimize RNA contaminations. Some optimization steps were necessary to successfully generate apoplastic washing fluid from barley leaves. The infiltration time as well as the centrifugation speed and time had to be increased to ensure efficient infiltration of leaf segments. Successful infiltration was verified by colouring of the leaves to dark green. The resulting apoplastic fluid was than treated as described for *Arabidopsis*. After centrifugation, the F40 fraction revealed vesicles with the known characteristics of a cup-shaped appearance and surrounded by a membrane (Fig. 20A). Most vesicles were in a size range of about 100 nm to 200 nm and average vesicle diameter was

167 nm for untreated and 156 nm for CYP3RNA treated leaves (Tab. 19). It was conspicuous that the overall number of vesicles was lower than for *Arabidopsis*. This can be partly explained by the fact that the amount of starting material (fresh weight) and also the amount of gained apoplastic fluid was lower. Similar to *Arabidopsis,* centrifugation speed of 40,000 xg was sufficient to isolate barley vesicles from apoplastic fluid. The F100 pellet contained no vesicles but only diffuse particles (Fig. 20B).
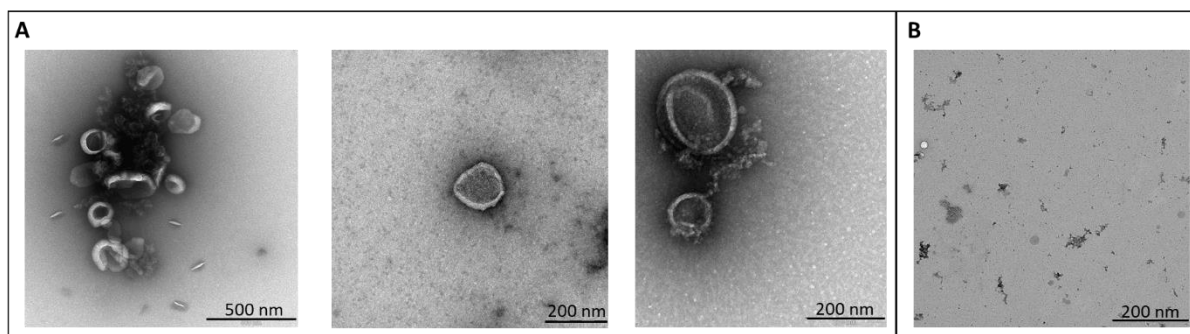
Fig. 20 Isolation of vesicle-like structures from the apoplastic fluid of barley leaves. Shown are negative staining and TEM of pellets after centrifugation at 40,000 xg (F40, **A**) and 100,000 xg (F100, **B**). Pictures are shown for CYP3RNA sprayed and untreated (TE buffer) leaves exemplary. Experiments were performed multiple times with similar results.

Despite the low yield of vesicles, RNA extraction from the F40 fraction generated a sufficient amount of RNA for cDNA library preparation and sequencing. In contrast to *Arabidopsis*, CYP3RNA sprayed samples and the TE control both, revealed siRNAs that mapped to CYP3RNA (Fig. 21). However, the CYP3RNA samples contained a substantial higher number of hits compared to the control and additionally the hits from both samples seemed not to overlap. You have to question whether hits that were observed in the control are specific or result from homology regions between the CYP3RNA and the barley genome. In general, the overall number of siRNAs that mapped to the CYP3RNA was lower compared to the two *Arabidopsis* samples (compare Fig. 17 and Fig. 19) and also read coverage (number of reads that overlap at a certain position of the sequence) was with a maximum of three very low. As seen before more siRNAs were identified that originated from the *FgCYP51A* fragment of the precursor but this was not as obvious as seen for the *Arabidopsis* samples.
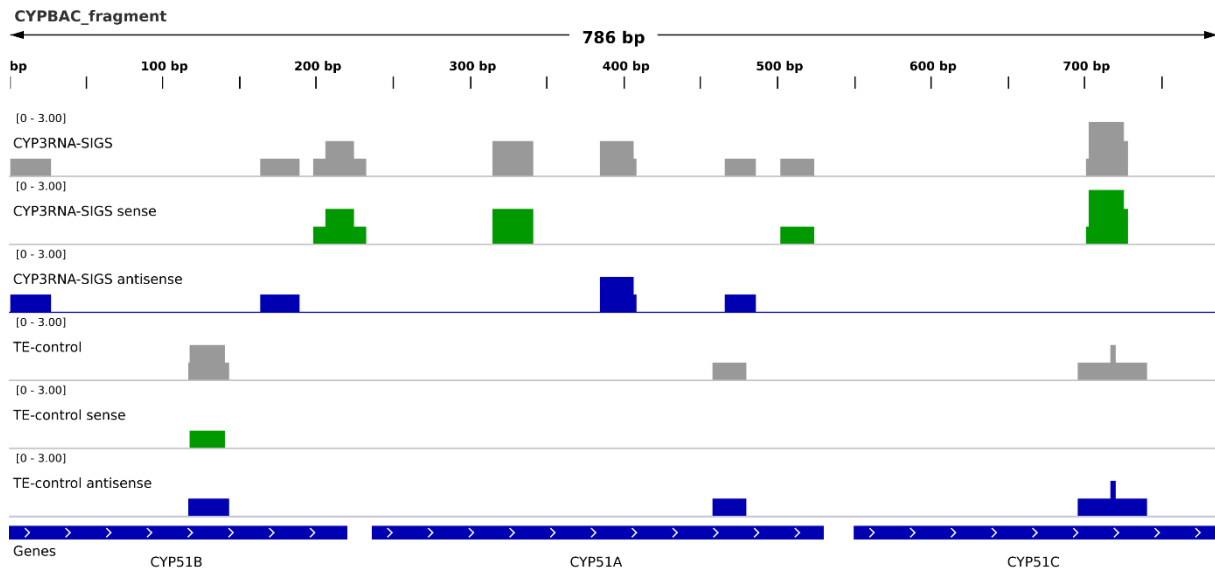
Fig. 21 Profiling of CYP3RNA-derived siRNAs in extracellular vesicles from the apoplast of barley leaves. Vesicles were isolated by apoplastic washes of barley leaves that were pre-treated with CYP3RNA (CYP3RNA-SIGS) or TE-buffer (TE-control) and subjected to RNAse A treatment. Total RNA extraction was performed from purified vesicles and analysed by RNA sequencing. sRNA reads of max. 25 nt from CYP3RNA (CYP3RNA-SIGS) and TE (TE-control) plants are mapped to the sequence of the CYP3RNA. Read coverage varied from 0-3 as indicated. Sequencing data are gained from the pooled RNA of two biological replicates each using 50 leaves of CYP3RNA and TE-sprayed leaves.

3.5 Establishment of Co-RNA immunoprecipitation (IP) of RNA-binding proteins in *Arabidopsis*

Although HIGS and SIGS approaches were widely used for plant protection against fungal pathogens, important mechanistic details are still missing. For successful gene silencing in the pathogen, the procession as well as transport of the dsRNA precursor in the plant itself might be an important factor. In *Cucurbita maxima* (*Cm*) the RNA-binding proteins (RBP) *Cm*PP16 and *Cm*RBP50 are known to enable long distance trafficking of RNAs through the phloem (Ham et al., 2009). The two proteins were overexpressed and purified from CYP3RNA expressing *Arabidopsis* plants. Co-purification of CYP3RNA originating RNA could give insight into CYP3RNA transport. The co-purified RNAs can be released from RBPs and analysed by RNA-sequencing. In the same objective also the five *Arabidopsis* dsRNA binding proteins (DRBs) were assessed concerning their roles in CYP3RNA procession and transport.

3.5.1 Expression and purification of PP16 and RBP50 from *Cucurbita maxima* in *Arabidopsis thaliana*

For specific purification from *Arabidopsis* cell extracts, proteins were cloned together with a tag. Therefore the family of pAUL vectors was chosen because they enable easy tagging of proteins by the Gateway cloning technology (Lyska et al., 2013). In the first step, coding

sequences (CDS) of *Cm*PP16 and *Cm*RBP50 were amplified from *Cm* cDNA and cloned into the pGEM-T vector. Successful amplification of the 453 bp PP16 and 1338 bp RBP50 fragment could be verified by agarose gel electrophoresis and insertion of the right sequence into pGEM-T was further verified by sequencing of the plasmid DNA (Fig. 22A). After fusion of att recombination sites, *Cm*RBPs were inserted into the pAUL vector by Gateway cloning (Fig. 22B).
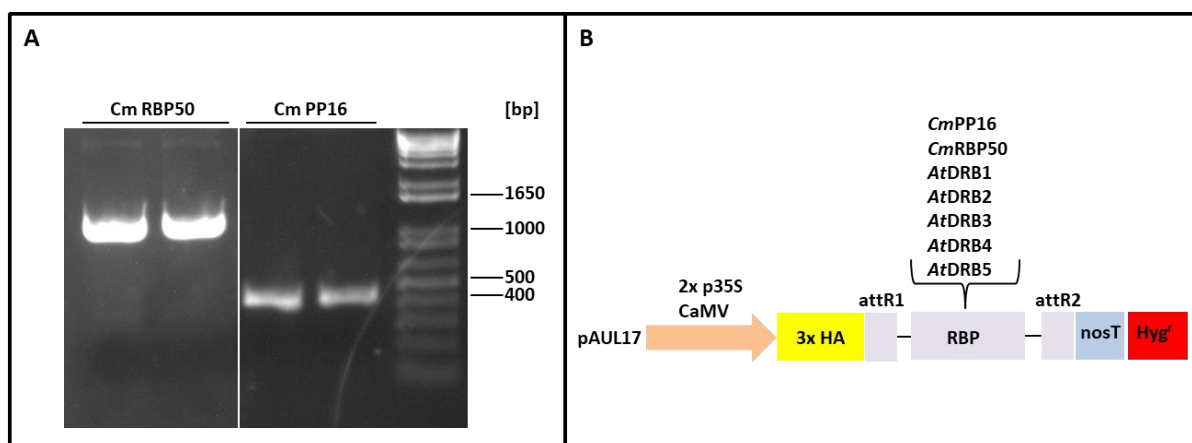
Fig. 22 Gateway cloning of RNA-binding proteins into pAUL vector. A, PCR amplification of RBP50 and PP16 from *Cm* cDNA. **B,** schematic representation of RBP containing pAUL17 vectors used for protein expression *in planta*.

To avoid interference of RNA-binding capability of the proteins, all proteins were planned to be N- and C-terminal tagged using pAUL13 and pAUL17. However following experiments showed that the C-terminal Strep-tag containing pAUL13 was not suitable for immunodetection in plants because of high background signals that could not be avoided by any optimization attempts. This has been already observed in earlier studies using anti-Strep-tag antibodies in plants (Lyska et al., 2013). Therefore, following experiments were performed with pAUL17 that contains a N-terminal HA-tag (Fig. 22B).

To assess whether the generated pAUL vectors can produce functional PP16 and RBP50 proteins *in planta* and because transformation of *Arabidopsis* takes some time until protein production can be analysed, proteins were transiently expressed in *Nicotiana benthamiana*. Leaf samples were taken 24 h and 48 h post infiltration (hpi) and protein expression was assessed by western blot and immunodetection using an HA-antibody (Roche). *Cm*RBP50 could be detected slightly higher than the 55 kDa marker band and *Cm*PP16 was detected between the 15 kDa and the 25 kDa band. Together with the 9 kDa HA-tag, a size of 59 kDa and 24 kDa was calculated for RBP50 and PP16, respectively, fitting with the size detected by western blot. For both proteins, sampling at 48 hpi resulted in better protein expression (Fig. 23A).

To analyse the ability of both pumpkin proteins in binding CYP3RNA-derived siRNAs, the vectors were transformed into *Arabidopsis* Col-0 wt as well as CYP3RNA expressing plants. To exclude unspecific binding of CYP3RNA-derived sRNAs to either the tag or the beads that were used during IP, the empty pAUL17 vector (ev) was transformed into CYP3RNA expressing plants. Transgenic plants were selected on ½ MS plates containing hygromycin as well as by PCR verification of the transgene. PCR positive plants were further characterized by qRT-PCR concerning mRNA expression as well as by western blot to verify successful protein production. It seems that expression of *Cm*RBP50 and *Cm*PP16 transcripts does not correlate with protein production. By testing two different lines for each protein, that showed expression of mRNA by qRT-PCR, in most cases only one line also showed protein production in western blot (Fig. 23B). Thereby also mRNA expression varied extremely among lines tested (data not shown), whereas only lines with the highest transcript expression were detectable by western blot. The protein level of weak expressing lines was probably under the detection level of the antibody or the detection system used. The size of both proteins was comparable to the size observed after transient expression in *N. benthamiana* and is in line with the expected size. Lines showing sufficient protein production (Fig. 23B L1, L3, L5, L8) were used for the establishment of co-RNA-immunoprecipitation (co-RNA-IP).

Co-RNA-IP was established according protocols that were used for co-RNA-IP of AGO proteins from *Arabidopsis* (Carbonell et al., 2012). Briefly, the leaves of 5-wk-old plants were harvested and ground to a fine powder in liquid nitrogen before subsequent resuspension in IP lysis buffer (Tab. 17). The cleared protein extract was first incubated with HA-antibody (Roche) before protein-antibody complexes were bound to protein-A-agarose (Roche). Unspecific binding was removed by six washing steps with IP buffer. After the last washing step, beads were divided into protein and RNA fraction to analyse whether *Cm*RBPs are bound to CYP3RNA-derived siRNAs. Generally, 20% of the IP was used for protein analysis and 80% for RNA extraction. Immunoprecipitated proteins were analysed by western blot (Fig. 23C). *Cm*RBP50 and *Cm*PP16 were detected in input (in) as well as in the immunoprecipitated (HA) fraction in CYP3RNA as well as in control plants. Rubisco bands were assessed in all fractions as loading controls and could be observed only in the input fractions indicating successful and specific purification of *Cm* proteins. In contrast, no bands in the expected size range were detected in the ev samples, underlining specificity of the IP.

After successful purification of *Cm*RBP50 and *Cm*PP16 from *Arabidopsis* cell extracts, the RBP bound RNA was released by proteinase K before subsequent extraction of RNAs by the single cell RNA purification kit (Norgen Biotek). The kit was used because only few amounts

of RNA were expected and because the kit purification provides highly pure RNA suitable for RNA sequencing. Analysis of the RNA concentrations by Nanodrop measurement revealed that around 60 ng RNA could be extracted from *Cm*RPB expressing lines (*Cm*RBP50/*Cm*PP16 ± CYP3). For ev plants only 30 ng RNA were determined. Before RNA sequencing the quality of the extracted RNA should be assessed but the amount would be sufficient for Illumina RNA sequencing technology.
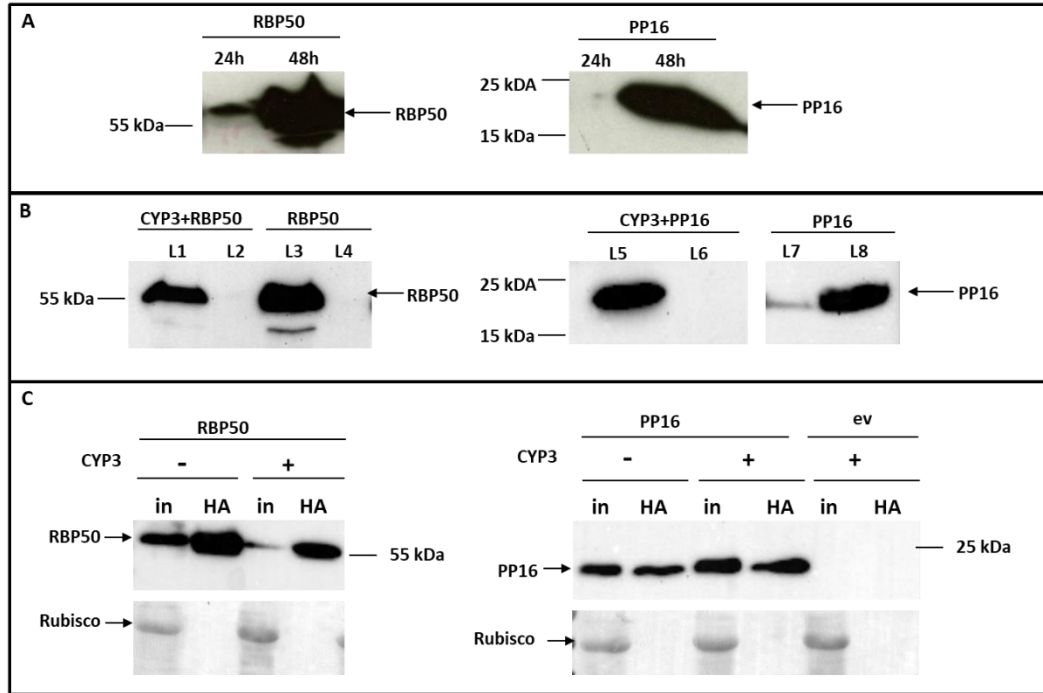

Fig. 23 Protein expression and purification of HA-tagged *Cm*RBP50 and *Cm*PP16 in *N. benthamiana* and *Arabidopsis*. A, transient expression of *Cm*RBP50 and *Cm*PP16 after infiltration of *N. benthamiana*. Protein samples from infiltrated leaves were taken 24 h and 48 h post infiltration and analysed by western blot using HA-antibody. **B**, stable transgenic expression of *Cm*RBP50 (L1-L4) and *Cm*PP16 (L5-L8) in CYP3RNA (L1-L2; L5-L6) expressing or wt (L3-L4; L7-L8) *Arabidopsis*. Proteins were extracted from the leaves of three to 4-wk-old plants and analysed by western blot using HA-antibody. Two different lines are shown for each protein expressing plant. **C**, immunoprecipitation of *Cm*RBP50 and *Cm*PP16 using HA-antibody (HA) as well as input fraction (in) in CYP3RNA expressing (+) and wt plants (-). Rubisco bands are shown as loading controls. ev = empty vector control. Lines indicate respective marker bands on the blot and arrows bands of the respective protein.

3.5.2 Co-RNA-IP of the five *Arabidopsis* DRBs

The DRB proteins from *Arabidopsis* are known to be important factors during RNAi-induced gene silencing by assisting in RNA procession and interaction with DCL proteins (Curtin et al., 2008). By the same approach as described above for *Cm* proteins, we wanted to find out which DRB proteins bind to CYP3RNA-derived RNAs and are possibly involved in CYP3RNA-derived siRNA generation. Therefore, the coding sequences (CDS) of DRB1-5 were first

amplified from *Arabidopsis* cDNA and cloned into pGEM-T vector (Promega). Correct lengths of CDS were verified by agarose gel electrophoresis as well as sequencing of pGEM-T plasmids (DRB1, 1260 bp; DRB2, 1305 bp; DRB3, 1080 bp; DRB4, 1068 bp; DRB5, 1182 bp) (Fig. 24). The following Gateway cloning of all DRBs into pAUL17 vector was done as described above (Fig. 22B) and verified by restriction digest and sequencing of the final vector.
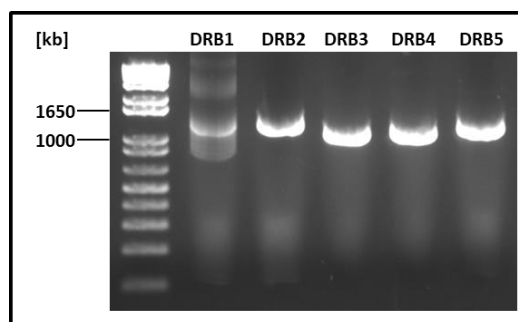
Fig. 24 Amplification of DRB coding sequences from *Arabidopsis* cDNA. CDS of DRB1, DRB2, DRB3, DRB4 and DRB5 were amplified with gene specific primers from cDNA of *Arabidopsis* Col-0 wt.

Efficient protein production from generated pAUL vectors was first assessed transiently in *N. benthamiana.* Western blot analysis of protein samples from infiltrated leaves revealed bands in the correct size ranges of 54 kDa, 56 kDa, 49 kDa, 47 kDa and 52 kDa for HA-*At*DRB1, HA-HA-*At*DRB2, HA-*At*DRB3, HA-*At*DRB4 and HA-*At*DRB5, respectively (Fig. 25A). For all proteins sampling at 48 hpi, and similar to above tested pumpkin proteins, resulted in better protein expression. Production of DRB5 was low also in comparison with the other DRB proteins.

To assess binding capability of *At*DRBs to CYP3RNA originating siRNAs, pAUL17-DRB vectors (Fig. 22B) were transformed into *Arabidopsis* plants expressing CYP3RNA (Tab. 1; Koch et al., 2013). As controls, all vectors were transformed in DRB knockout lines to ensure that only the tagged protein was present in plants (Tab. 1). For CYP3RNA plants this could not be excluded in this study because pre-transformation of DRB mutants with the CYP3RNA vector would have taken too much time. After transformation and selection of positive transgenic plants, only DRB1 and DRB2 were detectable after protein extraction (Fig. 25B). In contrast, DRB4 (Fig. 25B L11) was not detectable in the native protein extract but only after analysis by denaturing protein extraction (Quick & Dirty extraction see 2.2.19) using a different protocol. DRB3 and DBR5 were not detectable by western blot after analysis of more than ten positive transgenic lines using different protein extraction protocols. Analysis of transcript expression by qRT-PCR revealed successful mRNA production from DRB3 and DRB5 containing pAUL vectors (data not shown) suggesting that protein production was either under

the detection level or restricted to cellular compartments or plant tissues that could not be assessed using the applied methods.

Consequently co-RNA-IP could be done only with DRB1 and DRB2 proteins. Both proteins were successfully purified by immunoprecipitation with HA-antibody and agarose beads using the same protocols as described above for *Cm* proteins. DRB1 and DRB2 were detected in input and HA-fractions whereas Rubisco was only detectable in input fractions confirming specific purification of DRB proteins. Again, no bands of the expected size were visible in ev samples (Fig. 25C). RNA extraction from immunoprecipitated proteins and measurement of RNA concentrations by nanodrop revealed around 35 ng and 45 ng for DRB1 and DRB2 expressing plants respectively. From ev samples only 20 ng could be extracted.
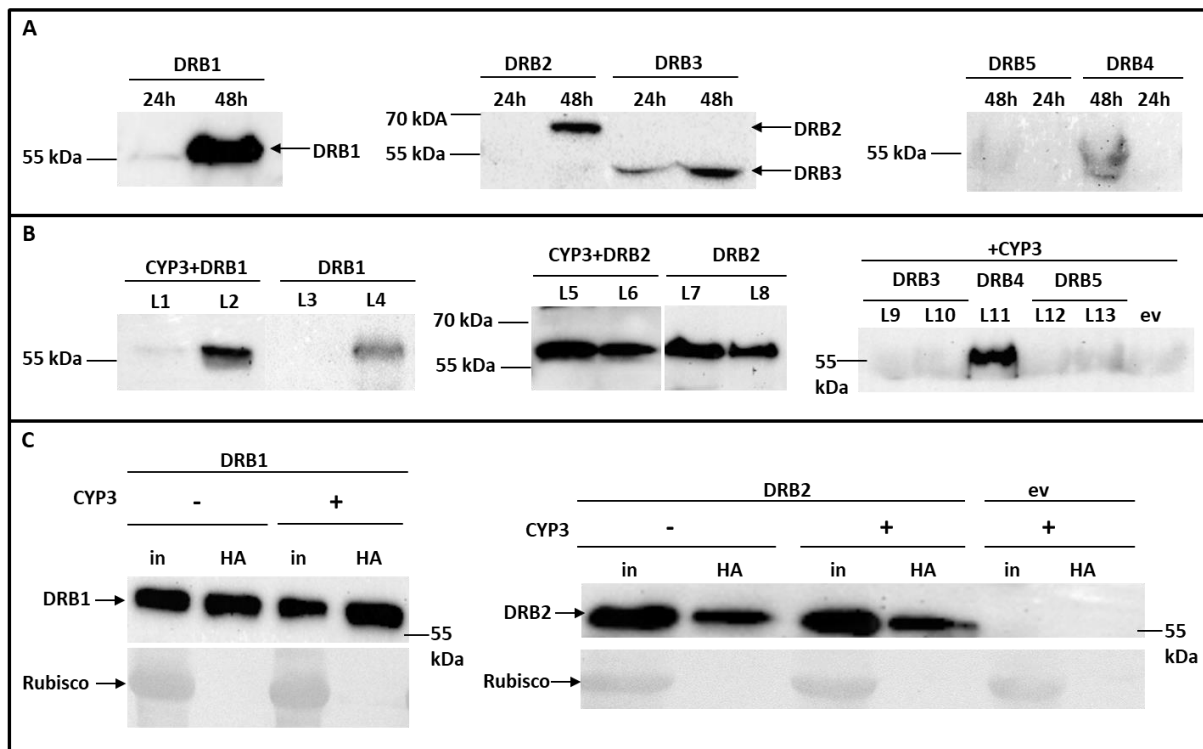

Fig. 25 Protein expression and purification of HA-tagged *At*DRBs in *N. benthamiana* and *Arabidopsis*. A, transient expression of *At*DRB1, *At*DRB2, *At*DRB3, *At*DRB4 and *At*DRB5 after infiltration of *N. benthamiana*. Protein samples from infiltrated leaves were taken 24 h and 48 h post infiltration and analysed by western blot using HA-antibody. **B**, stable transgenic expression of *At*DRB1 (L1-L4), *At*DRB2 (L5-L8), *At*DRB3 (L9-L10), *At*DRB4 (L11) and *At*DRB5 (L12-L13) in CYP3RNA expressing or wt *Arabidopsis*. Proteins were extracted from the leaves of three to 4-wk-old plants and analysed by western blot using HA-antibody. **C**, immunoprecipitation of *At*DRB1 and *At*DRB2 using HA-antibody. Shown is immunoprecipitation (HA) as well as input fraction (in) in CYP3 expressing (+) and control plants (-). Rubisco bands are shown as loading controls. ev = empty vector control. Lines indicate respective marker bands on the blot and arrows bands of the respective protein.

In further studies the isolated RNA from co-RNA-IP experiments using *Cm*RBPs as well as *Arabidopsis* DRB proteins could be used for RNA sequencing analysis. This could reveal new

insights into transgenic dsRNA procession and transport during RNAi based gene silencing approaches as well as general functions of DRB proteins in plants. Although modern RNA sequencing technologies are sensitive enough to analyse low amounts of starting material, as low as 10 ng, upscaling of the co-RNA-IP reactions could be considered to receive more reliable results (Lynch et al., 2010).

For DRB3, DRB4 and DRB5 which could not be detected with the used purification methods, specialized protocols for the extraction of proteins from specific plant tissues or cell organelles like the nucleus were considered. However preparation of the crude nuclear proteins extracts by using a protocol from Escobar et al., 2001 was only successful for DRB4 (Fig. 26A). Besides, DRB4 was detected in cytosolic as well as nuclear fractions suggesting that likely the protein extraction buffer used for IP experiments caused the problem and was not suitable for DRB4 extraction. In the attempt to further optimize the extraction of DRB4, several transgenic lines were propagated to generate more plant material. Additionally, 1 mM DTT was added to the IP extraction buffer and western blots were repeated with T2 plants. DTT can protect proteins from oxidative damage and it was included in the protocol from Escobar et al. as well as in the denaturing extraction buffer. After adjustment of the IP buffer, DRB4 could be perfectly detected in the native protein extract. This was independent of whether DTT was included or not suggesting that problems in detecting DRB4 were only caused by different expression levels between plant generations. In contrast DRB3 and DRB5 were not detected as seen before (Fig. 26B). After resolving the problem with DRB4 immunodetection, co-RNA-IP was performed successfully with the same protocol as used before for DRB1 and DRB2. DRB4 was detected in the expected size range of about 47 kDa in input and largely concentrated in HA-fraction (Fig. 26C). RNA extraction from HA-fractions yielded around 60 ng and 70 ng from DRB4 and ev samples, respectively. Future RNA sequencing analysis of both samples have to reveal whether this results from unspecific RNA attachment to the tag or the beads and which RNAs specifically bind to DRB4.
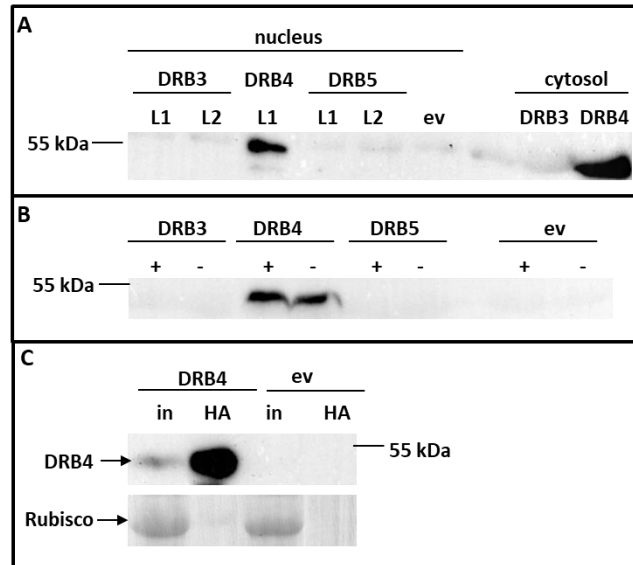
Fig. 26 Immunodetection of DRB3, DRB4 and DRB5 expressed in *Arabidopsis* using different protein extraction protocols. **A**, nuclear proteins were extracted from *Arabidopsis* leaves using a protocol from Escobar et al., 2001. Cytosolic and nuclear fractions were analysed from DRB expressing and empty vector lines (ev) using HA-antibody. **B**, native protein extraction using IP lysis buffer (Tab. 17) with (+) or without (-) 1 mM DTT. **C,** immunoprecipitation of *At*DRB4 and ev using HA-antibody. Shown is immunoprecipitation (HA) as well as input fraction (in) in CYP3 expressing (+) plants. Rubisco bands are shown as loading controls. Lines indicate respective marker bands on the blot and arrows bands of the respective protein.

In further studies expression of DRB3 and DRB5 should be analysed in specific plant tissues different from leaves. Additionally, co-transformation of DRB mutants with CYP3RNA producing vector and subsequent transfer of HA-tagged DRB proteins should be performed to exclude interference of the natural DRB proteins in this process. Moreover, analysis of C-terminal tagged proteins should be assessed additionally to exclude disruption of RNA binding capability by the tag.

4.   Discussion

4.1   Single and double CYP-constructs efficiently control *Fg* infection *in planta*

This project has been started based on previous studies using HIGS and SIGS approaches to silence the three *CYP51* genes of *Fg* by CYP3RNA and what has been shown to be really efficient in controlling *Fg* infection *in planta* (Koch et al., 2013; Koch et al., 2016). The aim of this PhD project was to find out whether simultaneous silencing of all three genes is required for successful disease control. Therefore, six constructs targeting either one or two *FgCYP51* genes were generated and assessed concerning their potential for plant protection. Considering that RNAi-based gene silencing has been used repeatedly to elucidate gene functions in a vast number of organisms (Blake et al., 2017; Lu, 2003; Mulot et al., 2016), this study was conducted to elucidate *CYP51* gene function in *Fusarium*. Until now, only one study has defined specific functions for the individual *CYP51* genes of *Fg* (Fan et al., 2013). In general, KO of *CYP51* reduces fungal growth by interfering with the ergosterol biosynthesis through inhibiting the sterol 14α-demethylase (Yoshida, 1988).

Surprisingly, all constructs, except CYP-C, provoked a remarkable reduction of *Fusarium* infection in *Arabidopsis* after inoculation of detached leaves (Fig. 5). It was even more striking that the published CYP3RNA expressing plants virtually showed the same phenotype as the new single and double constructs (Tab. 18). The results especially for the single constructs are contrasting to earlier studies showing that the deletion of individual *FgCYP51* genes can partly reduce conidiation, but otherwise causes no changes in *in vitro* morphology, mycelial growth rate or ergosterol content (Liu et al., 2011). In contrast, effects with double constructs could be expected seeing that double deletion mutants *cyp51A/cyp51C* and *cyp51B/cyp51C* reduced growth on potato dextrose agar (though not on SNA agar) (Fan et al., 2013). By using these mutants, *Fg*CYP51B could be identified as the major demethylase primarily responsible for sterol 14α-demethylation and having an essential role in ascospores formation, while *Fg*CYP51A is an additional 14α-demethylase, induced on ergosterol depletion and responsible for the intrinsic variation in azole sensitivity. In contrast, *FgCYP51C* does not encode a sterol 14α-demethylase; it is exclusively found in *Fusarium* species and is ubiquitous across the genus (Fan et al., 2013). Minor function of *FgCYP51C* in ergosterol synthesis would fit with the observed phenotype in *Arabidopsis* infection assays, where resistance enhancement by CYP-C single construct was only minor in comparison with the other constructs. Deletion of *FgCYP51C* results in reduced virulence on wheat ears, but not on *Arabidopsis* floral tissue (Fan et al., 2013). The observed phenotypes were proven to be based on *FgCYP51* silencing as shown

by qRT-PCR (Fig. 5). Considering the results from single and double constructs, conclusions about FgCYP51 functions must be reconceived, as all constructs seem to provoke co-silencing effects in the non-targeted *FgCYP51* genes. Surprisingly, this resulted in a downregulation of all *FgCYP51* genes. Consequently, it can be suggested that strong co-silencing of non-target genes by single constructs may explain why their effects on fungal morphology and virulence are much stronger than single *FgCYP51* gene deletions. Effects that were actually caused by silencing of a specific gene are masked and make it impossible to distinguish specific *CYP51* gene functions. This was aggravated by the fact that phenotypes of single and double constructs differed only weakly among each other and additionally could not be distinguished from the CYP3RNA in *Arabidopsis* infection assays.

To confirm the observed co-silencing effects, the sequences of the single constructs were bioinformatically fragmented into k-mers of 18 bp and aligned to *FgCYP51* mRNA sequences. Allowing one to three mismatches multiple off-targets were identified in non-target *FgCYP51* genes that could explain why single constructs provoke downregulation of all three genes. Nevertheless, there were some minor inconsistencies in off-target determination suggesting that the used software does not identify the complete set of possible off-targets. For CYP-B as well as for CYP-C, off-targets were detected in only one of the two non-target *FgCYP51* genes although qRT-PCR results showed that all three genes were downregulated. RNAi studies with human cell lines also identified unexpected off-targets by expression profiling additionally showing that 15 out of 19 bp identity seems to be sufficient to cause an effect (Jackson et al., 2003). Supporting this finding, it has been argued that specificity parameter for off-target prediction are often unfounded and that likely a substantial number of siRNAs remains undetected (Birmingham et al., 2006). Furthermore, it was assessed whether CYP single and double constructs would theoretically have additional off-targets in *Fg*. Using the same parameters as for the *FgCYP51* genes, several potential off-targets in the *Fg* genome were identified, raising the possibility that the virulence of the fungus is additionally affected by downregulation of these potential targets (Höfle et al., 2018 in revision). When it comes to plant protection, co-silencing on the three paralogous *FgCYP51* genes would be a desired effect of dsRNA-mediated inhibition of ergosterol biosynthesis and fungal virulence but when it comes to gene function the opposite is true. Undesired off-target effects leading to difficulties in identifying exact gene functions by RNAi-based silencing were reported in various organisms including plants and fungi (Qiu et al., 2005; Seinen et al., 2011; Senthil-Kumar and Mysore, 2011). However, most studies examining large-scale off-target analysis were performed on animal cells (Dahlgren et al., 2008; Jackson et al., 2003; Kamola et al., 2015). My results

suggest that off-target effects should be under consideration in fungi when it comes to gene function analysis and/or especially for applications in crop protection when it is critical that the respective RNAs constitute no harm for the environment, consumers or any beneficial organism. More research will be necessary in this area as it is likely that the parameters recommended for animals (Echeverri et al., 2006) are not applicable for fungi because of differences in RNAi machineries.

Of course, co-regulation of the *CYP51* genes also must be considered. Using *Fg* deletion mutants, it has been shown that reduced expression of *FgCYP51B* and subsequent depletion of ergosterol results in a compensatory induction of the *FgCYP51A* gene (Fan et al., 2013). The same effect can be observed after azole treatment (Becher et al., 2011; Liu et al., 2010). This has been confirmed recently in *Fusarium in vitro* cultures. The treatment of the fungi with single and double CYP-dsRNAs, targeting *FgCYP51B* alone or in combination resulted in upregulation of *FgCYP51A* (Höfle et al., 2018 in revision). Consistent with earlier reports, enhanced *FgCYP51A* expression was unable to fully compensate conidiation defects resulting from reduced activity of *FgCYP51B*. However, using the shown RNAi-based approach, no upregulation of *FgCYP51A* was observed *in planta* neither in HIGS nor SIGS setups, when targeting *FgCYP51B* alone or together with *FgCYP51C*, which cannot be fully explained yet. One can speculate that co-silencing effects in HIGS and SIGS setups are even stronger than in *in vitro* assays because of different mechanisms of siRNAs procession and/or amplification of the silencing signal through secondary siRNAs (Schwab and Voinnet, 2010).

Tab. 18 Growth inhibition of *Fg* during different RNAi-based silencing setups. Growth inhibition is shown as reduction in % of the infected leaf area or decrease of optical density (OD590) in comparison to the control (Höfle et al., 2018 in revision).

|	CYP-A	CYP-B	CYP-C	CYP-AC	CYP-BC	CYP-AB	CYP3RNA
In vitro	74%	71%	75%	69%	67%	73%	74%
HIGS (*A. thaliana*)	57%	66%	32%	63%	52%	60%	57%
HIGS (barley)	7%	40%	9%	39%	62%	53%	n. a
SIGS	80%	78%	82%	83%	88%	84%	93%

In contrast to *Arabidopsis*, obvious differences between single and double constructs were observed in barley HIGS setups (Tab. 18). Double constructs were in general more efficient than single constructs, what is in line with the above mentioned studies with double *Fg* deletion mutants (Fan et al., 2013). From the single constructs only CYP-B significantly reduced fungal infection what would be suggested considering the prominent function in ergosterol synthesis. Furthermore, infection strength on barley leaves seems to be reflected by *FgCYP51B* expression

as CYP-A and CYP-C showed stronger expression than the other constructs resulting in the same infection severity than the GUS control plants (Fig. 8). However, and similar to *Arabidopsis*, influences of individual *FgCYP51* genes were strongly concealed by co-silencing effects in non-target genes. Notably, the efficacy of single and double constructs in the barley HIGS setup correlates directly with the differential *in vitro* effect of these constructs on impairment of fungal morphology (Höfle et al., 2018 in revision). At this stage the different activities of single and double CYP constructs between the HIGS setups in barley vs. *Arabidopsis* (e.g. equal efficacy of single and double constructs in *Arabidopsis*) cannot be mechanistically explained. Possible explanations could be both, differences in the RNAi machinery of these two species and/or transfer routes of small RNAs from host cells to the interacting pathogen (Wang et al., 2016).

Seeing that the CYP3RNA was effective in controlling *Fg* infection by spray treatment of barley leaves, we also assessed single and double constructs. Under the conditions tested, resistance enhancement in general was stronger in comparison to HIGS setups and comparable to *Arabidopsis* all six constructs showed similar phenotypes (Tab. 18). Notably and consistent with earlier results (Koch et al., 2016), spraying CYP3RNA resulted in the strongest decrease in *Fg* infection by at least 90%. This was contrasting to HIGS in *Arabidopsis*, where no clear difference could be observed between constructs targeting one, two ore even three *FgCYP51* genes. A recent study showed that CYP3RNA, when sprayed onto barley leaves, is taken up by *Fg* and processed by the fungal RNAi machinery (Fig. 27B; Koch et al., 2016). Efficient uptake of CYP51-dsRNA could explain the high efficiency in the SIGS setups. It is not yet known whether in HIGS setups longer dsRNAs such as CYP3RNA are also transferred to the interacting fungus or whether cellularly expressed dsRNAs are processed by the plant's RNAi machinery into siRNAs in advance of an efficient uptake by the fungus (Fig. 27A). Treatment of *Fg* with CYP3RNA *in vitro* impaired fungal growth more than the single and double constructs (Höfle et al., 2018 in revision). Differences between CYP3RNA and the single and double constructs were observed only in setups (SIGS, *in vitro*), where dsRNA is suggested to be taken up directly and processed by the fungus whereas in HIGS setups probably siRNAs constitute the main transfer molecules. This would be an explanation for different activities of the same dsRNA constructs using different experimental setups. In aphids a comparative analysis of different dsRNA delivery strategies also revealed high variations in gene silencing efficiencies of the same target gene with a clear favour for dsRNA (Mulot et al., 2016).

A recent study showed that exogenously applied dsRNA can induce PTI leading to enhanced antiviral or antibacterial resistance (Niehl et al., 2016). In contrast, PTI triggering activity could

not be demonstrated with CYP3RNA as this dsRNA had no effects on marker genes indicative of salicylate- or jasmonate-mediated defence pathways (Koch et al., 2016). This is relevant considering the yield penalties of dsRNA-based plant protection strategies. Moreover, downregulation of the *FgCYP51* genes further argues that SIGS cannot rely on an unspecific resistance enhancement. Consistent with this, SIGS requires an intact fungal RNAi machinery as revealed by the fact that fungal *dicer-like 1* (*Fgdcl-1*) mutants widely tolerate spray treatments with CYP3RNA (Koch et al., 2016).
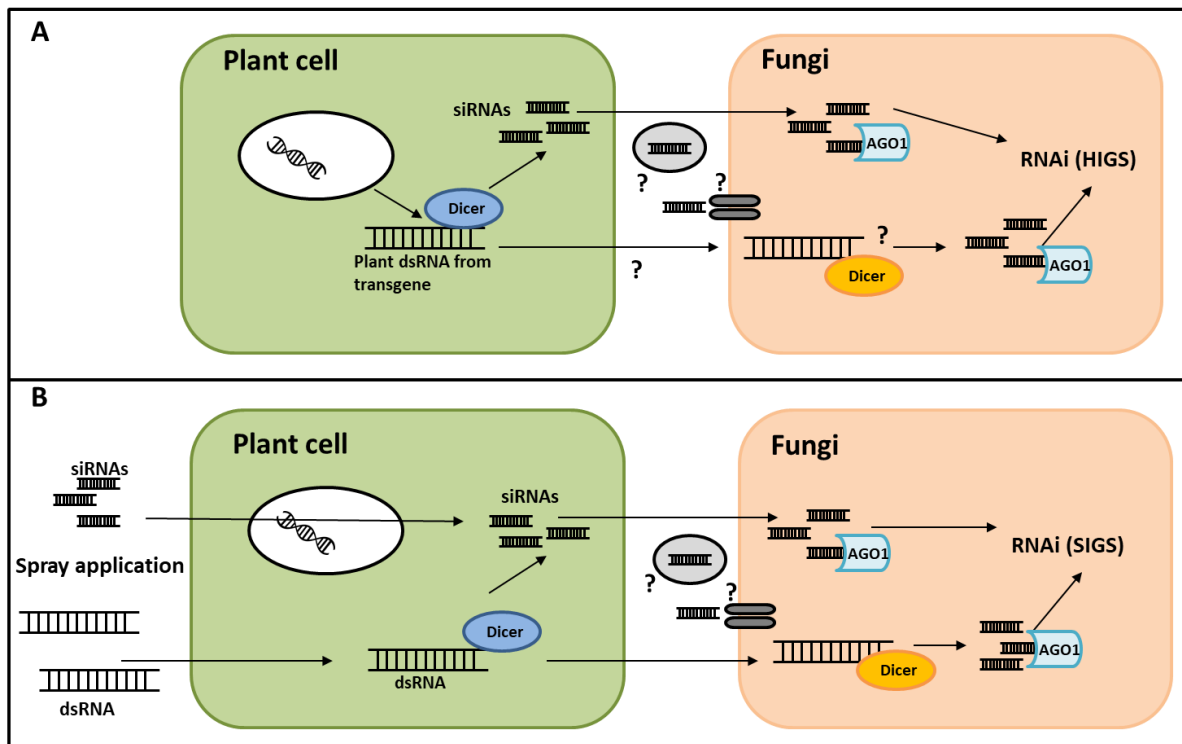
Fig. 27 Possible transfer routes and molecules in HIGS (A) and SIGS (B) against fungi. A, the transgene derived dsRNA is produced and processed in the plant. Whether the precursor itself can be transported into the fungus, where it could be processed by the fungal RNAi machinery, is unclear. **B**, the sprayed RNAs are taken up via unknown mechanisms by the plant and processed. The precursor dsRNA as well as siRNAs can be taken up by the fungus (Koch et al. 2016). Possible transfer routes for both mechanisms via vesicles or RNA-transporters are indicated. AGO1 seems to be essential for the RNAi response in *Fusarium* (Chen et al., 2015).

4.2 Gene silencing efficiency and co-silencing effects of *FgCYP51* genes increased with dsRNA length

RNAi-based gene silencing methods were reliably used to study gene functions in many organisms (Abdurakhmonov et al., 2016; Nguyen et al., 2008) and have been shown to have great potential for plant protection against fungal pathogens (Majumdar et al., 2017). Nevertheless, earlier studies and the here shown results suggest that important mechanistic

details and differences between HIGS and SIGS are still unresolved (Höfle et al., 2018 in revision; Koch et al., 2013; Koch et al., 2016). As shown in this study, the same dsRNA constructs lead to different silencing phenotypes using transgenic and exogenous dsRNA delivery, suggesting differences between the two mechanisms and also between different plant species. While HIGS probably relies on the plants RNAi machinery, SIGS studies suggest the involvement of both organism in the silencing process (Koch et al., 2016). This clarifies that further research is required to establish rules for an optimal dsRNA design, for example length of the dsRNA precursor. The elucidation of the molecular mechanism would be the key for future application. For the first time we assessed dsRNA constructs of increasing lengths in HIGS approaches against fungi. By comparing dsRNA lengths from about 500 bp to over 1500 bp no clear differences in the resistance enhancement against *Fg* could be detected (Fig. 11). The majority of the constructs reduced infection area by about 60%, what was similar to the shorter single constructs of around 250 bp (Tab. 18), suggesting that selection of the right target genes is superior than different dsRNA length. In RNAi feeding studies with insects, dsRNA lengths from 134 bp to 1842 bp were reported to work successfully on the same gene also indicating that target gene selection is superior as dsRNA length (Huvenne and Smagghe, 2010). In support to this, a study in aphids reported that the percentage of coverage of the target gene by the dsRNA does not impact the gene silencing efficiency. A dsRNA targeting *ALY* (mRNA export factor) transcripts covered a larger portion of the coding sequence compared to *Eph* (erythropoietin-producing hepatocellular) dsRNA, without inducing a higher gene inhibition (Mulot et al., 2016). The fact that only *Eph* could be silenced was explained by a higher abundance of *ALY* transcripts. Basal expression levels of the *FgCYP51* genes were not assessed in this study but this indicates that the gene silencing efficiency can be largely influenced from other factors apart from dsRNA design.

Again, and as discussed earlier, resistance was extensively boosted by co-silencing of non-target *FgCYP51* genes what makes each construct very effective in controlling *Fg* infection (Fig. 11). This was regardless of whether *FgCYP51A*, *FgCYP51B* or *FgCYP51C* was targeted. Contrasting to the phenotypes, gene silencing efficiency of the *FgCYP51* genes seems to increase with dsRNA lengths. Whereas gene silencing efficiency of target as well as non-target genes of 250 bp single constructs was within the scope of 60%, 800 bp constructs reduced expression of all *FgCYP51* genes by 80%. Why this doesn't additionally constitute a boost for resistance against *Fg* cannot be explained yet but would strengthen the argument that target gene selection goes superior to dsRNA length. Another explanation for these similar

phenotypes could be that the plants expressing single constructs were already highly resistant so that infection area could not be further restricted by enhanced *FgCYP51* silencing.

From theory a longer precursor can be processed into a greater number of active siRNAs, what could be already observed in some insect species. In the western corn rootworm, silencing efficiency increased with increasing dsRNA lengths (60-200 bp), whereas a minimum of 60 bp dsRNA is required for successful gene silencing (Bolognesi et al., 2012). By targeting the same gene in aphids only dsRNA and not siRNAs were able to achieve gene silencing (Mulot et al., 2016). In general the optimal dsRNA length varies hardly among insect species whereas in most studies 140 to 520 nucleotides were reported to provoke successful gene silencing (Andrade and Hunter, 2016). Probably precursor length limitations are only true for worms and higher eukaryotes as in fungi active uptake of long and short dsRNAs resulted in target gene silencing (Jöchl et al., 2009; Khatri and Rajam, 2007; Majumdar et al., 2017; Wang et al., 2016). It must also be considered that the incorporated dsRNA precursor seems to be processed by the insect itself while this is unclear in HIGS against fungi (Fig. 27A). For example it could be shown in bollworm that a higher dsRNA expression in plants correlates with a more efficient RNAi response (Mao et al., 2007). The same is true for aphids. A low accumulation of siRNAs in the plant did not result in less effective gene silencing, suggesting that the long dsRNA, rather than the siRNA, are the molecules that prime silencing (Mulot et al., 2016).

Considering that increasing the length of dsRNA constructs against *Fg* did not clearly increase the resistance, the use of shorter dsRNA under 500 bp is recommended. As shown by qRT-PCR especially with 800 bp constructs, off-target effects in non-targeted *FgCYP51* genes are amplified as well (Fig. 11). Obviously with increasing length of the precursor also off-targets in other non-target genes, organisms or the plant itself are more likely. This has been already proven by bioinformatics (Qiu et al., 2005; Senthil-Kumar and Mysore, 2011) and could be confirmed for the here assessed CYP constructs (Fig. 12). Unintended off-target silencing in the host have been observed for example in HIGS against *Aspergillus flavus*, what resulted in growth impairment of transgenic plants (Masanga et al., 2015). But this did not apply for CYP-dsRNA-expressing plants as no obvious phenotypic changes were observed. Besides widespread off-target analysis in *Arabidopsis* and barley have been performed for the CYP3RNA (Koch et al., 2013). Beside length, several other factors could influence the silencing efficiency including the expression level and accessibility of the target mRNA, the primary sequence and the secondary structure of the mRNA that can affect accessibility by the RISC complex, amount and sequence of dsRNA precursor, and the turnover of transcripts. For

example, plant DCLs seem to operate preferentially on GC-rich regions what could influence the plants ability to process the precursor into active siRNAs (Ho et al., 2007).

In general, the analysis of dsRNA constructs with different lengths from around 200 bp to over 1500 bp suggest that there is no size limitation for a dsRNA to function in HIGS. Although qRT-PCR results indicate that gene silencing efficiency increased with dsRNA length, phenotypes on plants do not clearly prove a correlation. Conclusions are additionally aggravated by the fact that off-target effects, like already discussed for *FgCYP51* gene function, mask the influence of the individual constructs on *Fg* infection.

4.3 Influence of the dsRNA design on the gene silencing efficiency of the *FgCYP51* genes

The above discussed results indicate that further research is needed to resolve the mechanism of HIGS against *Fusarium*. This was additionally highlighted by RNA sequencing of CYP3RNA expressing plants showing that most siRNAs seem to be processed from the *FgCYP51A* fragment of the precursor (Fig. 3). Nevertheless, the CYP3RNA has been shown to be highly effective in gene silencing of all three *FgCYP51* genes (Koch et al., 2013). Prominent off-target effects as observed in this study could probably explain why. To assess whether the efficiency of the CYP3RNA is caused by positional and/or sequence based effects several dsRNA designs (Fig. 13) were tested in *Fusarium* infection assays. Changing positions of the *FgCYP51* derived fragments like in CYP-ABC and CYP-BCA did not largely influence the gene silencing efficiency (Fig. 14). Comparable to CYP3RNA expressing plants, CYP-ABC reduced the expression of all target genes and CYP-BCA the expression of *FgCYP51A* and *FgCYP51C* by about 50% or more. Surprisingly *FgCYP51B* expression in CYP-BCA expressing plants was comparable to wt plants what cannot be explained at this stage. Also in the CYP3RNA, the *FgCYP51B* derived fragment is at the beginning of the precursor. In general, these experiments must be repeated because of large inconsistencies between phenotypes and gene expression. For example, the reduction of all *FgCYP51* genes in CYP-ABC did not lead to resistance against *Fg*. Additionally, experiments should be combined with RNA sequencing to clearly determine whether siRNA profiles changed in comparison to CYP3RNA plants.

By triplication of the single constructs as in CYP-AAA/BBB/CCC a higher gene silencing efficiency of target genes should be achieved, in theory by a higher number of precursor molecules. Unexpectedly this resulted in upregulation of all *FgCYP51* genes in CYP-CCC expressing plants (Fig. 14). One probable explanation would be that the precursor molecule folds in a 3D structure that is not recognized by the RNAi machinery and consequently not processed by DCL proteins. This could happen by incorrect base-pairing of ssRNA transcripts

for example by pairing of only one or two of the identical *FgCYP51C* sequence fragments or even by base-pairing between three ssRNA transcripts. This would result in inappropriate dsRNA generation. In CYP-AAA and CYP-BBB expressing plants only *FgCYP51C* was upregulated whereas the other two genes were silenced. Both plants were highly resistant against *Fg* infection suggesting that *FgCYP51C* is not crucial for *Fg* growth on leaves. This is supported by previous studies showing that *FgCYP51C* has only minor functions in ergosterol biosynthesis and is not necessary for infection of *Arabidopsis* floral tissue (Fan et al., 2013). In general, triplication of single constructs did not enhance the gene silencing efficiency of the *FgCYP51* genes, as also single constructs CYP-A, CYP-B and CYP-C provoked silencing of all three *FgCYP51* genes in a range of 50% or more. Aggravating CYP-CCC seems, because of unknown reasons, not to be processed by the plants RNAi machinery. This further suggest that silencing efficiency during HIGS is probably more dependent from an efficient transport of siRNAs into the fungus than from the amount of precursor molecules and/or siRNAs in the plant. This is clearly distinct from insects where it is shown that the amount of precursor molecule correlates with the gene silencing efficiency (Mao et al., 2007; Mulot et al., 2016).

The above-mentioned peak in the sequencing result of CYP3RNA (Fig. 3) plants led to the speculation that this specific sequence in the *FgCYP51A* derived fragment can be processed into a high number of active siRNAs by the plants RNAi machinery. Construct CYP-HSA was generated to analyse whether this is caused by the sequence itself and surprisingly this short sequence of only 100 bp provoked resistance enhancement by over 80% and strong target as well as non-target gene silencing (Fig. 14). This suggests that the peak observed in the CYP3RNA precursor is indeed caused by the sequence itself and not by the position of CYP-A in the middle of the construct. Certainly, this has to be confirmed by RNA-sequencing.

Sequence specific effects were analysed additionally by changing the position of the dsRNA in the respective *FgCYP51* gene as in CYP-A5', CYP-B5' and CYP-Cmiddle. Thereby CYP-Cmiddle strongly reduced the expression of his target gene by over 90% and additionally non-target genes *FgCYP51B* and *FgCYP51A* were reduced by 50% (Fig. 14). Though the phenotype on leaves was hardly contrasting and infection severity was similar to the wt. This phenomenon has been already observed with the CYP-C single construct where strong silencing of all *FgCYP51* genes by over 50% did not cause a significant resistance enhancement (Fig. 5). This cannot be explained, and the phenotypes should probably be analysed again. Especially for the here discussed constructs it is noticeable that infection assays had to be performed with T1 generation plants because no other plants were available at that time. For infection assays with the other constructs at least T2 generation plants were assessed. Other studies with aphids

already observed that silencing efficiency varies greatly between plant generations (Mulot et al., 2016). Switching the position of the dsRNA sequence in the respective *FgCYP51* gene led in the case of CYP-A5' to target gene silencing and non-significant co-silencing of *FgCYP51C* but not *FgCYP51B* (Fig. 14). As *FgCYP51B* is reported to be the major enzyme involved in sterol demethylation (Fan et al., 2013) this would explain why plants were not resistant against *Fg*. Co-silencing effects of CYP-A5' were not as prominent as seen with CYP-A single construct (compare Fig. 5 and Fig. 14). Supporting to this it is already reported that the beginning of a CDS has lower off-target errors. Nevertheless they do not recommend the 5' region for dsRNA design because this region is rich in binding sites for regulatory proteins (Qiu et al., 2005). This probably explains why CYP-B5' did not lead to target but only non-target gene silencing. Binding of regulatory proteins to the 5' region could impede the attachment of active siRNAs to the *FgCYP51B* mRNA and consequently gene silencing. Co-silencing siRNAs that are not binding to the 5' regions of *FgCYP51A* and *FgCYP51C* could in contrast lead to gene silencing.

4.4 Plant extracellular vesicles contain CYP3RNA originating siRNAs

Beside the already discussed questions about the nature of the transported RNA molecules during HIGS and SIGS also the mechanism of transport is unresolved. Several hypotheses include the transport via extracellular vesicles (EVs) that are comparable to mammalian exosomes or alternatively the uptake via membrane localized RNA transporters (Koch and Kogel, 2014; Majumdar et al., 2017). Recent research examples showing that EVs can be isolated from *Arabidopsis* and that vesicle production is enhanced after pathogen attack, make a vesicle-based transport a likely scenario (Rutter and Innes, 2017). Apart from this, no homologs of RNA uptake transporters like for example the SID-1 and SID-2 proteins from *C. elegans* (McEwan et al., 2012; Shih and Hunter, 2011) could be identified in fungi.

Therefore, I focused on the vesicle-based transport theory and successfully isolated exosome-like nanoparticles from CYP3RNA expressing *Arabidopsis* leaves. Thereby techniques like ultracentrifugation and sucrose purification, that are routinely used for the isolation of mammalian exosomes (Li et al., 2017), were shown to be suitable for plant vesicles. The isolated vesicles had an average diameter of around 100 nm (Tab. 19), what goes perfectly in line with the size range reported for mammalian exosomes of 30-150 nm (Raposo and Stoorvogel, 2013). The physical appearance after TEM analysis was similar to typical exosome preparations from cell culture supernatants (Fig. 15). Vesicles showed a cup-shaped morphology and were surrounded by a bilayer indicating that the isolated vesicles were comparable to exosomes (Li et al., 2017; Lobb et al., 2015). Together with the fact that plant

vesicles float in a sucrose gradient and were concentrated specifically in the interface of the 30% and 45% sucrose layer suggest that they are related to exosomes or similar vesicles observed in animals. Earlier studies using sucrose purification of exosomes also report that they locate between the 30% and 45% gradient (Mu et al., 2014; Sun et al., 2010).

Like mammalian exosomes, plant vesicles contained RNA cargo identified by RNA extraction from vesicle preparation and subsequent RNA sequencing. Sucrose gradient centrifugation has been used repeatedly for exosome purification and subsequent RNA sequencing and is shown to effectively separate exosomes and other extracellular vesicles from contaminants like protein aggregations and nucleic acids (Alexander et al., 2016; van Balkom et al., 2015). Consequently, the identified RNA was contained inside vesicles. RNA sequencing revealed siRNAs originating from the CYP3RNA precursor strongly indicating that plant processed siRNAs are incorporated in intracellular vesicles. After fusion with the plasma membrane these vesicles could cross the plant – fungal interface and enable siRNA transport during HIGS. This is supported by earlier studies. After fungal infection the formation of MVBs and paramural vesicles between cell wall and cell membrane seems to be enhanced (An et al., 2006a; Wang et al., 2014).

The here applied techniques include physical destruction of the cell wall during the isolation process, so the biogenesis of these vesicles or whether they are of intra- or extracellular origin, is questionable. Another characteristic of exosomes is their endosomal origin what distinguish them from other extracellular vesicles like microvesicles or apoptotic bodies that can be found in animals (Raposo and Stoorvogel, 2013). As the antibodies for suitable marker proteins that could prove an endosomal origin were not available for this study we cannot confirm that the isolated vesicles should be called exosomes. But considering that also the plasma membrane derived microvesicles can contain cell specific RNA cargo and are able to shuttle between cells, this is probably not necessary to answer our initial question (Cocucci et al., 2009; Hoy and Buck, 2012). As discussed, the isolated plant vesicles share multiple characteristics of mammalian exosomes, so it is likely that they also have similar functions in intercellular and interspecies communication in plants. The identification of CYP3RNA originating siRNAs inside the vesicles greatly suggest that they undertake important functions during HIGS against *Fusarium* and possibly constitute the main transport route of cross-kingdom silencing signals between these two species. The involvement of EVs in cross-kingdom communication has been shown for many different species before, including fungi (Peres da Silva et al., 2015), nematodes (Quintana et al., 2017) and plant pathogenic bacteria (Katsir and Bahar, 2017). In mammalian cells it is already proven that parasitic small RNAs are transported to host cells via

vesicles (Buck et al., 2014; Zhu et al., 2016). Until now it is highly unresolved how specificity is achieved in terms of which RNAs are packed into vesicles neither how RNAs are selectively incorporated into different classes of EVs. It is discussed that protein interaction partners, probably components of the RISC complex, are involved. For example AGO2 was identified in exosomes secreted from monocytes (Gibbings et al., 2009).

Until recently, the existence of exosomes or any type of EVs was questionable in plants so there are only few studies that can be used as reference. Rutter and Innes (2017) provided the first evident proof that EVs of endosomal origin exist in plants. By comparison of EVs from Rutter and Innes with the here shown vesicles the morphologies are greatly alike (Fig. 15) suggesting that comparable vesicles could be isolated by the method we used. However, to prove an extracellular origin, we repeated the vesicle isolation from CYP3RNA expressing plants by applying the same methods as described by Rutter and Innes. We were able to isolate EVs from the apoplastic fluid of *Arabidopsis* leaves that were in the same size range as described by Rutter and Innes. By light scattering they found the most abundant particles in a size range of 150 nm in diameter. Our average diameter by considering wt as well as CYP3RNA plants was about 130 nm (Tab. 19). These slight differences are probably also based on the measurement techniques. It has to be considered that light-scattering measurement of the whole isolation approach is probably more exact than measurement of individual vesicle diameters by ImageJ. The diameter of EVs from apoplastic fluid was also slightly bigger than from the previous method using cell lysate. Besides large differences of the experimental procedures this can be explained by the lack of the sucrose purification step. Consequently, probably distinct classes of EVs were isolated in the process. Also, cup-shaped appearance was not as prominent as observed before. The cup-shaped morphology can be explained by extreme dehydration of the vesicles during the sample preparation process of conventional electron microscopy (Li et al., 2017). Thus, it is not a quality feature for exosomes and can most likely vary from preparation to preparation. Rutter and Innes proved by immunodetection of several maker proteins for the plasma membrane, Golgi bodies as well as early and late endosome that vesicles formation was not caused by cellular damage neither are they reconstituted from the plasma membrane (Rutter and Innes, 2017). As we did not have any of these antibodies by hand we cannot provide this proof here. But we argue that by applying the exact same method it is certain that our EVs were extracted exclusively from apoplastic fluid and consequently are of extracellular origin. Whether they are of endosomal origin like mammalian exosomes or whether different classes of EVs were isolated was not relevant for our initial question. As the mechanism of RNA uptake

by the fungus is also unclear it is possible that also membrane derived vesicles like microvesicles could be involved.

RNA sequencing of EVs revealed CYP3RNA originating siRNAs as seen before in vesicles from whole leaves. RNAse A digest was performed previous to RNA extraction to prove that RNA was protected inside the lumen of EVs. This greatly suggest that siRNA contained vesicles are transported out of the cell most likely by fusion with the plasma membrane like seen in animals (Hoy and Buck, 2012). The results provide new inside into the mechanism of HIGS against fungi. They further provide another proof that EVs exist in plants and probably undertake similar functions in intercellular communication and probably cross-kingdom communication like in animals.

One characteristic of earlier siRNA profiling of CYP3RNA expressing plants or fungal cultures treated with CYP3RNA was a clear overrepresentation of *FgCYP51A* derived siRNAs (Fig. 3; Koch et al., 2016). This could be confirmed by the here shown sequencing results but not in the same extent as seen before, what can be probably explained by the smaller library size (Fig. 17; Fig. 19; Fig. 21). In earlier studies at least 5 million reads were analysed (Koch et al., 2016) whereas vesicle derived libraries contained mostly under 3 million reads (Tab. 15). Most notably was the extremely low number of siRNAs in EVs matching to *FgCYP51B* (Fig. 19). Such a minor transport of *FgCYP51B* targeting siRNAs to the fungus would strengthen the above discussed argument that the efficiency of the CYP3RNA is eminently boosted by co-silencing effects. The formation and amplification of secondary siRNAs in the fungus would explain why *FgCYP51B* can be silenced without an efficient generation and transport of *FgCYP51B* targeting siRNAs. Again, it is noteworthy that the library size was probably not sufficient to cover the whole range of vesicle contained siRNAs. Whole RNA profiling studies of human exosomes are performed with over 5 million reads (Huang et al., 2013; Rodríguez et al., 2017). For small RNA sequencing in general, 1-2 million and 5-8 million reads are recommended for differential expression and discovery of new microRNAs respectively. (Campbell et al., 2015; Metpally et al., 2013). Seeing that all vesicle libraries contained over 2 million reads (Tab. 15), I would expect that the data quality is sufficient for the simple yes or no question that has been analysed here. Nevertheless, one can probably not assume that the sequencing result reflects the full picture of plant transferred small RNAs. Therefore, upscaling of the vesicle isolation to improve the RNA yield should be considered.

Tab. 19 Average diameter of exosome-like nanoparticles from *Arabidopsis* and barley. Average diameter was analysed with the ImageJ Software based on microscopy scale bars. Standard errors (±SE) are given in parentheses.

sample	vesicle diameter [nm]	preparation method
Arabidopsis wt	94,8 [± 2,5]	whole leaves
Arabidopsis CYP3RNA	105,2 [± 3,6]	whole leaves
Arabidopsis wt	118,6 [± 6,5]	apoplastic washes
Arabidopsis CYP3RNA	141,4 [± 8,0]	apoplastic washes
barley TE	166,6 [±17,8]	apoplastic washes
barley CYP3	155,8 [±21,0]	apoplastic washes

4.5 Vesicles are involved in siRNA transport during SIGS

After showing that HIGS construct derived siRNAs are incorporated into plant vesicles and in this way probably transported into the fungus, the question whether this is happening also during SIGS emerged. The results shown in this work and earlier studies suggest that there are large differences between the two mechanisms (Höfle et al., 2018 in revision; Koch et al., 2016). Whereas HIGS is virtually based on the plants RNAi machinery, SIGS constitutes a more complex situation. The fact that the dsRNA precursor is transported and subsequently processed by the fungus, make it questionable whether siRNAs are transported as well (Koch et al., 2016). By application of the methods used for isolation of EVs from *Arabidopsis*, vesicles could be successfully isolated from the apoplastic fluid of barley leaves that were spray treated with CYP3RNA. In comparison to *Arabidopsis* the infiltration time had to be increased and multiple cycles of vacuum and derepression were necessary to assure complete infiltration of leaves. This was probably caused by a different leaf morphology of the plants like for example cuticula diameter that aggravated vacuum infiltration in barley. Nevertheless, vesicles showed the typical morphology and were surrounded by a bilayer as observed before. The vesicle diameter was slightly bigger than for EVs from *Arabidopsis*. As these are two complete different species this was not surprising and is probably not comparable. Additionally, the overall yield of vesicles was notably smaller than for *Arabidopsis* what caused higher variability in vesicle diameter resulting also in higher standard errors (Tab. 19). Because the production of dsRNA that was used for these experiments is highly expensive it was not possible to extensively increase the amount of starting material. However, the amount and quality of RNA extracted from the vesicles was sufficient for library generation as well as small RNA sequencing and the resulting library size was comparable to the *Arabidopsis* samples (Tab. 15). siRNA profiling revealed CYP3RNA matching hits, but these were considerably lower than seen before with *Arabidopsis* HIGS plants (Fig. 21). Because of the already mentioned fact that CYP3RNA can

be transported into the fungus and that the fungal RNAi machinery is crucial for gene silencing (Koch et al., 2016), the siRNA transport probably plays a more substantial role in HIGS than in SIGS. This is supported by a very recent study showing that after external application, dsRNAs instead of plant processed siRNAs are taken up by insects from tomato leaves (Gogoi et al., 2017). Nevertheless, the here shown results indicate that both, siRNA and dsRNA transport takes place during SIGS against fungi. Even in other studies examining this silencing approach externally applied siRNAs as well as dsRNA provoked gene silencing (Wang et al., 2016). Whether a vesicle based transport should be also considered for the transport of longer dsRNA molecules cannot be answered yet. Therefore, whole RNA profiling from plant EVs instead of small RNA sequencing should be considered for future studies.

4.6   RNA can be co-purified with RNA-binding proteins by immunoprecipitation

RNA-binding proteins (RBPs) have been shown to be indispensable for proper processing of small RNAs by Dicer-like proteins (DCL) during RNA interference and certainly also for the generation of siRNAs from transgenes (Curtin et al., 2008). The identification of RBPs that are bound to transgene derived dsRNA and/or siRNAs could provide insight into the processing mechanism of transgene derive dsRNA, the protein interaction partners involved in this process as well as the nature of the potential silencing signals. Furthermore, the transport mechanisms in the plant itself as well as cross-kingdom transport of silencing signals as discussed above are highly unresolved. It has been shown that microRNAs and siRNAs travel from cell to cell through plasmodesmata as well as systemically through the phloem (Brosnan and Voinnet, 2011; Molnar et al., 2010; Molnar et al., 2011). However, the protein machinery required for this process is unresolved. It is likely that RBPs are involved in long-distance trafficking of mRNA as well as sRNAs in plants probably through the phloem as shown in pumpkin (Ham et al., 2009; Ham et al., 2014). Here it was assessed whether two characterized pumpkin phloem RBPs, *Cm*PP16 and *Cm*RBP50 (Ham et al., 2009) can bind to CYP3RNA-derived RNA when expressed in *Arabidopsis*. This could be an indication for a phloem mediated transport happening during HIGS. The strategy was chosen because no similar proteins are characterized from *Arabidopsis* what is probably also due to experimental difficulties in obtaining the phloem sap (Tetyuk et al., 2013). Furthermore, it was assessed whether the five DRB proteins from *Arabidopsis* are involved in HIGS against *Fg* by either binding to the CYP3RNA precursor or originating siRNAs. Therefore, a method for purification of the RBPs from crude cell extracts had to be established that is also sensitive enough to leave RNA-protein binding intact. Co-RNA-IP has been used successfully to elucidate interactions between components of the RISC complex and microRNAs as well as siRNAs in *Arabidopsis*. Besides the method has been

shown reliable for RNA sequencing of the co-purified RNA (Carbonell et al., 2012; Garcia-Ruiz et al., 2015).

In this work the method was established for the above-mentioned RBPs that were expressed together with CYP3RNA in *Arabidopsis*. In the future this can help to elucidate RNA-trafficking and long-distance transport of silencing signals during HIGS and SIGS. From five RBPs that could be successfully co-purified in this work, all seem to bind to RNA as indicated by RNA extraction from immunoprecipitated proteins (Fig. 23 and Fig. 25). Although RNA amount was low, differences in the RNA yields from RBP containing samples and ev samples indicate that RNA-binding is not only due to unspecific attachment. The small amount of RNA that could be gained from ev samples is probably explained by unspecific binding to the antibodies, the tag or the beads itself. In further experiments this has to be confirmed by RNA sequencing from samples generated in this work or after collecting of additional RNA samples after upscaling of the experimental extent. To keep experimental costs within a limit, co-RNA-IP was performed on a 1 ml scale using a maximum of 500 mg plant input material and the obtained RNA amounts would be sufficient for sequencing. Modern RNA sequencing can be achieved with less than 10 ng input material but there are studies indicating that low quantities of starting RNA can influence the sequencing quality (Lynch et al., 2010). By duplication or triplication of the input material, it is certain that RNA yield could be increased but simultaneously also would experimental costs. For studies with AGO proteins the tenfold of our starting material was used, though to identify miRNA binding by northern blot where considerably more RNA is required (Carbonell et al., 2012).

In contrast to RBPs from pumpkin that could be detected without any problems after transient expression in *Nb* as well as transgenically in *Arabidopsis*, only three DRB proteins were detectable in *Arabidopsis* (Fig. 23 and Fig. 25). In T1 generation plants DRB4 was detectable only after denaturing protein extraction using SDS but not with the native extraction buffer that was necessary for co-RNA-IP. This is probably explained by the nuclear localization of DRB4 (Curtin et al., 2008) suggesting that the used buffer was not suitable for proper lysis of the nuclear membrane. However reassessment of T2 generation by preparation of the crude nuclear extracts using a previously published protocol (Escobar et al., 2001), revealed DRB4 expression in nuclear as well as cytosolic fractions (Fig. 26). Consequently, it was suggested that the buffer used for IP was not suitable for DRB4 extraction. The only important differences between the two buffers are that extraction buffer from Escobar et al., 2001 included DTT and Sucrose, with the latter probably only added for protection of the nuclei. DTT is normally added to protect sensible proteins against oxidative damage. In further experiments it could be excluded that this

constitutes a problem for DRB4 because immunodetection as well as immunoprecipitation was possible with or without DTT. Probably the problems in detecting DRB4 can be explained by different expression profiles and/or levels between plant generations. DRB4 probably constitutes the most interesting candidate for our questions because it is involved in the generation of 21 nt siRNAs from transgene-encoded or viral transcripts by interaction with DCL4 (Curtin et al., 2008; Eamens et al., 2009).

In contrast DRB3 and DRB5 were not detectable in *Arabidopsis* neither by denaturing nor native protein extraction and also after screening of up to ten different transgenic lines of T1 and T2 generation by western blot. Nevertheless, the successful mRNA production in leaves could be detected by qRT-PCR (data not shown), suggesting that the transgene is properly expressed and protein production probably only under the detection level of the methods used or protein production is restricted to specific plant tissues. Supporting to this DRB3 and DRB5 localization seems to be restricted to the SAM region (Eamens et al., 2012a) explaining why protein level in leaves was probably too low for immunodetection. Specific protein extraction from the SAM should be considered in this case, but whether this results in enough material for co-RNA-IP is questionable. Aggravating is additionally that DRB3 and DRB5 are not involved in the general production of sRNAs and clear functions of both proteins are not resolved (Curtin et al., 2008).

Contrasting to the other DRB proteins, DRB1 and DRB2 could be detected without problems in multiple transgenic lines and successfully purified by IP. DRB1 is one of the best studied DRB proteins and has a prominent role in miRNA processing by interaction with DCL1 to generate 21 nt microRNAs from precursor transcripts (Eamens et al., 2009). It is ubiquitously and constitutively expressed in all plant organs explaining why protein level was high and could be detected without any problems despite its nuclear localization. In contrast, like DRB3 and DRB5 the role of DRB2 in the general sRNA pathway is unknown (Curtin et al., 2008). The protein seems to be involved together with DRB3 and DRB5 in the biogenesis of developmental important miRNAs in the SAM region (Eamens et al., 2012a; Eamens et al., 2012b). Studies show furthermore that constitutive overexpression of DRB2, like performed here, can compensate loss of DRB1 in mutant plants (Eamens et al., 2012a). It is possible that overexpression led to an unnatural expression pattern explaining why DRB2 in contrast to DRB3 and DRB5 could be detected in high amounts in *Arabidopsis* leaves. Contrasting to this but in support with our results, recent studies show that DRB2 is similar to DRB1 expressed in all plant tissues and furthermore has a crucial role in gene regulation by determining whether a miRNA acts by cleavage or translational inhibition of its targets (Reis et al., 2015). In contrast

in the same study no similar function could be determined for DRB3 and DRB5 leaving their exact function unknown.

Altogether, these preliminary studies provided by this work can help to further elucidate the molecular mechanism of HIGS against fungi, what is a prerequisite for application of this technology. The co-purified RNA can be used for future RNA sequencing experiments to examine whether the assessed proteins are involved in CYP3RNA procession or transport. In this way the study could help to further elucidate DRB functions in *Arabidopsis*. Furthermore, after establishment the method could be expanded to other proteins involved in RNAi, like for example AGO proteins.

4.7   Conclusion and future prospects

This PhD project aimed at characterizing the unresolved mechanistic details about HIGS and SIGS against *Fg* that has been previously reported with the CYP3RNA (Koch et al., 2013; Koch et al., 2016). After testing various CYP3RNA derived dsRNA constructs that silence one, two or all three *FgCYP51* genes, it has become apparent that off-target effects should be under consideration in future experiments. On the other side these co-silencing effects make the *FgCYP51* genes to a very effective target for controlling *Fg* infection. Furthermore, the results suggest that selection of the right target gene is superior to dsRNA design. Although, increasing the dsRNA length seemed to enhance gene silencing efficiency as well as co-silencing, this did not constitute a considerable boost for *Fg* resistance. Neither did changing the dsRNA design. However, the results with one of the new constructs, CYP-HSA, which reached the efficiency of the CYP3RNA, indicate that some sequence based effects contribute to the efficiency of the CYP3RNA. This 100 bp construct, which targets *FgCYP51A*, was the shortest construct tested and contained a siRNA hot-spot that has earlier been detected in siRNA profiling of CYP3RNA plants (Fig. 3). The results suggest that this particular sequence can be processed into a high number of siRNAs by the plant's RNAi machinery. Considering that all interpretations were largely aggravated by co-silencing effects of CYP51-dsRNAs, this should be confirmed in future studies by RNA sequencing of these plants.

Showing that EVs from CYP3RNA expressing plants as well as from CYP3RNA sprayed leaves contain precursor derived siRNAs, is a large progress in understanding the RNA transport mechanisms during HIGS and SIGS. Future experiments could investigate whether plant EVs contain, beside siRNAs, also other RNA cargo like mRNAs or microRNAs like in animals (van Balkom et al., 2015). Additionally, the siRNA content could be analysed before and after pathogen infection.

Finally, this study provides some important preliminary work for the elucidation of transgenic siRNA procession and transport in the plant. By establishment of co-RNA-Immunoprecipitation of different RNA-binding proteins, like the five *Arabidopsis* DRB proteins, interactions of dsRNA-derived siRNAs with these proteins could be resolved. This could give further insight into the mechanism of HIGS on the plant's side and the protein interaction partners involved.

5.   Abstract

RNAi based approaches like Host-Induced Gene Silencing (HIGS) and Spray-Induced Gene Silencing (SIGS) have shown great potential in inhibiting pathogen infection in plants. In earlier studies it was demonstrated that inhibiting the sterol 14α-demethylase through silencing of the three *FgCYP51* genes, after delivery through transgene expression or external application of the double-stranded CYP3RNA, effectively controls *Fusarium graminearum* (*Fg*) infection *in planta* (Koch et al., 2013; Koch et al., 2016). In the attempt to silence only one or two of the *FgCYP51* genes, co-silencing effects in the respective non-target *FgCYP51* genes largely influenced the silencing efficiency in HIGS as well as SIGS approaches and masked the influence of individual constructs on *Fg* growth. Therefore, single and double constructs showed efficiencies in inhibiting *Fg* growth similar to the original CYP3RNA. By increasing the length of the single dsRNA constructs, silencing efficiency and co-silencing effects, proven by off-target analysis and qRT-PCR, were enhanced. The results suggest that up to 1500 bp – the longest construct analysed here - there is no length limitation for a dsRNA to function in HIGS. However, increasing the dsRNA length did not constitute a boost for *Fg* resistance, suggesting that target gene selection is more important than the length of dsRNA for effective fungal growth inhibition by HIGS. This was further supported by HIGS studies with constructs in which the design of the dsRNA was largely changed in comparison to the original single, double or the CYP3RNA construct. The changes involved switching the position of the dsRNA in the target gene, triplication of single constructs and transposition of the individual CYP51 fragments in the CYP3RNA.

With the objective to clarify how siRNAs are transferred between plant and fungus during HIGS and SIGS, two different methods were successfully used for the isolation of exosome-like nanoparticles or extracellular vesicles (EVs) from plants. The isolated vesicles shared characteristic features from known exosome preparations of mammalian cells and plant EVs that have been reported recently (Rutter and Innes, 2017). My work further confirmed that EVs from CYP3RNA-expressing plants contained siRNAs that originated from the dsRNA precursor, as proven by small RNA sequencing. The same was shown for EVs from CYP3RNA sprayed leaves. This indicates that the siRNAs, that are transferred during HIGS and SIGS, are indeed transported via vesicles, what was shown for the first time within this study. Therefore, the study gives new insight into the mechanism of RNA-based cross-kingdom communication. Altogether, this PhD project could clarify some important mechanistic details about HIGS and SIGS what is indispensable for a successful future application of these technologies as plant protection measure.

6. Zusammenfassung

RNAi basierte Pflanzenschutzmaßnahmen wie das *Host-Induced Gene Silencing* (HIGS) oder *Spray-Induced Gene Silencing* (SIGS) wurden bereits mit großem Erfolg zur Vermeidung von Pathogeninfektionen eingesetzt. In vorangegangenen Studien wurde gezeigt, dass die CYP3RNA, nach Expression in der Pflanze oder als Folge externer Applikation, zu einem *Silencing* der drei *FgCYP51* Gene führte wodurch eine Inhibierung der Sterol 14α-Demethylase in *Fusarium graminearum* ausgelöst wurde (Koch et al., 2013; Koch et al., 2016). Im Rahmen dieser Doktorarbeit sollten die Auswirkungen eines *Silencing* einzelner *FgCYP51* Gene untersucht werden. Dabei kam es sowohl in HIGS als auch SIGS Versuchen zum *Co-Silencing* von *FgCYP51* Nichtzielgenen wodurch die Auswirkungen der Einzel- bzw. Doppel-Konstrukte auf das pilzliche Wachstum kaschiert wurden. Dies begründete zudem, dass die Einzel- bzw. Doppel-Konstrukte vergleichbar effektiv waren wie die Referenz-dsRNA CYP3RNA. Durch eine Verlängerung der dsRNA wurden diese *Co-Silencing* Effekte und die generelle *Gen-Silencing* Effektivität erhöht. Die Ergebnisse lassen vermuten, dass dsRNAs bis zu einer Länge von 1500 bp erfolgreich in HIGS Studien eingesetzt werden können. Dennoch führte die Verlängerung der dsRNA nicht zu einer erhöhten Resistenz, was vermuten lässt, dass die Wahl eines geeigneten Target-Gens essentieller ist als das Design der eingesetzten dsRNA. Diese Annahme konnte durch weitere Konstrukte bestätigt werden, bei denen das dsRNA Design im Vergleich zur CYP3RNA weitreichend verändert wurde.

Ein weiteres Ziel dieser Arbeit war aufzuklären auf welche Weise siRNAs zwischen Pflanzen und Pilzen transportiert werden. Dabei wurden zwei verschiedene Methoden zur Isolation von Exosom-ähnlichen Vesikeln bzw. extrazellulären Vesikeln (EVs) aus Pflanzen erfolgreich implementiert. Die isolierten Vesikel zeigten die typischen Merkmale von Exsomen aus Humanzellen bzw. pflanzlichen EVs, die kürzlich entdeckt wurden (Rutter and Innes, 2017). Durch Sequenzierung der vesikulären RNA aus CYP3RNA-exprimerenden Pflanzen, konnten siRNAs identifiziert werden, welche dem dsRNA Vorläufermolekül abstammen. Ein ähnliches Ergebnis wurde für EVs aus Blättern erzielt, welche zuvor mit CYP3RNA besprüht wurden. Bislang wurde ausschließlich spekuliert, dass siRNAs während des HIGS sowie SIGS in Vesikeln transportiert werden. Die im Rahmen dieser Doktorarbeit gewonnenen Ergebnisse liefern somit neue Erkenntnisse zur RNA-basierten Kommunikation zwischen Spezies unterschiedlicher Abstammung. Zudem konnten wichtige mechanistische Details der HIGS- sowie SIGS-vermittelten Pathogenkontrolle aufgeklärt werden, was unabdingbar ist für einen zukünftigen Einsatz dieser Technologien und erfolgreichen Transfer als innovative Pflanzenschutzmaßnahme.

7. References

Abdellatef, E., Will, T., Koch, A., Imani, J., Vilcinskas, A. and Kogel, K.-H. (2015) Silencing the expression of the salivary sheath protein causes transgenerational feeding suppression in the aphid Sitobion avenae. *Plant biotechnology journal* **13**, 849–857.

Abdurakhmonov, I. Y., Ayubov, M. S., Ubaydullaeva, K. A., Buriev, Z. T., Shermatov, S. E., Ruziboev, H. S., Shapulatov, U. M., Saha, S., Ulloa, M., Yu, J. Z., Percy, R. G., Devor, E. J., Sharma, G. C., Sripathi, V. R., Kumpatla, S. P., van der Krol, A., Kater, H. D., Khamidov, K., Salikhov, S. I., Jenkins, J. N., Abdukarimov, A. and Pepper, A. E. (2016) RNA Interference for Functional Genomics and Improvement of Cotton (Gossypium sp.). *Frontiers in plant science* **7**, 202.

Abhishek Shrestha (2016). *Functional characterization of essential fungal CYP51 ergosterol biosynthesis genes using HIGS as well as SIGS strategies*. Masterthesis. JLU Gießen.

Admyre, C., Johansson, S. M., Qazi, K. R., Filen, J.-J., Lahesmaa, R., Norman, M., Neve, E. P. A., Scheynius, A. and Gabrielsson, S. (2007) Exosomes with Immune Modulatory Features Are Present in Human Breast Milk. *The Journal of Immunology* **179**, 1969–1978.

Alakonya, A., Kumar, R., Koenig, D., Kimura, S., Townsley, B., Runo, S., Garces, H. M., Kang, J., Yanez, A., David-Schwartz, R., Machuka, J. and Sinha, N. (2012) Interspecific RNA interference of SHOOT MERISTEMLESS-like disrupts Cuscuta pentagona plant parasitism. *The Plant cell* **24**, 3153–3166.

Alexander, P., Brown, C., Arneth, A., Finnigan, J., Moran, D. and Rounsevell, M. D. A. (2017) Losses, inefficiencies and waste in the global food system. *Agricultural systems* **153**, 190–200.

Alexander, R. P., Chiou, N.-T. and Ansel, K. M. (2016) Improved exosome isolation by sucrose gradient fractionation of ultracentrifuged crude exosome pellets. *Protocol Exchange*.

An, Q., Ehlers, K., Kogel, K.-H., van Bel, A. J. E. and Huckelhoven, R. (2006a) Multivesicular compartments proliferate in susceptible and resistant MLA12-barley leaves in response to infection by the biotrophic powdery mildew fungus. *The New phytologist* **172**, 563–576.

An, Q., Hückelhoven, R., Kogel, K.-H. and van Bel, A. J. E. (2006b) Multivesicular bodies participate in a cell wall-associated defence response in barley leaves attacked by the pathogenic powdery mildew fungus. *Cellular microbiology* **8**, 1009–1019.

Andrade, C. M., Tinoco, M. L. P., Rieth, A. F., Maia, F. C. O. and Aragão, F. J. L. (2016) Host-induced gene silencing in the necrotrophic fungal pathogen Sclerotinia sclerotiorum. *Plant Pathol* **65**, 626–632.

Andrade, E. C. de and Hunter, W. B. (2016) RNA Interference – Natural Gene-Based Technology for Highly Specific Pest Control (HiSPeC). In: *RNA Interference* (Abdurakhmonov, I.Y., ed): InTech.

Arunachalam, C. and Doohan, F. M. (2013) Trichothecene toxicity in eukaryotes: Cellular and molecular mechanisms in plants and animals. *Toxicology letters* **217**, 149–158.

Baulcombe, D. (2004) RNA silencing in plants. *Nature* **431**, 356–363.

Becher, R., Hettwer, U., Karlovsky, P., Deising, H. B. and Wirsel, S. G. R. (2010) Adaptation of Fusarium graminearum to tebuconazole yielded descendants diverging for levels of fitness, fungicide resistance, virulence, and mycotoxin production. *Phytopathology* **100**, 444–453.

Becher, R., Weihmann, F., Deising, H. B. and Wirsel, S. G. (2011) Development of a novel multiplex DNA microarray for Fusarium graminearum and analysis of azole fungicide responses. *BMC genomics* **12**, 52.

Bechtold, N. and Pelletier, G. (1998) In Planta AgrobacteriumMediated Transformation of Adult Arabidopsis thaliana Plants by Vacuum Infiltration. In: *Arabidopsis Protocols* (Martinez-Zapater, J.M. and Salinas, J., eds), pp. 259–266. Totowa, NJ: Humana Press.

Bhatia, V., Bhattacharya, R., Uniyal, P. L., Singh, R. and Niranjan, R. S. (2012) Host generated siRNAs attenuate expression of serine protease gene in Myzus persicae. *PloS one* **7**, e46343.

Birmingham, A., Anderson, E. M., Reynolds, A., Ilsley-Tyree, D., Leake, D., Fedorov, Y., Baskerville, S., Maksimova, E., Robinson, K., Karpilow, J., Marshall, W. S. and Khvorova, A. (2006) 3' UTR seed matches, but not overall identity, are associated with RNAi off-targets. *Nature methods* **3**, 199–204.

Blake, A. J., Finger, D. S., Hardy, V. L. and Ables, E. T. (2017) RNAi-Based Techniques for the Analysis of Gene Function in Drosophila Germline Stem Cells. *Methods in molecular biology (Clifton, N.J.)* **1622**, 161–184.

Bolognesi, R., Ramaseshadri, P., Anderson, J., Bachman, P., Clinton, W., Flannagan, R., Ilagan, O., Lawrence, C., Levine, S., Moar, W., Mueller, G., Tan, J., Uffman, J., Wiggins, E., Heck, G. and Segers, G. (2012) Characterizing the mechanism of action of double-stranded RNA activity against western corn rootworm (Diabrotica virgifera virgifera LeConte). *PloS one* **7**, e47534.

Borges, F. and Martienssen, R. A. (2015) The expanding world of small RNAs in plants. *Nature reviews. Molecular cell biology* **16**, 727–741.

Brosnan, C. A. and Voinnet, O. (2011) Cell-to-cell and long-distance siRNA movement in plants: Mechanisms and biological implications. *Current opinion in plant biology* **14**, 580–587.

Brown, N. A., Evans, J., Mead, A. and Hammond-Kosack, K. E. (2017) A spatial temporal analysis of the Fusarium graminearum transcriptome during symptomless and symptomatic wheat infection. *Molecular plant pathology*.

Brown, N. A., Urban, M., van de Meene, A. M. L. and Hammond-Kosack, K. E. (2010) The infection biology of Fusarium graminearum: Defining the pathways of spikelet to spikelet colonisation in wheat ears. *Fungal biology* **114**, 555–571.

Buck, A. H., Coakley, G., Simbari, F., McSorley, H. J., Quintana, J. F., Le Bihan, T., Kumar, S., Abreu-Goodger, C., Lear, M., Harcus, Y., Ceroni, A., Babayan, S. A., Blaxter, M., Ivens, A. and Maizels, R. M. (2014) Exosomes secreted by nematode parasites transfer small RNAs to mammalian cells and modulate innate immunity. *Nature communications* **5**, 5488.

Buhtz, A., Springer, F., Chappell, L., Baulcombe, D. C. and Kehr, J. (2008) Identification and characterization of small RNAs from the phloem of Brassica napus. *The Plant journal for cell and molecular biology* **53**, 739–749.

Caby, M.-P., Lankar, D., Vincendeau-Scherrer, C., Raposo, G. and Bonnerot, C. (2005) Exosomal-like vesicles are present in human blood plasma. *International immunology* **17**, 879–887.

Campbell, J. D., Liu, G., Luo, L., Xiao, J., Gerrein, J., Juan-Guardela, B., Tedrow, J., Alekseyev, Y. O., Yang, I. V., Correll, M., Geraci, M., Quackenbush, J., Sciurba, F., Schwartz, D. A., Kaminski, N., Johnson, W. E., Monti, S., Spira, A., Beane, J. and Lenburg, M. E. (2015) Assessment of microRNA differential expression and detection in multiplexed small RNA sequencing data. *RNA (New York, N.Y.)* **21**, 164–171.

Carbonell, A., Fahlgren, N., Garcia-Ruiz, H., Gilbert, K. B., Montgomery, T. A., Nguyen, T., Cuperus, J. T. and Carrington, J. C. (2012) Functional analysis of three Arabidopsis ARGONAUTES using slicer-defective mutants. *The Plant cell* **24**, 3613–3629.

Cerutti, H. and Casas-Mollano, J. A. (2006) On the origin and functions of RNA-mediated silencing: From protists to man. *Current genetics* **50**, 81–99.

Chen, W., Kastner, C., Nowara, D., Oliveira-Garcia, E., Rutten, T., Zhao, Y., Deising, H. B., Kumlehn, J. and Schweizer, P. (2016) Host-induced silencing of Fusarium culmorum genes protects wheat from infection. *Journal of experimental botany* **67**, 4979–4991.

Chen, Y., Gao, Q., Huang, M., Liu, Y., Liu, Z., Liu, X. and Ma, Z. (2015) Characterization of RNA silencing components in the plant pathogenic fungus Fusarium graminearum. *Scientific reports* **5**, 12500.

Cheng, W., Song, X.-S., Li, H.-P., Cao, L.-H., Sun, K., Qiu, X.-L., Xu, Y.-B., Yang, P., Huang, T., Zhang, J.-B., Qu, B. and Liao, Y.-C. (2015) Host-induced gene silencing of an essential chitin synthase gene confers durable resistance to Fusarium head blight and seedling blight in wheat. *Plant biotechnology journal* **13**, 1335–1345.

Cocucci, E., Racchetti, G. and Meldolesi, J. (2009) Shedding microvesicles: Artefacts no more. *Trends in cell biology* **19**, 43–51.

Colombo, M., Raposo, G. and Thery, C. (2014) Biogenesis, secretion, and intercellular interactions of exosomes and other extracellular vesicles. *Annual review of cell and developmental biology* **30**, 255–289.

Crescitelli, R., Lasser, C., Szabo, T. G., Kittel, A., Eldh, M., Dianzani, I., Buzas, E. I. and Lotvall, J. (2013) Distinct RNA profiles in subpopulations of extracellular vesicles: Apoptotic bodies, microvesicles and exosomes. *Journal of extracellular vesicles* **2**.

Curtin, S. J., Watson, J. M., Smith, N. A., Eamens, A. L., Blanchard, C. L. and Waterhouse, P. M. (2008) The roles of plant dsRNA-binding proteins in RNAi-like pathways. *FEBS letters* **582**, 2753–2760.

Dahlgren, C., Zhang, H.-Y., Du, Q., Grahn, M., Norstedt, G., Wahlestedt, C. and Liang, Z. (2008) Analysis of siRNA specificity on targets with double-nucleotide mismatches. *Nucleic acids research* **36**, e53.

Di Tommaso, P., Chatzou, M., Floden, E. W., Barja, P. P., Palumbo, E. and Notredame, C. (2017) Nextflow enables reproducible computational workflows. *Nature biotechnology* **35**, 316–319.

Ding, M., Zhu, Q., Liang, Y., Li, J., Fan, X., Yu, X., He, F., Xu, H., Liang, Y. and Yu, J. (2017) Differential roles of three FgPLD genes in regulating development and pathogenicity in Fusarium graminearum. *Fungal genetics and biology FG & B* **109**, 46–52.

Doll, S. and Danicke, S. (2011) The Fusarium toxins deoxynivalenol (DON) and zearalenone (ZON) in animal feeding. *Preventive veterinary medicine* **102**, 132–145.

Dunoyer, P., Melnyk, C., Molnar, A. and Slotkin, R. K. (2013) Plant mobile small RNAs. *Cold Spring Harbor perspectives in biology* **5**.

Eamens, A. L., Kim, K. W., Curtin, S. J. and Waterhouse, P. M. (2012a) DRB2 is required for microRNA biogenesis in Arabidopsis thaliana. *PloS one* **7**, e35933.

Eamens, A. L., Smith, N. A., Curtin, S. J., Wang, M.-B. and Waterhouse, P. M. (2009) The Arabidopsis thaliana double-stranded RNA binding protein DRB1 directs guide strand selection from microRNA duplexes. *RNA (New York, N.Y.)* **15**, 2219–2235.

Eamens, A. L., Wook Kim, K. and Waterhouse, P. M. (2012b) DRB2, DRB3 and DRB5 function in a non-canonical microRNA pathway in Arabidopsis thaliana. *Plant signaling & behavior* **7**, 1224–1229.

Echeverri, C. J., Beachy, P. A., Baum, B., Boutros, M., Buchholz, F., Chanda, S. K., Downward, J., Ellenberg, J., Fraser, A. G., Hacohen, N., Hahn, W. C., Jackson, A. L., Kiger, A., Linsley, P. S., Lum, L., Ma, Y., Mathey-Prévôt, B., Root, D. E., Sabatini, D. M., Taipale, J., Perrimon, N. and Bernards, R. (2006) Minimizing the risk of reporting false positives in large-scale RNAi screens. *Nature methods* **3**, 777–779.

Eddy, S. R. (2011) Accelerated Profile HMM Searches. *PLoS computational biology* **7**, e1002195.

Escobar, C., Aristizéabal, F., Navas, A., Del Campo, F. F. and Fenoll, C. (2001) Isolation of active DNA-binding nuclear proteins from tomato galls induced by root-knot nematodes. *Plant Mol Biol Rep* **19**, 375–376.

Fan, J., Urban, M., Parker, J. E., Brewer, H. C., Kelly, S. L., Hammond-Kosack, K. E., Fraaije, B. A., Liu, X. and Cools, H. J. (2013) Characterization of the sterol 14α-demethylases of Fusarium graminearum identifies a novel genus-specific CYP51 function. *The New phytologist* **198**, 821–835.

Felippes, F. F. de, Marchais, A., Sarazin, A., Oberlin, S. and Voinnet, O. (2017) A single miR390 targeting event is sufficient for triggering TAS3-tasiRNA biogenesis in Arabidopsis. *Nucleic acids research* **45**, 5539–5554.

Fernández-Ortuño, D., Loza-Reyes, E., Atkins, S. L. and Fraaije, B. A. (2010) The CYP51C gene, a reliable marker to resolve interspecific phylogenetic relationships within the Fusarium species complex and a novel target for species-specific PCR. *International journal of food microbiology* **144**, 301–309.

Finn, R. D., Coggill, P., Eberhardt, R. Y., Eddy, S. R., Mistry, J., Mitchell, A. L., Potter, S. C., Punta, M., Qureshi, M., Sangrador-Vegas, A., Salazar, G. A., Tate, J. and Bateman, A.

(2016) The Pfam protein families database: towards a more sustainable future. *Nucleic acids research* **44**, D279-85.

Fire, A., Xu, S., Montgomery, M. K., Kostas, S. A., Driver, S. E. and Mello, C. C. (1998) Potent and specific genetic interference by double-stranded RNA in Caenorhabditis elegans. *Nature* **391**, 806–811.

Garcia-Ruiz, H., Carbonell, A., Hoyer, J. S., Fahlgren, N., Gilbert, K. B., Takeda, A., Giampetruzzi, A., Garcia Ruiz, M. T., McGinn, M. G., Lowery, N., Martinez Baladejo, M. T. and Carrington, J. C. (2015) Roles and programming of Arabidopsis ARGONAUTE proteins during Turnip mosaic virus infection. *PLoS pathogens* **11**, e1004755.

Ghag, S. B., Shekhawat, U. K. S. and Ganapathi, T. R. (2014) Host-induced post-transcriptional hairpin RNA-mediated gene silencing of vital fungal genes confers efficient resistance against Fusarium wilt in banana. *Plant biotechnology journal* **12**, 541–553.

Gibbings, D. J., Ciaudo, C., Erhardt, M. and Voinnet, O. (2009) Multivesicular bodies associate with components of miRNA effector complexes and modulate miRNA activity. *Nature cell biology* **11**, 1143–1149.

Gogoi, A., Sarmah, N., Kaldis, A., Perdikis, D. and Voloudakis, A. (2017) Plant insects and mites uptake double-stranded RNA upon its exogenous application on tomato leaves. *Planta* **246**, 1233–1241.

Gould, S. J. and Raposo, G. (2013) As we wait: Coping with an imperfect nomenclature for extracellular vesicles. *Journal of extracellular vesicles* **2**.

Gross, J. C., Chaudhary, V., Bartscherer, K. and Boutros, M. (2012) Active Wnt proteins are secreted on exosomes. *Nature cell biology* **14**, 1036–1045.

Halperin, W. and Jensen, W. A. (1967) Ultrastructural changes during growth and embryogenesis in carrot cell cultures. *Journal of ultrastructure research* **18**, 428–443.

Ham, B.-K., Brandom, J. L., Xoconostle-Cázares, B., Ringgold, V., Lough, T. J. and Lucas, W. J. (2009) A polypyrimidine tract binding protein, pumpkin RBP50, forms the basis of a phloem-mobile ribonucleoprotein complex. *The Plant cell* **21**, 197–215.

Ham, B.-K., Li, G., Jia, W., Leary, J. A. and Lucas, W. J. (2014) Systemic delivery of siRNA in pumpkin by a plant PHLOEM SMALL RNA-BINDING PROTEIN 1-ribonucleoprotein complex. *The Plant journal for cell and molecular biology* **80**, 683–694.

Hamakawa, M. and Hirotsu, T. (2017) Establishment of Time- and Cell-Specific RNAi in Caenorhabditis elegans. *Methods in molecular biology (Clifton, N.J.)* **1507**, 67–79.

Han, L. and Luan, Y.-S. (2015) Horizontal Transfer of Small RNAs to and from Plants. *Frontiers in plant science* **6**, 1113.

Hiraguri, A., Itoh, R., Kondo, N., Nomura, Y., Aizawa, D., Murai, Y., Koiwa, H., Seki, M., Shinozaki, K. and Fukuhara, T. (2005) Specific interactions between Dicer-like proteins and HYL1/DRB-family dsRNA-binding proteins in Arabidopsis thaliana. *Plant molecular biology* **57**, 173–188.

Ho, T., Wang, H., Pallett, D. and Dalmay, T. (2007) Evidence for targeting common siRNA hotspots and GC preference by plant Dicer-like proteins. *FEBS letters* **581**, 3267–3272.

Hoffmann, S., Otto, C., Kurtz, S., Sharma, C. M., Khaitovich, P., Vogel, J., Stadler, P. F. and Hackermüller, J. (2009) Fast mapping of short sequences with mismatches, insertions and deletions using index structures. *PLoS computational biology* **5**, e1000502.

Höfle, L., Koch, A., Zwarg, J., Schmitt, A., Stein, E., Jelonek, L. and Kogel, K.-H. (2018 in revision) SIGS vs HIGS: A comparative study on the efficacy of antifungal double-stranded RNAs targeting Fusarium FgCYP51 genes. *Scientific reports*.

Hoy, A. M. and Buck, A. H. (2012) Extracellular small RNAs: What, where, why? *Biochemical Society transactions* **40**, 886–890.

Huang, X., Yuan, T., Tschannen, M., Sun, Z., Jacob, H., Du, M., Liang, M., Dittmar, R. L., Liu, Y., Liang, M., Kohli, M., Thibodeau, S. N., Boardman, L. and Wang, L. (2013) Characterization of human plasma-derived exosomal RNAs by deep sequencing. *BMC genomics* **14**, 319.

Hückelhoven, R. and Panstruga, R. (2011) Cell biology of the plant-powdery mildew interaction. *Current opinion in plant biology* **14**, 738–746.

Hunter, J. D. (2007) Matplotlib: A 2D Graphics Environment. *Comput. Sci. Eng.* **9**, 90–95.

Huvenne, H. and Smagghe, G. (2010) Mechanisms of dsRNA uptake in insects and potential of RNAi for pest control: a review. *Journal of insect physiology* **56**, 227–235.

Imani, J., Li, L., Schäfer, P. and Kogel, K.-H. (2011) STARTS--a stable root transformation system for rapid functional analyses of proteins of the monocot model plant barley. *The Plant journal for cell and molecular biology* **67**, 726–735.

Jackson, A. L., Bartz, S. R., Schelter, J., Kobayashi, S. V., Burchard, J., Mao, M., Li, B., Cavet, G. and Linsley, P. S. (2003) Expression profiling reveals off-target gene regulation by RNAi. *Nature biotechnology* **21**, 635–637.

Jöchl, C., Loh, E., Ploner, A., Haas, H. and Hüttenhofer, A. (2009) Development-dependent scavenging of nucleic acids in the filamentous fungus Aspergillus fumigatus. *RNA biology* **6**, 179–186.

Johnstone, R. M., Adam, M., Hammond, J. R., Orr, L. and Turbide, C. (1987) Vesicle formation during reticulocyte maturation. Association of plasma membrane activities with released vesicles (exosomes). *The Journal of biological chemistry* **262**, 9412–9420.

Kalluri, R. (2016) The biology and function of exosomes in cancer. *The Journal of clinical investigation* **126**, 1208–1215.

Kamola, P. J., Nakano, Y., Takahashi, T., Wilson, P. A. and Ui-Tei, K. (2015) The siRNA Non-seed Region and Its Target Sequences Are Auxiliary Determinants of Off-Target Effects. *PLoS computational biology* **11**, e1004656.

Karlovsky, P. (2011) Biological detoxification of the mycotoxin deoxynivalenol and its use in genetically engineered crops and feed additives. *Applied microbiology and biotechnology* **91**, 491–504.

Katsir, L. and Bahar, O. (2017) Bacterial outer membrane vesicles at the plant-pathogen interface. *PLoS pathogens* **13**, e1006306.

Kazan, K., Gardiner, D. M. and Manners, J. M. (2012) On the trail of a cereal killer: Recent advances in Fusarium graminearum pathogenomics and host resistance. *Molecular plant pathology* **13**, 399–413.

Kent, W. J., Zweig, A. S., Barber, G., Hinrichs, A. S. and Karolchik, D. (2010) BigWig and BigBed: Enabling browsing of large distributed datasets. *Bioinformatics (Oxford, England)* **26**, 2204–2207.

Khatri, M. and Rajam, M. V. (2007) Targeting polyamines of Aspergillus nidulans by siRNA specific to fungal ornithine decarboxylase gene. *Medical mycology* **45**, 211–220.

Kim, J., Shin, H. and Park, J. (2017) RNA in Salivary Extracellular Vesicles as a Possible Tool for Systemic Disease Diagnosis. *Journal of dental research*, 22034517702100.

Koch, A., Biedenkopf, D., Furch, A., Weber, L., Rossbach, O., Abdellatef, E., Linicus, L., Johannsmeier, J., Jelonek, L., Goesmann, A., Cardoza, V., McMillan, J., Mentzel, T. and Kogel, K.-H. (2016) An RNAi-Based Control of Fusarium graminearum Infections Through Spraying of Long dsRNAs Involves a Plant Passage and Is Controlled by the Fungal Silencing Machinery. *PLoS pathogens* **12**, e1005901.

Koch, A. and Kogel, K.-H. (2014) New wind in the sails: improving the agronomic value of crop plants through RNAi-mediated gene silencing. *Plant biotechnology journal* **12**, 821–831.

Koch, A., Kumar, N., Weber, L., Keller, H., Imani, J. and Kogel, K.-H. (2013) Host-induced gene silencing of cytochrome P450 lanosterol C14alpha-demethylase-encoding genes

confers strong resistance to Fusarium species. *Proceedings of the National Academy of Sciences of the United States of America* **110**, 19324–19329.

Kuo, H. Y., Jacobsen, E. L., Long, Y., Chen, X. and Zhai, J. (2017) Characteristics and processing of Pol IV-dependent transcripts in Arabidopsis. *Journal of genetics and genomics = Yi chuan xue bao* **44**, 3–6.

Langmead, B. and Salzberg, S. L. (2012) Fast gapped-read alignment with Bowtie 2. *Nature methods* **9**, 357–359.

Law, J. A. and Jacobsen, S. E. (2010) Establishing, maintaining and modifying DNA methylation patterns in plants and animals. *Nature reviews. Genetics* **11**, 204–220.

Li, P., Kaslan, M., Lee, S. H., Yao, J. and Gao, Z. (2017) Progress in Exosome Isolation Techniques. *Theranostics* **7**, 789–804.

Li, W., Koutmou, K. S., Leahy, D. J. and Li, M. (2015) Systemic RNA Interference Deficiency-1 (SID-1) Extracellular Domain Selectively Binds Long Double-stranded RNA and Is Required for RNA Transport by SID-1. *The Journal of biological chemistry* **290**, 18904–18913.

Li, Z., Zhou, M., Zhang, Z., Ren, L., Du, L., Zhang, B., Xu, H. and Xin, Z. (2011) Expression of a radish defensin in transgenic wheat confers increased resistance to Fusarium graminearum and Rhizoctonia cerealis. *Functional & integrative genomics* **11**, 63–70.

Liegeois, S., Benedetto, A., Garnier, J.-M., Schwab, Y. and Labouesse, M. (2006) The V0-ATPase mediates apical secretion of exosomes containing Hedgehog-related proteins in Caenorhabditis elegans. *The Journal of cell biology* **173**, 949–961.

Lilley, C. J., Davies, L. J. and Urwin, P. E. (2012) RNA interference in plant parasitic nematodes: a summary of the current status. *Parasitology* **139**, 630–640.

Liu, X., Fu, J., Yun, Y., Yin, Y. and Ma, Z. (2011a) A sterol C-14 reductase encoded by FgERG24B is responsible for the intrinsic resistance of Fusarium graminearum to amine fungicides. *Microbiology (Reading, England)* **157**, 1665–1675.

Liu, X., Jiang, J., Shao, J., Yin, Y. and Ma, Z. (2010) Gene transcription profiling of Fusarium graminearum treated with an azole fungicide tebuconazole. *Applied microbiology and biotechnology* **85**, 1105–1114.

Liu, X., Yu, F., Schnabel, G., Wu, J., Wang, Z. and Ma, Z. (2011b) Paralogous cyp51 genes in Fusarium graminearum mediate differential sensitivity to sterol demethylation inhibitors. *Fungal genetics and biology FG & B* **48**, 113–123.

Livak, K. J. and Schmittgen, T. D. (2001) Analysis of relative gene expression data using real-time quantitative PCR and the 2(-Delta Delta C(T)) Method. *Methods (San Diego, Calif.)* **25**, 402–408.

Lobb, R. J., Becker, M., Wen, S. W., Wong, C. S. F., Wiegmans, A. P., Leimgruber, A. and Möller, A. (2015) Optimized exosome isolation protocol for cell culture supernatant and human plasma. *Journal of extracellular vesicles* **4**, 27031.

Lori, G. A., Sisterna, M. N., Sarandón, S. J., Rizzo, I. and Chidichimo, H. (2009) Fusarium head blight in wheat: Impact of tillage and other agronomic practices under natural infection. *Crop Protection* **28**, 495–502.

Lough, T. J. and Lucas, W. J. (2006) Integrative plant biology: role of phloem long-distance macromolecular trafficking. *Annual review of plant biology* **57**, 203–232.

Lu, R. (2003) Virus-induced gene silencing in plants. *Methods (San Diego, Calif.)* **30**, 296–303.

Lu, S. and Edwards, M. (2017) Molecular Characterization and Functional Analysis of PR-1-like Proteins Identified from the Wheat Head Blight Fungus Fusarium graminearum. *Phytopathology*.

Lynch, A. G., Hadfield, J., Dunning, M. J., Osborne, M., Thorne, N. P. and Tavaré, S. (2010) The cost of reducing starting RNA quantity for Illumina BeadArrays: A bead-level dilution experiment. *BMC genomics* **11**, 540.

Lyska, D., Engelmann, K., Meierhoff, K. and Westhoff, P. (2013) pAUL: a gateway-based vector system for adaptive expression and flexible tagging of proteins in Arabidopsis. *PloS one* **8**, e53787.

Machado, A. K., Brown, N. A., Urban, M., Kanyuka, K. and Hammond-Kosack, K. (2017) RNAi as an emerging approach to control Fusarium Head Blight disease and mycotoxin contamination in cereals. *Pest management science*.

Majumdar, R., Rajasekaran, K. and Cary, J. W. (2017) RNA Interference (RNAi) as a Potential Tool for Control of Mycotoxin Contamination in Crop Plants: Concepts and Considerations. *Frontiers in plant science* **8**, 200.

Manavella, P. A., Koenig, D. and Weigel, D. (2012) Plant secondary siRNA production determined by microRNA-duplex structure. *Proceedings of the National Academy of Sciences of the United States of America* **109**, 2461–2466.

Mao, Y.-B., Cai, W.-J., Wang, J.-W., Hong, G.-J., Tao, X.-Y., Wang, L.-J., Huang, Y.-P. and Chen, X.-Y. (2007) Silencing a cotton bollworm P450 monooxygenase gene by plant-

mediated RNAi impairs larval tolerance of gossypol. *Nature biotechnology* **25**, 1307–1313.

Martin, M. (2011) Cutadapt removes adapter sequences from high-throughput sequencing reads. *EMBnet j.* **17**, 10.

Masanga, J. O., Matheka, J. M., Omer, R. A., Ommeh, S. C., Monda, E. O. and Alakonya, A. E. (2015) Downregulation of transcription factor aflR in Aspergillus flavus confers reduction to aflatoxin accumulation in transgenic maize with alteration of host plant architecture. *Plant cell reports* **34**, 1379–1387.

Matzke, M. A. and Mosher, R. A. (2014) RNA-directed DNA methylation: An epigenetic pathway of increasing complexity. *Nature reviews. Genetics* **15**, 394–408.

Maximilian Metze (2016). *Creating constructs for a host-indced gene silencing resistance approach in Arabidopsis thaliana against Fusarium graminearum*. Masterthesis. JLU Gießen.

McEwan, D. L., Weisman, A. S. and Hunter, C. P. (2012) Uptake of extracellular double-stranded RNA by SID-2. *Molecular cell* **47**, 746–754.

Melnyk, C. W., Molnar, A. and Baulcombe, D. C. (2011) Intercellular and systemic movement of RNA silencing signals. *The EMBO journal* **30**, 3553–3563.

Mesterházy, Á., Lemmens, M. and Reid, L. M. (2012) Breeding for resistance to ear rots caused by Fusarium spp. in maize - a review. *Plant Breeding* **131**, 1–19.

Metpally, R. P. R., Nasser, S., Malenica, I., Courtright, A., Carlson, E., Ghaffari, L., Villa, S., Tembe, W. and van Keuren-Jensen, K. (2013) Comparison of Analysis Tools for miRNA High Throughput Sequencing Using Nerve Crush as a Model. *Frontiers in genetics* **4**, 20.

Micali, C. O., Neumann, U., Grunewald, D., Panstruga, R. and O'Connell, R. (2011) Biogenesis of a specialized plant-fungal interface during host cell internalization of Golovinomyces orontii haustoria. *Cellular microbiology* **13**, 210–226.

Michael DroettboomNIH, Thomas A CaswellBrookhaven National Lab, John Hunter, Eric FiringUniversity of Hawaii, Jens Hedegaard Nielsen@qdev-dk, Nelle VaroquauxUC Berkeley, Benjamin Root, Phil Elson, Darren DaleCornell University, Jae-Joon Lee, Elliott Sales de Andrade, Jouni K. Seppänen, Damon McDougallUniversity of Texas at Austin, Ryan MayUCAR/@Unidata, Antony Lee, Andrew Straw, David Stansby, Paul Hobson@Geosyntec, Tony S Yu, Eric MaMIT, Christoph Gohlke, Steven SilvesterContinuum Analytics, Charlie Moad, Jan Schulz, Adrien F. VincentUniv. Paris-Sud, Peter Würtz, Federico Ariza, Cimarron, Thomas Hisch and Nikita Kniazev (2017). *Matplotlib/Matplotlib V2.0.2*: Zenodo.

Mitter, N., Worrall, E. A., Robinson, K. E., Li, P., Jain, R. G., Taochy, C., Fletcher, S. J., Carroll, B. J., Lu, G. Q. M. and Xu, Z. P. (2017) Clay nanosheets for topical delivery of RNAi for sustained protection against plant viruses. *Nature plants* **3**, 16207.

Molnar, A., Melnyk, C. and Baulcombe, D. C. (2011) Silencing signals in plants: A long journey for small RNAs. *Genome biology* **12**, 215.

Molnar, A., Melnyk, C. W., Bassett, A., Hardcastle, T. J., Dunn, R. and Baulcombe, D. C. (2010) Small silencing RNAs in plants are mobile and direct epigenetic modification in recipient cells. *Science (New York, N.Y.)* **328**, 872–875.

Mu, J., Zhuang, X., Wang, Q., Jiang, H., Deng, Z.-B., Wang, B., Zhang, L., Kakar, S., Jun, Y., Miller, D. and Zhang, H.-G. (2014) Interspecies communication between plant and mouse gut host cells through edible plant derived exosome-like nanoparticles. *Molecular nutrition & food research* **58**, 1561–1573.

Mukherjee, K., Campos, H. and Kolaczkowski, B. (2013) Evolution of animal and plant dicers: early parallel duplications and recurrent adaptation of antiviral RNA binding in plants. *Molecular biology and evolution* **30**, 627–641.

Mulot, M., Boissinot, S., Monsion, B., Rastegar, M., Clavijo, G., Halter, D., Bochet, N., Erdinger, M. and Brault, V. (2016) Comparative Analysis of RNAi-Based Methods to Down-Regulate Expression of Two Genes Expressed at Different Levels in Myzus persicae. *Viruses* **8**.

Nguyen, Q. B., Kadotani, N., Kasahara, S., Tosa, Y., Mayama, S. and Nakayashiki, H. (2008) Systematic functional analysis of calcium-signalling proteins in the genome of the rice-blast fungus, Magnaporthe oryzae, using a high-throughput RNA-silencing system. *Molecular microbiology* **68**, 1348–1365.

Niehl, A., Wyrsch, I., Boller, T. and Heinlein, M. (2016) Double-stranded RNAs induce a pattern-triggered immune signaling pathway in plants. *The New phytologist* **211**, 1008–1019.

Nosaka, M., Itoh, J.-I., Nagato, Y., Ono, A., Ishiwata, A. and Sato, Y. (2012) Role of transposon-derived small RNAs in the interplay between genomes and parasitic DNA in rice. *PLoS genetics* **8**, e1002953.

Nowara, D., Gay, A., Lacomme, C., Shaw, J., Ridout, C., Douchkov, D., Hensel, G., Kumlehn, J. and Schweizer, P. (2010) HIGS: host-induced gene silencing in the obligate biotrophic fungal pathogen Blumeria graminis. *The Plant cell* **22**, 3130–3141.

Nybakken, K., Vokes, S. A., Lin, T.-Y., McMahon, A. P. and Perrimon, N. (2005) A genome-wide RNA interference screen in Drosophila melanogaster cells for new components of the Hh signaling pathway. *Nature genetics* **37**, 1323–1332.

OERKE, E.-C. and Dehne, H.-W. (2004) Safeguarding production—losses in major crops and the role of crop protection. *Crop Protection* **23**, 275–285.

Osborne, L. E. and Stein, J. M. (2007) Epidemiology of Fusarium head blight on small-grain cereals. *International journal of food microbiology* **119**, 103–108.

Papp, I. (2003) Evidence for Nuclear Processing of Plant Micro RNA and Short Interfering RNA Precursors. *Plant physiology* **132**, 1382–1390.

Parent, J.-S., Martínez de Alba, A. E. and Vaucheret, H. (2012) The origin and effect of small RNA signaling in plants. *Frontiers in plant science* **3**, 179.

Peres da Silva, R., Puccia, R., Rodrigues, M. L., Oliveira, D. L., Joffe, L. S., César, G. V., Nimrichter, L., Goldenberg, S. and Alves, L. R. (2015) Extracellular vesicle-mediated export of fungal RNA. *Scientific reports* **5**, 7763.

Pisitkun, T., Shen, R.-F. and Knepper, M. A. (2004) Identification and proteomic profiling of exosomes in human urine. *Proceedings of the National Academy of Sciences of the United States of America* **101**, 13368–13373.

Plasterk, R. H. A. (2002) RNA silencing: The genome's immune system. *Science (New York, N.Y.)* **296**, 1263–1265.

Pratt, A. J. and MacRae, I. J. (2009) The RNA-induced silencing complex: A versatile gene-silencing machine. *The Journal of biological chemistry* **284**, 17897–17901.

Price, C. L., Parker, J. E., Warrilow, A. G. S., Kelly, D. E. and Kelly, S. L. (2015) Azole fungicides - understanding resistance mechanisms in agricultural fungal pathogens. *Pest management science* **71**, 1054–1058.

Qiu, S., Adema, C. M. and Lane, T. (2005) A computational study of off-target effects of RNA interference. *Nucleic acids research* **33**, 1834–1847.

Quinlan, A. R. and Hall, I. M. (2010) BEDTools: A flexible suite of utilities for comparing genomic features. *Bioinformatics (Oxford, England)* **26**, 841–842.

Quintana, J. F., Babayan, S. A. and Buck, A. H. (2017) Small RNAs and extracellular vesicles in filarial nematodes: From nematode development to diagnostics. *Parasite immunology* **39**.

Raposo, G. and Stoorvogel, W. (2013) Extracellular vesicles: Exosomes, microvesicles, and friends. *The Journal of cell biology* **200**, 373–383.

Regente, M., Corti-Monzon, G., Maldonado, A. M., Pinedo, M., Jorrin, J. and La Canal, L. de (2009) Vesicular fractions of sunflower apoplastic fluids are associated with potential exosome marker proteins. *FEBS letters* **583**, 3363–3366.

Reis, R. S., Hart-Smith, G., Eamens, A. L., Wilkins, M. R. and Waterhouse, P. M. (2015) Gene regulation by translational inhibition is determined by Dicer partnering proteins. *Nature plants* **1**, 14027.

Rocha, O., Ansari, K. and Doohan, F. M. (2005) Effects of trichothecene mycotoxins on eukaryotic cells: a review. *Food additives and contaminants* **22**, 369–378.

Rodríguez, M., Bajo-Santos, C., Hessvik, N. P., Lorenz, S., Fromm, B., Berge, V., Sandvig, K., Linē, A. and Llorente, A. (2017) Identification of non-invasive miRNAs biomarkers for prostate cancer by deep sequencing analysis of urinary exosomes. *Molecular cancer* **16**, 156.

Rutter, B. D. and Innes, R. W. (2017) Extracellular Vesicles Isolated from the Leaf Apoplast Carry Stress-Response Proteins. *Plant physiology* **173**, 728–741.

Saumet, A. and Lecellier, C.-H. (2006) Anti-viral RNA silencing: Do we look like plants? *Retrovirology* **3**, 3.

Savary, S., Ficke, A., Aubertot, J.-N. and Hollier, C. (2012) Crop losses due to diseases and their implications for global food production losses and food security. *Food Sec.* **4**, 519–537.

Sawano, H., Matsuzaki, T., Usui, T., Tabara, M., Fukudome, A., Kanaya, A., Tanoue, D., Hiraguri, A., Horiguchi, G., Ohtani, M., Demura, T., Kozaki, T., Ishii, K., Moriyama, H. and Fukuhara, T. (2017) Double-stranded RNA-binding protein DRB3 negatively regulates anthocyanin biosynthesis by modulating PAP1 expression in Arabidopsis thaliana. *Journal of plant research* **130**, 45–55.

Schwab, R. and Voinnet, O. (2010) RNA silencing amplification in plants: Size matters. *Proceedings of the National Academy of Sciences of the United States of America* **107**, 14945–14946.

Seinen, E., Burgerhof, J. G. M., Jansen, R. C. and Sibon, O. C. M. (2011) RNAi-induced off-target effects in Drosophila melanogaster: Frequencies and solutions. *Briefings in functional genomics* **10**, 206–214.

Senthil-Kumar, M. and Mysore, K. S. (2011) Caveat of RNAi in plants: The off-target effect. *Methods in molecular biology (Clifton, N.J.)* **744**, 13–25.

Shih, J. D. and Hunter, C. P. (2011) SID-1 is a dsRNA-selective dsRNA-gated channel. *RNA (New York, N.Y.)* **17**, 1057–1065.

Shin, S., Mackintosh, C. A., Lewis, J., Heinen, S. J., Radmer, L., Dill-Macky, R., Baldridge, G. D., Zeyen, R. J. and Muehlbauer, G. J. (2008) Transgenic wheat expressing a barley class II chitinase gene has enhanced resistance against Fusarium graminearum. *Journal of experimental botany* **59**, 2371–2378.

Shivakumara, T. N., Chaudhary, S., Kamaraju, D., Dutta, T. K., Papolu, P. K., Banakar, P., Sreevathsa, R., Singh, B., Manjaiah, K. M. and Rao, U. (2017) Host-Induced Silencing of Two Pharyngeal Gland Genes Conferred Transcriptional Alteration of Cell Wall-Modifying Enzymes of Meloidogyne incognita vis-à-vis Perturbed Nematode Infectivity in Eggplant. *Frontiers in plant science* **8**, 473.

Skog, J., Noerholm, M., Bentink, S., Romain, C., Fishbeck, J., Sinclair, I., Scott, A., Mueller, R., Koestler, T. and Belzer, S. (2014) Abstract B34: Development of a urine microvesicle/exosome RNA biomarker panel to identify prostate cancer. *Molecular Cancer Therapeutics* **12**, B34-B34.

Stack, R. W. (1989) A comparison of the inoculum potential of ascospores and conidia of Gibberella zeae. *Canadian Journal of Plant Pathology* **11**, 137–142.

Stefanato, F. L., Abou-Mansour, E., Buchala, A., Kretschmer, M., Mosbach, A., Hahn, M., Bochet, C. G., Métraux, J.-P. and Schoonbeek, H.-j. (2009) The ABC transporter BcatrB from Botrytis cinerea exports camalexin and is a virulence factor on Arabidopsis thaliana. *The Plant journal for cell and molecular biology* **58**, 499–510.

Sun, D., Zhuang, X., Xiang, X., Liu, Y., Zhang, S., Liu, C., Barnes, S., Grizzle, W., Miller, D. and Zhang, H.-G. (2010) A novel nanoparticle drug delivery system: The anti-inflammatory activity of curcumin is enhanced when encapsulated in exosomes. *Molecular therapy the journal of the American Society of Gene Therapy* **18**, 1606–1614.

Tetyuk, O., Benning, U. F. and Hoffmann-Benning, S. (2013) Collection and analysis of Arabidopsis phloem exudates using the EDTA-facilitated Method. *Journal of visualized experiments JoVE*, e51111.

Thorvaldsdóttir, H., Robinson, J. T. and Mesirov, J. P. (2013) Integrative Genomics Viewer (IGV): High-performance genomics data visualization and exploration. *Briefings in bioinformatics* **14**, 178–192.

Trail, F. (2009) For blighted waves of grain: Fusarium graminearum in the postgenomics era. *Plant physiology* **149**, 103–110.

Unver, T. and Budak, H. (2009) Virus-induced gene silencing, a post transcriptional gene silencing method. *International journal of plant genomics* **2009**, 198680.

van Balkom, B. W. M., Eisele, A. S., Pegtel, D. M., Bervoets, S. and Verhaar, M. C. (2015) Quantitative and qualitative analysis of small RNAs in human endothelial cells and exosomes provides insights into localized RNA processing, degradation and sorting. *Journal of extracellular vesicles* **4**, 26760.

Vazquez, F. and Hohn, T. (2013) Biogenesis and Biological Activity of Secondary siRNAs in Plants. *Scientifica* **2013**, 783253.

Walawage, S. L., Britton, M. T., Leslie, C. A., Uratsu, S. L., Li, Y. and Dandekar, A. M. (2013) Stacking resistance to crown gall and nematodes in walnut rootstocks. *BMC genomics* **14**, 668.

Wang, F., Shang, Y., Fan, B., Yu, J.-Q. and Chen, Z. (2014) Arabidopsis LIP5, a positive regulator of multivesicular body biogenesis, is a critical target of pathogen-responsive MAPK cascade in plant basal defense. *PLoS pathogens* **10**, e1004243.

Wang, M., Weiberg, A., Lin, F.-M., Thomma, B. P. H. J., Huang, H.-D. and Jin, H. (2016) Bidirectional cross-kingdom RNAi and fungal uptake of external RNAs confer plant protection. *Nature plants* **2**, 16151.

Weiberg, A., Wang, M., Lin, F.-M., Zhao, H., Zhang, Z., Kaloshian, I., Huang, H.-D. and Jin, H. (2013) Fungal small RNAs suppress plant immunity by hijacking host RNA interference pathways. *Science (New York, N.Y.)* **342**, 118–123.

Xoconostle-Cázares, B., Xiang, Y., Ruiz-Medrano, R., Wang, H. L., Monzer, J., Yoo, B. C., McFarland, K. C., Franceschi, V. R. and Lucas, W. J. (1999) Plant paralog to viral movement protein that potentiates transport of mRNA into the phloem. *Science (New York, N.Y.)* **283**, 94–98.

Xu, H. and Mendgen, K. (1994) Endocytosis of 1,3-?: -glucans by broad bean cells at the penetration site of the cowpea rust fungus (haploid stage). *Planta* **195**.

Yoo, B.-C., Kragler, F., Varkonyi-Gasic, E., Haywood, V., Archer-Evans, S., Lee, Y. M., Lough, T. J. and Lucas, W. J. (2004) A systemic small RNA signaling system in plants. *The Plant cell* **16**, 1979–2000.

Yoshida, Y. (1988) Cytochrome P450 of fungi: Primary target for azole antifungal agents. *Current topics in medical mycology* **2**, 388–418.

Zhang, J., Khan, S. A., Heckel, D. G. and Bock, R. (2017) Next-Generation Insect-Resistant Plants: RNAi-Mediated Crop Protection. *Trends in Biotechnology* **35**, 871–882.

Zhang, L., Hou, D., Chen, X., Li, D., Zhu, L., Zhang, Y., Li, J., Bian, Z., Liang, X., Cai, X., Yin, Y., Wang, C., Zhang, T., Zhu, D., Zhang, D., Xu, J., Chen, Q., Ba, Y., Liu, J., Wang, Q., Chen, J., Wang, J., Wang, M., Zhang, Q., Zhang, J., Zen, K. and Zhang, C.-Y. (2012)

Exogenous plant MIR168a specifically targets mammalian LDLRAP1: evidence of cross-kingdom regulation by microRNA. *Cell research* **22**, 107–126.

Zhou, B., Bailey, A., Niblett, C. L. and Qu, R. (2016) Control of brown patch (Rhizoctonia solani) in tall fescue (Festuca arundinacea Schreb.) by host induced gene silencing. *Plant cell reports* **35**, 791–802.

Zhu, L., Liu, J., Dao, J., Lu, K., Li, H., Gu, H., Liu, J., Feng, X. and Cheng, G. (2016) Molecular characterization of S. japonicum exosome-like vesicles reveals their regulatory roles in parasite-host interactions. *Scientific reports* **6**, 25885.

Zhu, S., Jeong, R.-D., Lim, G.-H., Yu, K., Wang, C., Chandra-Shekara, A. C., Navarre, D., Klessig, D. F., Kachroo, A. and Kachroo, P. (2013) Double-stranded RNA-binding protein 4 is required for resistance signaling against viral and bacterial pathogens. *Cell reports* **4**, 1168–1184.

8.   Attachment

8.1   List of figures

8.2   List of tables

8.3 Sequences of dsRNAs, proteins and genes mentioned in this study

dsRNAs:

CYP-A:

CGGTCCATTGACAATCCCCGTCTTTGGTAGCGATGTCGTATACGATTGTCCCAACTCGAAGCTCATGGAACAAAAGAAGTTTG
TCAAGTTTGGCCTTACGCAAAAAGCACTCGAGTCACACGTCCAGTTAATCGAGCGAGAGGTTCTTGACTACGTCGAAACTGAT
CCATCCTTTTCTGGCAGAACTAGCACCATCGATGTCCCCAAGGCAATGGCTGAGATAACAATCTTTACTGCCTCACGTTCTTTG
CAGGGTGAGGAAGTTCGGAGAAAACTCACTGCCGAGTTTGCTGC

CYP-B:

CAGCAAGTTTGACGAGTCCCTGGCCGCTCTCTACCACGACCTCGATATGGGCTTCACCCCCATCAACTTCATGCTTCACTGGG
CCCCTCTCCCCTGGAACCGTAAGCGCGACCACGCCCAGCGCACTGTTGCCAAGATCTACATGGACACTATCAAGGAGCGCCG
CGCCAAGGGCAACAACGAATCCGAGCATGACATGATGAAGCACCTTATGAACTCT

CYP-C:

ATTGGAAGCACCGTACAATATGGCATCGACCCGTACGCTTTTTTCTTCGACTGCAGAGATAAATACGGCGACTGCTTTACCTT
TATTCTCCTTGGCAAATCAACGACTGTCTTTCTTGGTCCCAAGGGCAATGACTTTATCCTCAACGGCAAACACGCCGATCTCA
ACGCCGAGGACGTTTATGGGAAACTTACCACGCCCGTGTTTGGTGAGGAGGTTGTTTATGACTGCTCCAATG

CYP-AC:

CGGTCCATTGACAATCCCCGTCTTTGGTAGCGATGTCGTATACGATTGTCCCAACTCGAAGCTCATGGAACAAAAGAAGTTTG
TCAAGTTTGGCCTTACGCAAAAAGCACTCGAGTCACACGTCCAGTTAATCGAGCGAGAGGTTCTTGACTACGTCGAAACTGAT
CCATCCTTTTCTGGCAGAACTAGCACCATCGATGTCCCCAAGGCAATGGCTGAGATAACAATCTTTACTGCCTCACGTTCTTTG
CAGGGTGAGGAAGTTCGGAGAAAACTCACTGCCGAGTTTGCTGCATTGGAAGCACCGTACAATATGGCATCGACCCGTACGC
TTTTTTCTTCGACTGCAGAGATAAATACGGCGACTGCTTTACCTTTATTCTCCTTGGCAAATCAACGACTGTCTTTCTTGGTCCC
AAGGGCAATGACTTTATCCTCAACGGCAAACACGCCGATCTCAACGCCGAGGACGTTTATGGGAAACTTACCACGCCCGTGT
TTGGTGAGGAGGTTGTTTATGACTGCTCCAATG

CYP-BC:

CAGCAAGTTTGACGAGTCCCTGGCCGCTCTCTACCACGACCTCGATATGGGCTTCACCCCCATCAACTTCATGCTTCACTGGG
CCCCTCTCCCCTGGAACCGTAAGCGCGACCACGCCCAGCGCACTGTTGCCAAGATCTACATGGACACTATCAAGGAGCGCCG
CGCCAAGGGCAACAACGAATCCGAGCATGACATGATGAAGCACCTTATGAACTCTATTGGAAGCACCGTACAATATGGCATC
GACCCGTACGCTTTTTTCTTCGACTGCAGAGATAAATACGGCGACTGCTTTACCTTTATTCTCCTTGGCAAATCAACGACTGTC
TTTCTTGGTCCCAAGGGCAATGACTTTATCCTCAACGGCAAACACGCCGATCTCAACGCCGAGGACGTTTATGGGAAACTTAC
CACGCCCGTGTTTGGTGAGGAGGTTGTTTATGACTGCTCCAATG

CYP-AB:

CGGTCCATTGACAATCCCCGTCTTTGGTAGCGATGTCGTATACGATTGTCCCAACTCGAAGCTCATGGAACAAAAGAAGTTTG
TCAAGTTTGGCCTTACGCAAAAAGCACTCGAGTCACACGTCCAGTTAATCGAGCGAGAGGTTCTTGACTACGTCGAAACTGAT
CCATCCTTTTCTGGCAGAACTAGCACCATCGATGTCCCCAAGGCAATGGCTGAGATAACAATCTTTACTGCCTCACGTTCTTTG
CAGGGTGAGGAAGTTCGGAGAAAACTCACTGCCGAGTTTGCTGCCAGCAAGTTTGACGAGTCCCTGGCCGCTCTCTACCACG
ACCTCGATATGGGCTTCACCCCCATCAACTTCATGCTTCACTGGGCCCCTCTCCCCTGGAACCGTAAGCGCGACCACGCCCAG
CGCACTGTTGCCAAGATCTACATGGACACTATCAAGGAGCGCCGCGCCAAGGGCAACAACGAATCCGAGCATGACATGATGA
AGCACCTTATGAACTCT

CYP3RNA:

CAGCAAGTTTGACGAGTCCCTGGCCGCTCTCTACCACGACCTCGATATGGGCTTCACCCCCATCAACTTCATGCTTCACTGGG
CCCCTCTCCCCTGGAACCGTAAGCGCGACCACGCCCAGCGCACTGTTGCCAAGATCTACATGGACACTATCAAGGAGCGCCG
CGCCAAGGGCAACAACGAATCCGAGCATGACATGATGAAGCACCTTATGAACTCTCGGTCCATTGACAATCCCCGTCTTTGGT
AGCGATGTCGTATACGATTGTCCCAACTCGAAGCTCATGGAACAAAAGAAGTTTGTCAAGTTTGGCCTTACGCAAAAAGCAC
TCGAGTCACACGTCCAGTTAATCGAGCGAGAGGTTCTTGACTACGTCGAAACTGATCCATCCTTTTCTGGCAGAACTAGCACC
ATCGATGTCCCCAAGGCAATGGCTGAGATAACAATCTTTACTGCCTCACGTTCTTTGCAGGGTGAGGAAGTTCGGAGAAAACT
CACTGCCGAGTTTGCTGCATTGGAAGCACCGTACAATATGGCATCGACCCGTACGCTTTTTTCTTCGACTGCAGAGATAAATA
CGGCGACTGCTTTACCTTTATTCTCCTTGGCAAATCAACGACTGTCTTTCTTGGTCCCAAGGGCAATGACTTTATCCTCAACGG

CAAACACGCCGATCTCAACGCCGAGGACGTTTATGGGAAACTTACCACGCCCGTGTTTGGTGAGGAGGTTGTTTATGACTGCT
CCAATG

GUS-dsRNA:

CACCCAGGTGTTCGGCGTGGTGTAGAGCATTACGCTGCGATGGATTCCGGCATAGTTAAAGAAATCATGGAAGTAAGACTGC
TTTTTCTTGCCGTTTTCGTCGGTAATCACCATTCCCGGCGGGATAGTCTGCCAGTTCAGTTCGTTGTTCACACAAACGGTGATA
CGTACACTTTTCCCGGCAATAACATACGGCGTGACATCGGCTTCAAATGGCGTATAGCCGCCCTGATGCTCCATCACTTCCTG
ATTATTGACCCACACTTTGCCGTAATGAGTGACCGCATCGAAACGCAGCACGATACGCTGGCCTGCCCAACCTTTCGGTATAA
AGACTTCGCGCTGATACCAGACGTTGCCCGCATAATTACGAATATCTGCATCGGCGAACTGATCGTTAAAACTGCCTGGCACA
GCAATTGCCCGGCTTTCTTGTAACGCGCTTTCCCACCAACGCTGATCAATTCCACAGTTTTCGCGATCCAGACTGAATGCCCAC
AGGCCGTCGAGTTTTTTGATTTCACGGGTTGGGGTTTCTACAGGACGTAAC

Full sequences of dsRNAs CYPA-500/800/full, CYPB-400/800/full and CYPC-400/800/full
are available in the Master thesis of Abhishek Shrestha (Abhishek Shrestha, 2016).

Full sequences of dsRNAs CYP-HSA, CYP-A5`, CYP-B5', CYP-Cmiddle, CYP-ABC, CYP-
BCA, CYP-AAA, CYP-BBB and CYP-CCC are available in the Master thesis of Maximilian
Metze (Maximilian Metze, 2016).

protein sequences:

Sequences of the five *Arabidopsis* DRB proteins were obtained from the TAIR database
(DRB1: AT1G09700.1; DRB2: AT2G28380.1; DRB3: AT3G26932.1; DRB4: AT3G62800.1;
DRB5: AT5G41070.1)

Sequences of RBP50 and PP16 from *Cucurbita maxima* are available from pubmed under the
accession numbers EU793994.1 and AF079170.1 respectively.

gene sequences:

FgCYP51A (FGSG_04092); *FgCYP51B* (FGSG_01000); *FgCYP51C* (FGSG_11024); *EF1-α*
(FGSG_08811)

8.4   Own work

Experiments, data analysis and writing of the present thesis unless otherwise indicated and with
exception of the following items, were all done by myself.

Small RNA sequencing of vesicle RNA as described in 2.2.18 was performed in Bielefeld by
Dr. Tobias Busche (Center for Biotechnology – CeBiTec).

The bioinformatic off-target analysis as shown in Fig. 12 as well as siRNA profiling as shown
in Fig. 17, Fig. 19 and Fig. 21 were done by Lukas Jelonek (Department of Bioinformatic and
Systems Biology, JLU Gießen).

The siRNA profiling of CYP3RNA plants as shown in Fig. 3 was provided by Dr. Aline Koch
(Institute for Phytopathology, JLU Gießen).

9. Danksagung

An dieser Stelle möchte ich meinen besonderen Dank nachstehenden Personen entgegenbringen, ohne deren Mithilfe die Anfertigung dieser Promotionsschrift niemals zustande gekommen wäre:

An erster Stelle gilt mein Dank Herrn Prof. Dr. Karl-Heinz Kogel für seine wissenschaftliche und methodische Unterstützung während der gesamten Bearbeitungsphase meiner Dissertation sowie der Überlassung dieses hochinteressanten Forschungsthemas.

Ich danke Frau Prof. Dr. Annette Becker für die hilfsbereite und wissenschaftliche Betreuung als Zweitgutachterin.

Mein ganz besonderer Dank gilt Frau Dr. Aline Koch. Jederzeit gewährte sie mir bei der Planung, Durchführung und Auswertung der vorliegenden Arbeit außerordentlich fachliche, und wertvolle Unterstützung. Ihre wegweisenden und kreativen Ideen haben wesentlich zum Erstellen der Arbeit beigetragen. Besonders bedanken will ich mich auch für die Freiheit und das Vertrauen, welches sie mir während des gesamten Forschungsprojektes entgegnete und was maßgeblich zum Gelingen dieser Arbeit beitrug. Auch die vielen nichtwissenschaftlichen und motivierenden Gespräche haben meine Arbeit unterstützt und gaben der Laborarbeit immer eine ganz besondere und persönliche Komponente.

Großer Dank gebührt Frau Dagmar Biedenkopf, Frau Martina Claar und Frau Elke Stein. Mit ihrer außerordentlichen methodischen Kompetenz und Erfahrung haben sie viele Experimente vorangebracht und den Laboralltag auch in stressigen Phasen erleichtert. Bei Frau Dagmar Biedenkopf möchte ich mich besonders für die gemeinsame Laborarbeit, ihre nie endende Hilfsbereitschaft sowie die zahlreichen Gespräche, die jederzeit Freude in den Laboralltag brachten, bedanken.

Ich danke unserer Gärtnerin Christina Birkenstock sowie unseren Gärtnern Udo Schnepp und Volker Weisel für ihren unermüdlichen Einsatz bei der Aufzucht unserer Pflanzen.

Allen Mitarbeitern des Institutes für Phytopathologie bin ich sehr dankbar für die zahlreiche Unterstützung sowie die freundliche und angenehme Zusammenarbeit. Innerhalb sowie außerhalb des Laboralltags gab es mit euch immer viel zu lachen.

Ich danke des Weiteren den Studenten, die mich im Rahmen ihrer Abschlussarbeiten in zahlreichen Projekten unterstützt haben. Herrn Maximilian Metze und Herrn Abishek Shretka danke ich für ihre große und kompetente Mithilfe bei der Klonierung und Pflanzentransformation, die diese Arbeit maßgeblich vorangebracht hat. Frau Alexandra Schmitt danke ich für die Mithilfe bei den Gerste Pathogenassays.

Mein Dank gilt auch der Imaging Unit der JLU Gießen, besonders Herrn Dr. Martin Hardt sowie Anna Möbus, die mich in die Methodik der Elektronenmikroskopie eingeführt haben und ihr Labor, ihre Geräte sowie ihre Arbeitszeit zur Verfügung gestellt haben.

Bei Herrn Lukas Jelonek bedanke ich mich für die bioinformatischen Analysen, die innerhalb dieser Arbeit durchgeführt wurden. Ohne seine Kompetenz wären viele Projekt nicht zustande gekommen.

Besonders möchte ich an dieser Stelle auch meiner Mama und meiner Schwester, für die unermüdliche Stärkung und Motivation danken, sowie für das stets offene Ohr für meine Gedanken und Zweifel. Danke Mama, dass du immer an mich glaubst und mir bei meinem bisherigen Lebensweg stets zur Seite gestanden hast.

Meinem Lieblingsmenschen Fabian Weipert, der bereits seit Beginn meines Studiums an meiner Seite ist, danke ich für die gemeinsame Zeit in der wir bis jetzt jeden Abschnitt erfolgreich zusammen gemeistert haben und hoffentlich auch in Zukunft werden. Du warst für mich immer ein Rückhalt auf den ich mich verlassen konnte und der es mir ermöglicht hat alle Probleme zu vergessen.